THESIS
3

MICHIGAN STATE UNIVERSITY LIBRARIES
3 1293 01417 2112

This is to certify that the

dissertation entitled

PARAMETRIC MODULATION: A NOVEL COMPUTER-ASSISTED OPTIMIZATION METHOD FOR LIQUID CHROMATOGRAPHY

presented by

Patrick Hassan Sao Lukulay

has been accepted towards fulfillment
of the requirements for

Doctorate degree in Analytical Chemistry

Victoria McGuffin
Major professor

Date 4 August 1995

MSU is an Affirmative Action/Equal Opportunity Institution

O-12771

LIBRARY
Michigan State
University

PLACE IN RETURN BOX to remove this checkout from your record.
TO AVOID FINES return on or before date due.

DATE DUE	DATE DUE	DATE DUE
JUL 1 6 2007		

MSU Is An Affirmative Action/Equal Opportunity Institution
c:\circ\datedue.pm3-p.1

PARAMETRIC MODULATION: A NOVEL COMPUTER-ASSISTED OPTIMIZATION METHOD FOR LIQUID CHROMATOGRAPHY

By

Patrick Hassan Sao Lukulay

A DISSERTATION

Submitted to

Michigan State University

in partial fulfillment of the requirements

for the degree of

DOCTOR OF PHILOSOPHY

Department of Chemistry

1995

Copyright by

Patrick Hassan Sao Lukulay

1995

ABSTRACT

PARAMETRIC MODULATION: A NOVEL COMPUTER-ASSISTED OPTIMIZATION METHOD FOR LIQUID CHROMATOGRAPHY

by

Patrick Hassan Sao Lukulay

A novel computer-assisted optimization method called parametric modulation has been developed for univariate and multivariate optimization in liquid chromatography. The fundamental strategy of his approach is that chromatographic retention may be accurately predicted if the solute is constrained to undergo interaction independently within each mobile phase, stationary phase, and temperature environment. Thus, the overall solute retention may be calculated by summation of its retention within each individual environment. In this method, the predicted solute retention time is more accurate because it is calculated by summation of the known and measured behavior in discrete environments rather than by numerical regression in unknown or poorly characterized environments.

In this dissertation, the general concept and theory of solute retention and band dispersion under the condition of parametric modulation have been developed and a computer program written to implement the technique. Semi-empirical equations have been developed to predict solute retention and band broadening as a function of the length dimension of stationary phase, mobile phase and temperature environments.

Experimental verification of this technique is demonstrated for both univariate and multivariate optimization. In the univariate optimization, mobile

phase is optimized for the separation of eight common corticosteroids. The separation was compared to that obtained by conventional premixed solvents and the results were comparable with respect to accuracy, total analysis time, resolution of the least resolved solute pair, and the overall quality of the separation.

The verification of the multivariate optimization is demonstrated in two independent studies for the separation of isomeric polynuclear aromatic hydrocarbons (PAH). In the first study, mobile and stationary phases are optimized simultaneously. By measuring solute retention times at various aqueous compositions of methanol and acetonitrile on both Octadecylsilica and β-cyclodextrinsilica stationary phases, the optimum combination of stationary phases and mobile phase was predicted by the computer program. Under these optimum conditions, all solutes were predicted to be baseline resolved (Resolution = 1.5), except for two solutes with resolution of 0.88. The experimental retention time and peak width for each solute agreed well with the predicted values, with an average error of ±3.5% for retention time and ±21% for peak width.

In the second study, temperature and mobile phase were optimized simultaneously. By measuring retention times of PAHs at 23, 35, 40, and 45°C on polymeric octadecylsilica stationary phase using mobile phases of pure methanol and acetonitrile, the optimum conditions of temperature and mobile phase were predicted. Under these optimum conditions, the experimental chromatogram shows excellent separation of all PAH standards with average relative errors of 0.9% and ±16%, in predicted retention times and peak withs, respectively. Based on these results, the parametric modulation approach appears to be a powerful and versatile strategy for the multivariate optimization of chromatographic separations.

This dissertation is dedicated to my family for their unconditional love and support

ACKNOWLEDGEMENT

I would like to express my sincere thanks and gratitude to my advisor, Dr. Victoria L. McGuffin for her guidance and direction through out the course of my graduate study. I would also like to thank the members of my committee; Dr. Stan Crouch, Dr. Ned Jackson, Dr. Carl Lira and for their critical evaluation and helpful feedback about my work.

This work would not have been fun without the many discussions and words of encouragement from my colleagues in the laboratory including, Dr. Jon Wahl, Dr. Marina Tavares, Daniel Hopkins, Dr. Chris Evans, Dr. Shu Hui Chen, John Jugde, Dr. Peiru Wu, and Chomin Lee. My thanks go especially to Dr. Jon Wahl and Dr. Thomas Atkinson for making the transition to computer optimization less tasking.

I wish to send a special message of thanks to Helen, for her hospitality toward me and my family. To my friends, at Fourah Bay College, especially Maada King, Munir and Leo for the wonderful companionship during rough times.

I owe my accomplishments to my lovely wife and son; Adjoa and Aruna, for their encouragement and for being there for me during the course of this work. To the rest of the Lukulay family, in Potoru and Freetown, especially by parents and Bra sheku, I say *Be Seah*.

Finally, I thank the almighty God for his blessing and protection through out the course of my academic and social development.

TABLE OF CONTENTS

	LIST OF TABLES	xi
	LIST OF FIGURES	xiii
CHAPTER 1	FUNDAMENTAL CONSIDERATION OF LIQUID CHROMATOGRAPHIC SEPARATIONS AND THEIR OPTIMIZATION	
	1.1 Introduction	1
	1.2 Modes of Liquid Chromatography Adsorption Partition Ion Exchange Size Exclusion	3
	1.3 Partition Theory of Solute Retention Solubility Parameter Model Solvophobic Model Lattice Model	5
	1.4 Optimization Procedures Simultaneous Method Sequential Method Regression Method Theoretical Method	11
	1.5 Univariate Optimization Mobile Phase Composition Stationary Phase Composition Temperature Other Parameters	25
	1.6 Multivariate Optimization Multiple Mobile Phase Parameters Mobile and Stationary Phases Mobile Phase Composition and Temperature Temperature and Flow Rate	31
	1.7 Conclusion	38
	1.8 References	42

CHAPTER 2 THEORY OF PARAMETRIC MODULATION

2.1 Theoretical Development 48
Theory of Solute Retention
Theory of Solute Band Broadening
Theory of Solvent Zone Broadening

2.2 Optimization Strategy 55

2.3 Conclusion 62

2.4 References 64

CHAPTER 3 UNIVARIATE OPTIMIZATION OF MOBILE PHASE BY SOLVENT MODULATION

3.1 Introduction 65

3.2 Theoretical Concept and Optimization Strategies 65
Premixed Mobile Phases
Solvent Modulation

3.3 Experimental Methods 69
Experimental System
Materials and Methods
Computer-Assisted Optimization Programs

3.4 Results and Discussion 73
Premixed Solvents
Solvent Modulation

3.5 Conclusion 95

3.6 References 96

CHAPTER 4 MULTIVARIATE OPTIMIZATION OF MOBILE AND STATIONARY PHASES BY SOLVENT MODULATION ON SERIALLY COUPLED COLUMNS

4.1 Introduction 97

4.2 Theoretical Development 97

4.3 Experimental Methods 99
Materials and Methods
Experimental System
Computer-Assisted Optimization Program

4.4 Results and Discussion 102

4.4 Results and Discussion 102

4.5 Conclusion 136

4.6 References 137

CHAPTER 5 MULTIVARIATE OPTIMIZATION OF MOBILE PHASE AND TEMPERATURE BY PARAMETRIC MODULATION

5.1 Introduction 138

5.2 Theoretical Development 138

5.3 Experimental Methods 142
Materials and Methods
Experimetal System
Computer-Assisted Optimization Program

5.4 Results and Discussion 145

5.5 Conclusion 170

5.6 References 171

CHAPTER 6 EXPERIMENTAL AND COMPUTER SIMULATION STUDIES OF SOLUTE-SOLUTE INTERACTIONS IN LIQUID CHROMATOGRAPHY

6.1 Introduction 172

6.2 Experimental Methods 175
Materials and Methods
Experimental System
Molecular Mechanics and Dynamics Simulations

6.3 Results 180
Experimental Studies
Computer Simulation Studies

6.4 Discussion 208

6.5 Conclusion 210

6.6 References 211

CHAPTER 7 SUMMARY AND FUTURE WORK

7.1 Summary 214

7.2 Future Work 217

7.3 References 219

APPENDIX 1 COMPUTER PROGRAM

A1.1 Program Description 220

A1.2 Optimization Program
Program name: paramod1.for 224

A1.3 References 236

LIST OF TABLES

Table 3.1 Capacity Factors for Corticosteroids on Octadecylsilica Stationary Phase using Methanol and Acetonitrile Mobile Phases. 74

Table 3.2 Comparison of Experimental and Theoretical Capacity Factors under the Predicted Optimum Conditions for Premixed Mobile Phases. 82

Table 3.3 Evaluation of the Permutations for a Two-Solvent Modulation Sequence. 84

Table 3.4 Comparison of Experimental and Theoretical Capacity Factors under the Predicted Optimum Conditions for Solvent Modulation. 94

Table 4.1 Capacity factors (k_{ijp}) for polynuclear aromatic hydrocarbons on octadecylsilica stationary phase using aqueous methanol and acetonitrile mobile phases. 105

Table 4.2 Capacity factors (k_{ijp}) for polynuclear aromatic hydrocarbons on β-cyclodextrinsilica stationary phase using aqueous methanol and acetonitrile mobile phases. 106

Table 4.3 Evaluation of the permutations of a two-column/two-solvent chromatographic system for the separation of polynuclear aromatic hydrocarbons. The columns are octadecylsilica (ODS) and β-cyclodextrinsilica (β-CD); the solvents are aqueous mixtures of methanol (CH_3OH) and acetonitrile (CH_3CN) as given in Tables 4.1 and 4.2. The analysis time (t_f), minimum resolution ($(R_{i,i+1})_{min}$) and minimum Chromatographic Resolution Statistic (CRS_{min}) function corresponding to the optimum conditions are given. 108

Table 4.4 Evaluation of the permutations of a two-column/two-solvent chromatographic system for the separation of polynuclear aromatic hydrocarbons. The columns are octadecylsilica (ODS) and β-cyclodextrinsilica (β-CD); the solvents are aqueous mixtures of methanol (CH_3OH) and acetonitrile (CH_3CN) as given in Tables 4.1 and 4.2. The analysis time (t_f), minimum resolution ($(R_{i,i+1})_{min}$) and minimum Chromatographic Resolution Statistic (CRS_{min}) function corresponding to the optimum conditions are given, when analysis time is not considered to be a goal of the optimization. 110

Table 4.5 Comparison of experimental (EXPT) and theoretical (THEORY) retention time and peak width under the predicted optimum conditions illustrated in Figures 4.7 and 4.8. 134

Table 5.1 Capacity factors (k_{ijp}) for polynuclear aromatic hydrocarbons on polymeric octadecylsilica stationary phase obtained at different temperatures using 100% methanol as mobile phase. 152

Table 5.2 Capacity factors (k_{ijp}) for polynuclear aromatic hydrocarbons on polymeric octadecylsilica stationary phase obtained at different temperatures using 100% acetonitrile as mobile phase. 153

Table 5.3 Evaluation of the selected permutations of a two-temperature/one-solvent and two-temperature/two-solvent chromatographic system for the separation of polynuclear aromtic hydrocarbons. The column is polymeric octadecylsilica; the solvents are 100% methanol and acetonitrile as given in Tables 5.1 and 5.2. The analysis time (t_f), minimum resolution ($(R_{i,i+1})_{min}$) and minimum hromatogrphic Resolution Statistic (CRS_{min}) function correponding to the optimum conditions are given. 159

Table 5.4 Comparison of experimental (EXPT) and theoretical (Theory) retention time and peak width under the predicted optimum conditions illustrated in Figures 5.7 and 5.8. 169

Table 6.1 Comparison of the chromatographic figures of merit for corticosteroids analyzed individually and in mixtures. Experimental conditions as given in Figure 6.2. 185

Table 6.2 Total energy (E) and the components of van der Waals energy (E_{vdw}), electrostatic energy (E_Q), and hydrogen bonding energy (E_{hb}) at infinite separation distance (∞) and at the optimum separation distance (opt) for the pairwise configurations of corticosteroids shown in Figures 6.4A to 6.4C. 199

Table 6.3 Total energy (E) and the components of van der Waals energy (E_{vdw}), electrostatic energy (E_Q), and hydrogen bonding energy (E_{hb}) at infinite separation distance (∞) and at the optimum separation distance (opt) for the pairwise configurations of corticosteroids shown in Figures 6.5A to 6.5C. 207

LIST OF FIGURES

Figure 1.1 The sequential method of optimization for two parameters using the simplex approach. The initial simplex is comprised of vertices 1, 2, and 3. The vertex with worst response is identified, then replaced by projection through the midpoint of the remaining vertices. The simplex eventually converges at the optimum, which is located in the vicinity of vertex 6 in this example. 17

Figure 1.2 The regression method of optimization for one parameter using the window diagram approach. The resolution or other quality criterion is calculated by regression for each solute pair. the shaded window regions represent the limiting resolution of the least-resolved solute pair. The optimum is located at the highest point in the highest window, which is approximately 0.8 for parameter 1 in this example. 21

Figure 1.3 The regression method of optimization for two parameters using the overlapping resolution mapping approach. The resolution or other quality criterion is calculated by regression for each solute pair. The regions with resolution less than a threshold value (e.g., $R_{i,i+1}$ = 1.5) are shaded. The optimum is located by overlapping the maps for all solute pairs, which is approximately 0.7 for parameter 1 and 0.6 for parameter 2 in this example. 24

Figure 1.4 Schematic illustration of the parametric modulation concept for n solvent zones in q serially coupled columns. 40

Figure 2.1 Schematic illustration of solvent zone broadening ($1 - \xi$ = 0.95). 54

Figure 2.2 Effect of solvent zone length on zone purity according to Equations (3.12) to (3.14). (A) Constant particle diameter (5 µm) with varying column lengths of 10 cm (—), 25 cm (–), and 100 cm (-). (B) Constant column length (25 cm) and varying particle diameters of 3 µm (—), 5 µm (–), and 10 µm (-). 57

Figure 3.1 Structure of corticosteroids. 71

Figure 3.2 Critical resolution as a function of the mobile phase composition for aqueous acetonitrile mixtures. Column: 47 × 0.46 cm i.d., packed with octadecylsilica material. Solutes: (1) prednisone, (2) cortisone, (3) prednisolone, (4) hydrocortisone, (5) dehydrocorticosterone, (6) methylprednisolone, (7) tetrahydrocortisol, (8) tetrahydrocortisone. 77

Figure 3.3 Critical resolution as a function of the mobile phase composition for aqueous methanol mixtures. Experimental conditions as given in Figure 3.2. 79

Figure 3.4 Experimental chromatogram of corticosteroids obtained under the predicted optimum conditions for premixed mobile phases. Column: 47 × 0.46 cm i.d., packed with octadecylsilica material. Mobile phase: 56% methanol, 0.5 mL/min. Detector: UV-visible absorbance detector, 240 nm, 0.005 AUFS. Solutes: (1) prednisone, (2) cortisone, (3) prednisolone, (4) hydrocortisone, (5) dehydrocorticosterone, (6) methylprednisolone, (7) tetrahydrocortisol, (8) tetrahydrocortisone. 81

Figure 3.5 Separation of corticosteroids in individual mobile phases for solvent modulation. Mobile phase: (A) 60% methanol, (B) 35% acetonitrile, 0.5 mL/min. All other experimental conditions as given in Figure 3.4. 86

Figure 3.6 Topographic (A) and contour (B) maps of the CRS response surface as a function of the fractional zone lengths for 35% acetonitrile and 60% methanol. 88

Figure 3.7 Experimental chromatogram of corticosteroids obtained under the predicted optimum conditions for solvent modulation. Mobile phase: solvent modulation sequence of 35% acetonitrile and 60% methanol in fractional zone lengths of 0.4 and 4.8, respectively, 0.5 mL/min. All other experimental conditions as given in Figure 3.4. 93

Figure 4.1 Structures of isomeric four- and five-ring polynuclear aromatic hydrocarbons. 104

Figure 4.2 Topographic (A) and contour (B) maps of the CRS response surface as a function of the column length (cm) for octadecylsilica and β-cyclodextrinsilica. 112

Figure 4.3 Topographic (A) and contour (B) maps of the CRS response surface as a function of the solvent zone length (cm) for 80% methanol and 50% acetonitrile. 116

Figure 4.4 Predicted chromatogram for the isomeric PAH with a 75 cm octadecylsilica column using the optimal solvent modulation sequence of 80% methanol and 50% acetonitrile in zones of 167 and 318 cm length, respectively. Solutes: (1) pyrene, (2) triphenylene, (3) benzo[c]phenanthrene, (4) chrysene, (5) benz[a]anthracene, (6) benzo[e]pyrene, (7) perylene, (8) benzo[a]pyrene, (9) dibenz[a,c]anthracene, (10) dibenz[a,h]anthracene. 121

Figure 4.5 Topographic (A) and contour (B) maps of the CRS response surface as a function of the column length (cm) for octadecylsilica and β-cyclodextrinsilica. 123

Figure 4.6 Topographic (A) and contour (B) maps of the CRS response surface as a function of the solvent zone length (cm) for 70% acetonitrile and 80% methanol. 127

Figure 4.7 Predicted chromatogram for the isomeric PAH with a 75 cm octadecylsilica column using the optimal solvent modulation sequence of 70% acetonitrile and 80% methanol in zones of 203 and 634 cm length, respectively. Solutes as given in Figure 4.4. 132

Figure 4.8 Experimental chromatogram obtained under the predicted optimum conditions. Column: 200 µm I.D. x 75 cm fused silica capillary, packed with 5 µm octadecylsilica. Mobile phase: solvent modulation sequence of 70% acetonitrile and 80% methanol in zones of 203 and 634 cm length, respectively, 0.95 µL/min. Detectors: (A) UV-visible absorbance at 254 nm to indicate solvent modulation sequence, (B) Laser-induced fluorescence with excitation at 325 nm and emission at 420 nm to indicate solute retention. Solutes: (0) injection solvent, (1) pyrene, (2) triphenylene, (3) benzo[c]phenanthrene, (4) chrysene, (5) benz[a]anthracene, (6) benzo[e]pyrene, (7) perylene, (8) benzo[a]pyrene, (9) dibenz[a,c]anthracene, (10) dibenz[a,h]anthracene. 134

Figure 5.1 Schematic illustration of the parametric modulation concept for the simultaneous optimization of mobile phase and temperature. 140

Figure 5.2 Structure of polynuclear aromatic hydrocarbons. 148

Figure 5.3 Effect of temperature on the selectivity of polynuclear aromatic hydrocarbons using 100% methanol as mobile phase. Experimental conditions as given in Figure 5.3. Solutes: (1) Benzo[c]phenanthrene, (2) pyrene, (3) phenanthrophenanthrene, (4) benz[a]anthracene, (5) tetrabenzonaphthacene, (6) chrysene, (7) benzo[e]pyrene, (8) perylene, (9) benzo[a]pyrene. 151

Figure 5.4 Effect of temperature on logarithm of capacity factor for polynuclear aromatic hydrocarbons using 100% methanol as mobile phase at 1.2 µL/min. Column: 200 mm I.D. x 75 cm fused silica capillary, packed with 5.5 mm polymeric octadecylsilica. Detector: Laser-induced fluorescence with excitation at 325 nm and emission at 420 nm. Solutes: (Δ) benzo[c]phenanthrene, (●) pyrene, (❑) phenanthrophenanthrene, (▲) benz[a]anthracene, (◊) tetrabenzonaphthacene, (■) chrysene, (O) benzo[e]pyrene, (♦) perylene, (∇) benzo[a]pyrene. 155

Figure 5.5 Effect of temperature on logarithm of capacity factor for polynuclear aromatic hydrocarbons using 100% acetonitrile

as mobile phase at 1.2 µL/min. Experimetal conditions and solutes as given in Figure 5.3. 157

Figure 5.6 Topographic map (A) and contour map (B) of the CRS response surface as a function of the column length (cm) at temperatures 23° C (Temp. 1) and 40° C (Temp. 2). 162

Figure 5.7 Predicted chromatogram for the polynuclear aromatic hydrocarbons on polymeric octadecylsilica column using the optimal conditions of 5 cm of column maintained at 23° C and 85 cm maintained at 40° C; using 100% methanol as the mobile phase. Solutes: (1) benzo[c]phenanthrene, (2) pyrene, (3) phenanthrophenanthrene, (4) benz[a]anthracene, (5) tetrabenzonaphthacene, (6) chrysene, (7) benzo[e]pyrene, (8) perylene, (9) benzo[a]pyrene. 166

Figure 5.8 Experimental chromatogram obtained under the predicted optimum conditions. Column: 200 mm I.D. x 75 cm fused silica capillary, packed with 5.5 mm polymeric octadecylsilica. Mobile phase: 100% methanol at 1.2 µL/min. Detector: Laser-induced fluorescence with excitation at 325 nm and emission at 420 nm. Solutes as given in Figure 5.7. 168

Figure 6.1 Structures of corticosteroids. 177

Figure 6.2 Chromatograms of corticosteroids analyzed individually and in mixtures. Column: 47 x 0.46 cm i.d., packed with 5-µm octadecylsilica material. Mobile phase: 35% aqueous acetonitrile; 0.5 mL/min. Detector: UV–VIS absorbance detector (240 nm, 0.005 AUFS). Solutes: (A) cortisone (10^{-6} M), (B) tetrahydrocortisol (10^{-3} M), (C) mixture of cortisone and tetrahydrocortisol. 182

Figure 6.3 Chromatograms of corticosteroids analyzed individually and in mixtures. Solute: (A) methylprednisolone (10^{-6} M), (B) tetrahydrocortisone (10^{-3} M), (C) mixture of methylprednisolone and tetrahydrocortisone. Experimental conditions as given in Figure 2. 188

Figure 6.4 The optimum configuration for interaction between (A) two cortisone molecules, (B) two tetrahydrocortisol molecules and (C) cortisone and tetrahydrocortisol. (O) carbon, (o) hydrogen, (●) oxygen, (- - -) nonbonding atoms that meet the defined energy and distance constraints for hydrogen bonds according to Equation [6.3]. 193

Figure 6.5 The optimum configuration for interaction between (A) two methylprednisolone molecules, (B) two tetrahydrocortisone molecules, and (C) methylprednisolone and tetrahydrocortisone molecules. (O) carbon, (o) hydrogen, (●) oxygen, (- - -) nonbonding atoms that meet

the defined energy and distance constraints for hydrogen bonds according to Equation [6.3]. 202

Figure A1.1 A flow chart of the computer program used to optimize chromatographic parameters by the parametric modulation method. 222

CHAPTER 1

FUNDAMENTAL CONSIDERATION OF LIQUID CHROMATOGRAPHIC SEPARATIONS AND THEIR OPTIMIZATION

1.1 Introduction

Chromatography is a separation technique in which molecules or ions are distributed between two immiscible phases, one of which is stationary and the other mobile. Because the molecules or ions are distributed between the two phases to different extents, they migrate at different velocities, thus leading to their separation. The goal of any chromatographic technique is to achieve maximum separation of all the components in their mixture. The degree of separation between any two solutes, known as the resolution, is governed by two independent processes, namely solute retention and band broadening. The functional relationship between resolution and these two processes is given by (1)

$$R_{i,i+1} = \frac{2\ (t_{i+1} - t_i)}{(w_{i+1} + w_i)} \qquad [1.1]$$

where t represents the retention time, and w represents the band widths of adjacent solutes i, i+1. The retention time is controlled mainly by thermodynamic processes, whereas the band width is controlled by kinetic processes such as the rate of diffusion and mass transfer processes. The above resolution equation

can be expressed in terms of fundamental parameters of the chromatographic process. It can be shown (1) that for symmetrical Gaussian peaks, Equation [1.1] can be represented in a useful form as shown below

$$R_S = \frac{N^{1/2}}{4} \left(\frac{\alpha - 1}{\alpha} \right) \left(\frac{k'}{1 + k'} \right) \qquad [1.2]$$

where N is the number of theoretical plates, k' is the average capacity factor, and α is the selectivity factor. The capacity factor is a thermodynamic measure of retention and is given by

$$k = \frac{t_i - t_o}{t_o} \qquad [1.3]$$

where t_i and t_o are the elution time of a retained and unretained solute, respectively. The selectivity factor is the ratio of capacity factors of two adjacent solutes expressed as k_{i+1} / k_i such that $\alpha \geq 1$.

Optimization of resolution can generally be achieved by optimizing each term in the resolution equation separately. For a given stationary phase, the selectivity and capacity factor are generally optimized by controlling the type and composition of organic modifier in aqueous solution, respectively. The plate number is be optimized by changing column length, column diameter, and particle size. Of the three terms, selectivity has the greatest influence on resolution (2). Thus, chromatographic optimization is readily achieved by optimizing selectivity. In order to influence solute selectivity, an understanding of the different modes of liquid chromatography and the model of solute retention are necessary. In this introductory chapter, the various modes of liquid chromatography are presented, followed by a discussion of the various theories

which have been proposed to describe the partition model of solute retention. Also, a review of current methods of univariate and multivariate optimization is presented. Then, a novel strategy for univariate and multivariate optimization called parametric modulation is introduced and the advantages over current optimization methods are discussed.

1.2 Modes of Liquid Chromatography

Retention in liquid chromatography is thought to occur by different mechanisms. These different mechanisms give rise to the different types of liquid chromatographic methods.

Adsorption. Separations by an adsorption mechanism result largely from the attraction of polar functional groups on the solute to discrete adsorption sites on the surface of the stationary phase. The strength of these polar interactions determine solute retention and selectivity. The type of chromatography in which adsorption is the predominant retention mode is known as adsorption chromatography or liquid-solid chromatography. It involves the use of polar stationary phases with relatively nonpolar mobile phases. Silica gel is the most widely used adsorbent (1), although alumina, clay, diatomaceous earth, charcoal and other solids have also been used. The adsorption characteristics of silica gel and alumina are due predominantly to surface hydroxyl groups which provide their polar surface. Additionally, these surfaces are known to have one or more layers of adsorbed water molecules. Thus, the activity of the surface depends not only on the number and orientation of the hydroxyl groups but also on the amount of adsorbed water (3).

Partition. Partition is a separation mechanism in which solute molecules are distributed between the two immiscible liquid phases, similar to liquid-liquid extraction. Thus, unlike adsorption, the partition process involves interaction of the solute with the bulk mobile and stationary phases (1,4). The type of chromatography where partition is the predominant mode of retention is called liquid-liquid chromatography. This is divided into two categories: normal-phase chromatography where the stationary phase is more polar than the mobile phase, and reversed-phase chromatography where the mobile phase is more polar than the stationary phase. For normal phase separations, typical stationary phases are χψανοπροπψλσιλιχα ανδ αμινοπροπψλσιλιχα, whereas for reversed phase stationary phases separations, typical include octylsilica (C8) and octadecylsilica (C18). Retention by a partition mode is highly suited for the separation of homologues and oligomers. Various theories have been proposed to explain the partition mode of solute retention and these are discussed in Section (1.3).

Ion Exchange. The ion-exchange mechanism involves the dynamic interaction of charged solutes with the stationary phase. The stationary phase is characterized by the presence of a weak or strong acid or base bearing exchangeable counter ions. In this mode of chromatography, sample ions in the mobile phase compete with the counter ions for sites (S) on the stationary phase

$$A^- + S^+B^- \leftrightarrow B^+ + S^+A^- \quad \text{(Anion exchange)}$$

$$C^+ + S^-B^+ \leftrightarrow B^+ + S^-C^+ \quad \text{(Cation exchange)}$$

Retention in ion exchange is governed by the extent to which the ions compete with B for the charged sites. Thus, selectivity is obtained for ionic species such

as organic acids and bases with different ionization constants. An important parameter used to control selectivity is pH of the mobile phase (5,6). In addition to the ion-exchange mechanism, it is argued that retention in ion-exchange chromatography also occurs by partitioning (3) and ion-pairing (7,8) mechanisms. In ion pairing, solutes form an ion-pair with a counter ion and partition into the stationary phase which is often an organic polymeric support. The formation of the ion-pair increases the lipophilic character of the solute and increases its affinity for the stationary phase. The true mechanism is controversial and it is suggested that it may be a convolution of the two mechanisms discussed (8).

Size Exclusion. In size exclusion, the column packing is a porous material with uniform size distribution. Molecules that are too large are excluded from all the pores, where small molecules can penetrate most of the pores. Consequently, small molecules are retained longer than large molecules. Separation by this mode is governed mainly by molecular size (9). Additionally, size exclusion may occur in restricted cavities, such a cyclodextrins and crown ethers. Retention in these cavities is thought to occur by inclusion complexation; thus solute retention is driven mainly by entropic rather than enthalpic interaction with the restricted cavity.

1.3 Partition Theory of Solute Retention

Since solute retention in reversed-phase liquid chromatography is thought to occur mainly by a partition mechanism (1), the various theories advanced for this mode of chromatography are discussed. These theories provide an insight

into the important parameters which must be controlled in order to optimize chromatographic retention and selectivity.

The theoretical models can be divided into two categories, classical thermodynamic treatments and statistical thermodynamic treatments. The classical thermodynamic models include the Hildebrand solubility parameter (10,11) and the solvophobic theory of Horvath and co-workers (12,13). The statistical thermodynamic models include the lattice model by Martire, Boehm and Dill (14-16)

Solubility Parameter Model. The concept of solubility parameter arises from the regular solution theory of Hildebrand and Scott (10). This theory defines the square root of the cohesive energy density of a pure liquid as the solubility parameter (δ), which is characteristic of its polarity.

$$\delta = (-E/v_i)^{1/2} \qquad [1.4]$$

where E is the cohesive energy required to transfer one mole of the substance from the ideal gas state into its liquid state and v_i is the molar volume of the liquid. While the model in its original form considered only dispersive interactions (δ_d), it has been extended to include other types of molecular interactions such as permanent dipole orientation (δ_o), dipole induction (δ_{ind}), and hydrogen bonding interactions of acidic (δ_a) and basic nature (δ_b). By assuming that these interactions are independent of one another, the overall solubility parameter can be expressed as

$$\delta^2 = \delta_d^2 + \delta_p^2 + \delta_h^2 \qquad [1.5]$$

where the polar (δ_p) and the hydrogen bonding (δ_h) components are defined as

$$\delta_p^2 = \delta_o^2 + 2\delta_{ind}\delta_d \qquad [1.6]$$

$$\delta_h^2 = 2\delta_a\delta_b \qquad [1.7]$$

Thus, the magnitude of the solubility parameter is a measure of the overall polarity or strength of the solvent, with non-polar solvents having low δ values (around 7 $cal^{1/2}\ cm^{-3/2}$) and polar solvents having high δ values (around 10 $cal^{1/2}\ cm^{-3/2}$).

The solubility parameter can be extended to mixed solvent systems and is expressed as the arithmetic sum of the individual solubility parameters weighted according to their volume fraction (ϕ) in the mixture.

$$\delta = \Sigma\, \phi_j\, \delta_j \qquad [1.8]$$

According to the regular solution theory, the activity coefficient (γ) for solute (i) dissolved in solvent (j) is related to the individual solubility parameters by the following equation

$$RT \ln \gamma_i = v_i\, (\delta_i - \delta_j)^2 \qquad [1.9]$$

where v_i is the molar volume of the solute and is presumed identical to the solvent at infinite dilution, R is the gas constant, and T is the absolute temperature. The capacity factor of the solute (k) is related to the distribution constant (K), which in turn is mathematically related to the ratio of solute activity coefficient in the mobile and stationary phases (11).

$$\ln k_i = \ln\left(\frac{K_i}{\beta}\right) = \frac{v_i}{RT}\left[(\delta_i - \delta_M)^2 - (\delta_i - \delta_S)^2\right] - \ln\beta \qquad [1.10]$$

Thus, solute retention is a function of the solubility parameters of the solute (δ_i), the mobile phase (δ_M), and the stationary phase (δ_S) as well as the volume ratio of the mobile and stationary phases (β). According to Equation [1.10], separation is most favorable when the difference in solubility parameter of the mobile and stationary phases is greatest.

If the solubility parameter model accounts for all solute-solvent and solvent-solvent interactions, then a quadratic relationship should exist between the logarithm of the capacity factor and the volume fraction of one component in the mobile phase. This quadratic relationship is obtained by combining Equations [1.9] and [1.10] for a simple binary mobile-phase mixture of component 1 and 2, and expressing the result as a function of the volume fraction (ϕ_1)

$$\ln k_i = A_o + A_1\phi_1 + A_{11}\phi_1^2 \qquad [1.11]$$

where the coefficients are equivalent to

$$A_o = \frac{v_i}{RT}\left[(\delta_i - \delta_2)^2 - (\delta_i - \delta_s)^2\right] - \ln\beta$$

$$A_1 = \frac{v_i}{RT}\left[(\delta_i - \delta_1)^2 - (\delta_i - \delta_2)^2 - (\delta_1 - \delta_2)^2\right]$$

$$A_{11} = \frac{v_i}{RT}(\delta_1 - \delta_2)^2$$

Generally, the predictive value of the model is only qualitative or semi-quantitative at best. This limitation arises from the assumptions inherent in the model (11). First, Equation [1.8] assumes that solvent-solvent interactions are negligible, and thus each solute is assumed to interact independently with each solvent component in a mixture. Secondly, the solute and mobile phase solvent are randomly mixed, thus neglecting clustering which may be significant in polar solvents. More importantly, the model assumes that the stationary phase is isotropic and independent of the mobile phase composition. In view of these assumptions, the solubility parameter model may not always adequately represent molecular interactions in mixed solvents.

Solvophobic Theory. The solvophobic theory developed by Horvath and co-workers (12,13) is derived from the solvophobic theory of Sinanoglu (17). Unlike the solubility parameter model, the solvophobic theory emphasizes the importance of only the mobile phase in the retention of solutes. According to this theory, the driving force for solute retention is the repulsion of solute from the more polar mobile phase, rather than attraction between solute and stationary phase. Thus, this theory propounds that solute retention is a passive process rather than an active process. Horvath *et al.* (12,13) have carried out a detailed theoretical analysis of the factors responsible for solute retention in liquid chromatography using the solvophobic theory. They characterize the solvophobic strength of the eluent by its physical properties, among which the surface tension plays the dominant role. This model is successful in predicting trends in retention upon changes in mobile phase composition and upon altering certain molecular properties of the solute, principally its size. However, the

model is incomplete because it does not provide a detailed explanation of the dependence of retention on stationary phase variables (18). Cole and Dorsey (18) have observed that stationary phase bonding density plays a significant role in the retention mechanism of reversed-phase chromatography. Consequently, they concluded that the stationary phase must be considered in order to accurately describe the retention process.

Lattice Model. The lattice model is a statistical thermodynamic model developed by Martire and Boehm to describe retention and selectivity in liquid chromatography (14-16). Unlike the solvophobic theory, this model emphasizes the role of the mobile phase as well as the stationary phase in solute retention and selectivity. It is based on the competitive equilibrium at the molecular level among solute and solvent molecules distributed between non-ideal mobile and stationary phases. In the general form of the model, the stationary phase is considered as a heterogeneous planar surface containing many types of chemically or energetically different adsorption sites. Solute retention is considered in terms of both enthalpic and entropic contributions in the mobile and stationary phases. The partition coefficient (K) may be computed from the chemical potentials of the solute S in the mobile phase mixture of components A and B and in the stationary phase consisting of a bonded alkyl chain C (16). If A and B with relative concentrations ϕ_A and ϕ_B, respectively, are randomly mixed, then the partition coefficient is given as

$$\ln k_i = \ln \left(\frac{K}{\beta} \right) =$$

$$\left[(\chi_{SA} - \chi_{SB}) + \phi_B(\chi_{SB} - \chi_{SA} - \chi_{AB}) + \phi_B^2 \chi_{AB} \right] - \ln \beta \qquad [1.12]$$

where χ is the binary interaction parameter.

Thus, both the solubility parameter model and the lattice model predict a quadratic dependence of the logarithm of solute capacity factor on the mobile phase composition. It has been suggested (16) that this quadratic dependence can be expressed in a more convenient form for the purpose of graphing the dependence of retention on mobile phase composition

$$\left(\frac{1}{\phi_B}\right) \ln \left(\frac{k}{k_o}\right) = [(\chi_{SB} - \chi_{SA} - \chi_{AB}) + \phi_B \chi_{AB}] \qquad [1.13]$$

where k_o is the value of k when $\phi_B = 0$. By combining Equations [1.10] and [1.12], it can be shown that the solubility parameter model is related to the lattice model through the dependence of the interaction parameters and the solubility parameters (19).

$$\chi_{AB} = \text{constant } (\delta_A - \delta_B)^2 \qquad [1.14]$$

1.4 Optimization Procedures

In chromatography, optimization refers to the process of identifying the experimental conditions required to achieve the most desirable separation in the most time- and cost-effective manner. Because of the numerous experimental parameters that directly and indirectly influence chromatographic retention and band broadening, optimization is a nontrivial process and has been the subject of numerous theoretical and practical studies (1,2,20,21). In this section, a review of the present strategies for univariate optimization and their logical extension to

multivariate optimization are presented. The existing methods are described, together with recent applications, and their advantages and limitations are evaluated.

In order to determine unequivocally the most appropriate experimental conditions, a systematic approach must be adopted in the optimization process. This process consists of three distinct steps: selection of the quality criterion, selection of the experimental parameters, and selection of the method to identify the most optimal value or level of each parameter. These steps are discussed sequentially below.

The Quality Criteria. The first step involves the formulation of a criterion which is a quantitative measure of the quality of the separation. Because this criterion is used to guide the decision-making process, it must inherently define and rank the goals of the optimization. One of the most important goals in chromatography is to maximize the resolution between adjacent solutes ($R_{i,i+1}$), which may be calculated as shown in Equation [1.2]. Several quality criteria have been developed based on resolution alone, ranging from simple functions such as the limiting resolution of the least-resolved solute pair (22-24) to more complex functions such as the sum or product of the resolution for all adjacent solute pairs, without or with weighting factors (25,26). In addition to resolution, other goals have been incorporated or applied in either a simultaneous or sequential manner (20). These more complex quality criteria include the chromatographic response function (CRF) (27) and the chromatographic optimization function (COF) (28), both of which optimize resolution and analysis time. The CEF function developed by Vajda and Leisztner (29) optimizes the resolution and the number of solutes, whereas the chromatographic resolution statistic (CRS) of Schlabach and Excoffier (30) attempts to optimize resolution of

all solutes, provide uniform spacing, and minimize analysis time simultaneously. Each of these quality criteria has inherent advantages and limitations which should be considered in view of the specific application and its goals (2,20,31-34).

The Parameter Space. Next, the experimental parameters that have the greatest influence on the quality criterion are identified. These parameters may have a limited number of discrete or finite values, or they may be continuously variable within a specified range. Among the examples of chromatographic parameters that are discrete in nature are the type of mobile and stationary phases. In addition, physical dimensions such as the particle size, column diameter, and column length may be discrete if restricted to columns that are commercially available. Parameters that are continuously variable in nature include the composition of the mobile and stationary phases, as well as the temperature, pressure, and flow rate. The proper selection of these parameters is crucial, since the success of any optimization strategy is dependent exclusively upon them. It is, therefore, assumed that all experimental factors not explicitly chosen as parameters will be held constant during the optimization.

Depending upon the number and nature of the parameters, the relationship with the quality criterion can be represented by individual point(s), by line(s) in two-dimensional space, by plane(s) in three-dimensional space, or by higher-order surface(s) in N-dimensional space. For simplicity in the subsequent discussion, the relationship between the parameter(s) and the quality criterion will be referred to as the response surface, regardless of its continuity and dimensionality.

The Optimization Method. Once the quality criterion and the experimental parameters are chosen, a logical procedure must be used to locate the optimum value of the criterion on the response surface. Because the response surface may be highly complex, with many local minima and maxima, this procedure must be sufficiently robust and reliable to locate the primary or global optimum rather than secondary or local optima. The procedures that have been adopted to locate the optimum can be classified into four categories, as described below.

Simultaneous Method Simultaneous methods are those in which all of the parameters to be varied, as well as their levels, are chosen *a priori*. Experimental data are acquired at each level for each of the parameters chosen. The optimum is then identified by the experimental conditions that yield the best value of the quality criterion. The simultaneous method is also referred to as a grid search or mapping method, since the parameter space can be likened to a grid or framework of experimental conditions, generally spaced in uniform increments. The number of experiments to be performed depends on the number of the parameters and their levels (2); for n parameters at q levels, the number of experiments is q^n. In order to describe the response surface completely and accurately, each parameter must be examined over a wide range in small increments of the level. However, this may require a prohibitively large number of experiments. In order to reduce the number of experiments, constrained parameters may be chosen to reduce the degrees of freedom of the parameter space. A constrained parameter is one in which the sum of the levels is constrained to a constant value; for example, the sum of the volume fractions of the mobile phase solvents is unity. Another approach to reduce the number of experiments is through experimental design, common examples of which are the factorial and star design methods (35,36).

Because of the inherent nature of simultaneous methods, they are most suitable for parameters that are discrete and independent. An advantage of these methods is that they do not require or rely on a theoretical or mathematical model to locate the optimum. These methods can be used to elucidate the complete response surface if the parameter levels are varied over a wide range in small increments. Thus, it is possible in principle to identify the global optimum in the presence of other local optima. The most significant disadvantage is that the number of experiments increases rapidly with the number of parameters and their levels.

Sequential Method In the sequential method, a few initial experiments are performed at selected levels of the parameter(s) and the results are used to direct and guide subsequent experiments. The success of this method is highly dependent upon the type of quality criterion and the type of search routine used to locate the optimum. A variety of search routines have been developed (36,37), the most common of which is the simplex routine (38-43). A simplex is a geometric figure that consist of N+1 vertices in N-dimensional space; for example, a two-dimensional simplex is a triangle. To illustrate the search procedure, consider the response surface shown as a contour diagram in Figure 1.1 The vertices 1, 2, and 3 define the initial simplex and represent the initial levels of the parameters at which an experiment is performed. The results of these experiments are then compared by means of the quality criterion; in this example, vertex 2 has the worst response. Consequently, the simplex routine replaces this vertex with one obtained by reflection through the midpoint of the line connecting vertices 1 and 3. The simplex is now described by vertices 1, 3, and 4. An experiment is performed at the new vertex 4, and the quality criterion is compared to that obtained previously at vertices 1 and 3. Vertex 1 now has

Figure 1.1 The sequential method of optimization for two parameters using the simplex approach. The initial simplex is comprised of vertices 1, 2, and 3. The vertex with worst response is identified, then replaced by projection through the midpoint of the remaining vertices. The simplex eventually converges at the optimum, which is located in the vicinity of vertex 6 in this example.

Figure 1.1

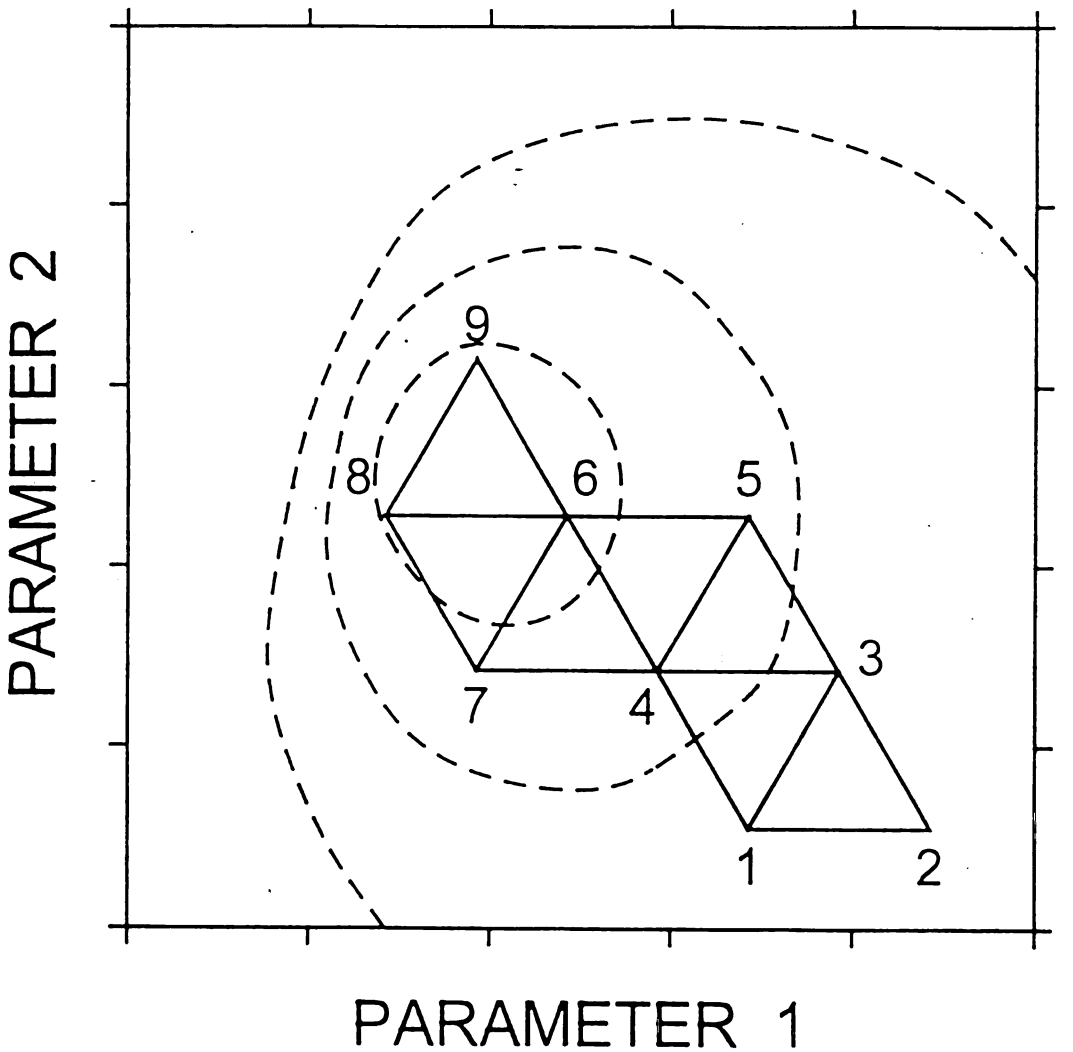

the worst response, and reflection in the opposite direction leads to vertex 5. The objective of this iterative procedure is to direct successive experiments toward more favorable regions of the response surface. This procedure is continued within the defined boundary conditions of the parameters until the optimum is obtained in the vicinity of vertex 6. In the sequential simplex method originally proposed by Spendley *et al.* (38), the vertices are equally spaced to create a simplex that is an equilateral polyhedron. Such equilateral simplexes may not readily converge, in some cases circling around the optimum or becoming stranded on a surface ridge. These limitations have been largely overcome by the modified procedure of Nelder and Mead (39), which allows for expansion of the simplex in a favorable direction and contraction in an unfavorable direction during the search procedure.

The simplex and related sequential methods are most suitable for parameters that are continuous, since an experiment must be performed at each new vertex that is calculated. An important advantage is that these methods are able to optimize several parameters simultaneously with no prior knowledge about their interaction. Additionally, these methods do not rely on any theoretical or mathematical model to identify the optimum conditions. However, the sequential procedures have some disadvantages, foremost among which is that an indeterminate number of experiments are required to locate the optimum. Moreover, for response surfaces consisting of many local maxima and minima, a local optimum may be erroneously identified as the global optimum. This problem may be circumvented by repeating the optimization procedure with the initial simplex of various sizes and in various locations on the response surface. A convergence of the simplex to the same optimum indicates that a global optimum has been found. Additionally, because the quality criterion is only evaluated at selected points, a limited insight is provided about the response

surface. Despite these potential drawbacks, sequential optimization procedures such as the simplex method are versatile with wide applicability in chromatography (40-43).

Regression Method Regression methods, otherwise known as interpretive methods, rely on the use of a semi-empirical mathematical model to describe the quality criterion as a function of the experimental parameters. In these techniques, a chromatographic property, such as capacity factor, plate number, etc., that is related to the quality criterion is measured at certain levels of the parameters. The resulting data are analyzed by the least-squares method in order to determine the best value for the coefficient(s) in the model equation. The number of experiments depends on the mathematical model; a linear model requires a minimum of two experiments, a quadratic model requires three experiments, etc. However, it is generally desirable to acquire data at additional levels of the parameter in excess of the minimum requirements in order to allow for greater statistical confidence in the results of the regression.

Once the regression coefficients have been determined, the equation may be used to calculate the chromatographic property and, hence, the quality criterion at any intermediate level of the parameter. Numerical or graphical methods may then be used to represent the response surface and to determine the most optimal value of the parameter. A well-known method of representation for a single parameter is the window diagram approach, originally developed by Laub and Purnell (44-46). As shown in Figure 1.2, the quality criterion (usually the resolution for each solute pair) is graphed as a function (usually linear) of the parameter. The regions of the graph beneath the limiting resolution for the least-resolved solute pair are shaded to create "windows". The optimum value of the parameter may then be identified from the highest point in the highest window,

Figure 1.2 The regression method of optimization for one parameter using the window diagram approach. The resolution or other quality criterion is calculated by regression for each solute pair. The shaded window regions represent the limiting resolution of the least-resolved solute pair. The optimum is located at the highest point in the highest window, which is approximately 0.8 for parameter 1 in this example.

Figure 1.2

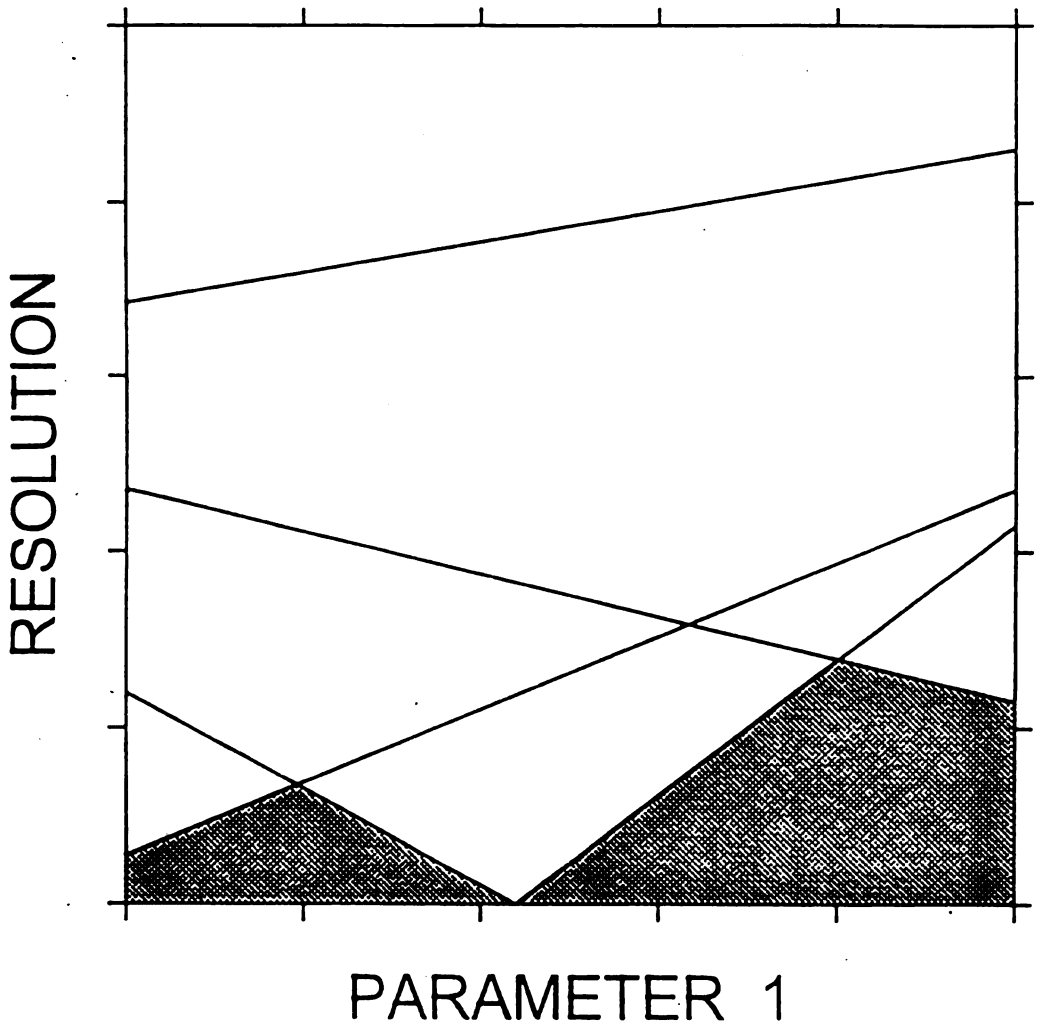

which represents the maximum value of the quality criterion. This approach may be extended to two parameters by using the overlapping resolution mapping (ORM) technique described by Glajch and Kirkland (47). In this case, the resolution of each solute pair is represented by a surface, rather than a line, and the regions of intersection must be determined in order to create the three-dimensional "windows". A simpler graphical approach, illustrated in Figure 1.3, is to shade those regions with resolution less than a selected threshold value (e.g., $R_{i,i+1} = 1.5$) for each solute pair and then overlap these maps to identify the optimum value of the two parameters. The extension of these graphical techniques to three or more parameters remains a challenging problem (48).

When compared with the simultaneous and sequential methods, the regression techniques require fewer experiments to describe the complete response surface. However, the successful application of this method is greatly reliant on the accuracy of the mathematical model. For this reason, regression methods are most appropriate for continuous parameters with a well-defined and verifiable relationship to the chromatographic property or quality criterion, such as mobile phase composition and temperature.

Theoretical Method Theoretical methods, like regression methods, use a mathematical equation to describe the effect of the parameter on a chromatographic property such as capacity factor, plate number, etc. The important distinction is that the equation is theoretically derived and requires no preliminary experimental data for implementation. This approach is most appropriate for discrete or continuous parameters that have an invariant and theoretically predictable effect, such as flow rate, column diameter, and column length. The optimal value of the parameter may be determined by any of the numerical or graphical methods discussed previously.

Figure 1.3 The regression method of optimization for two parameters using the overlapping resolution mapping approach. The resolution or other quality criterion is calculated by regression for each solute pair. The regions with resolution less than a threshold value (e.g., $R_{i,i+1}$ = 1.5) are shaded. The optimum is located by overlapping the maps for all solute pairs, which is approximately 0.7 for parameter 1 and 0.6 for parameter 2 in this example.

Figure 1.3

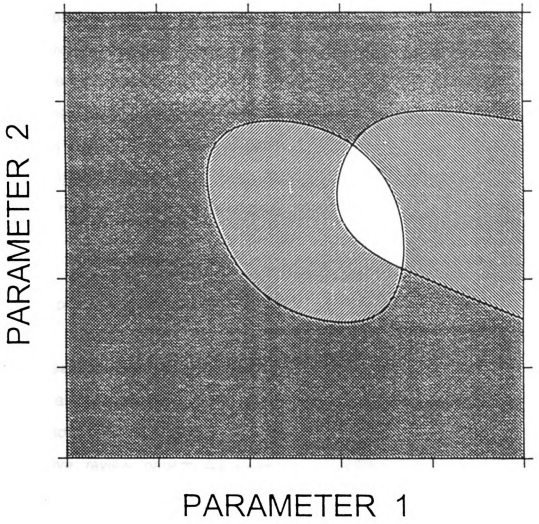

1.5 Univariate Optimization

Univariate optimization involves the optimization of a single parameter or of multiple parameters in a wholly independent manner. This is achieved by varying a given parameter to investigate its influence on the quality criterion, while all other parameters are held constant. When an optimum value for that parameter has been established, its value is held constant while the next parameter is varied to determine its own optimum value. This approach is relatively simple and is adequate for parameters that do not interact with one another, but may be problematic for mutually dependent parameters. Univariate optimization can be accomplished by any of the procedures discussed previously. In this section, the univariate optimization of important chromatographic parameters will be reviewed.

Mobile Phase Composition. The mobile phase composition is, by far, the most common parameter used for optimization in liquid chromatography (1). As such, it has already been the subject of several excellent books (1,2,20) and comprehensive review papers (26,49-51). Mobile phase optimization will generally include the type of solvent or other modifier, which influences the selectivity, as well as its concentration, which influences the strength. Because of the discrete nature of solvent or modifier type, optimization is most often performed by the simultaneous method. This approach has been utilize to select from among several organic solvents, buffers, ion pair agents, etc. (50,52,53). However, the simultaneous approach is time-consuming and ineffective to optimize solvent or modifier concentration, which is most often performed by regression methods (1).

1.5 Univariate Optimization

Univariate optimization involves the optimization of a single parameter or of multiple parameters in a wholly independent manner. This is achieved by varying a given parameter to investigate its influence on the quality criterion, while all other parameters are held constant. When an optimum value for that parameter has been established, its value is held constant while the next parameter is varied to determine its own optimum value. This approach is relatively simple and is adequate for parameters that do not interact with one another, but may be problematic for mutually dependent parameters. Univariate optimization can be accomplished by any of the procedures discussed previously. In this section, the univariate optimization of important chromatographic parameters will be reviewed.

Mobile Phase Composition. The mobile phase composition is, by far, the most common parameter used for optimization in liquid chromatography (1). As such, it has already been the subject of several excellent books (1,2,20) and comprehensive review papers (26,49-51). Mobile phase optimization will generally include the type of solvent or other modifier, which influences the selectivity, as well as its concentration, which influences the strength. Because of the discrete nature of solvent or modifier type, optimization is most often performed by the simultaneous method. This approach has been utilize to select from among several organic solvents, buffers, ion pair agents, etc. (50,52,53). However, the simultaneous approach is time-consuming and ineffective to optimize solvent or modifier concentration, which is most often performed by regression methods (1).

For normal- and reversed-phase chromatography, regression models have been developed to describe solute retention as a function of mobile phase composition. By extension of classical thermodynamics to non-interacting binary solvent mixtures, the capacity factor can be described as a quadratic function of the volume fraction ϕ_i of each component

$$\ln k = A_0 + A_1 \phi_1 + A_{11} \phi_1^2 + A_2 \phi_2 + A_{22} \phi_2^2 + A_{12} \phi_1 \phi_2 \qquad [1.15]$$

where A_i are the regression coefficients. If the volume fraction is a constrained parameter (e.g., $\phi_2 = 1 - \phi_1$), this expression can be simplified as follows (54-56)

$$\ln k = A_0 + A_1 \phi_1 + A_{11} \phi_1^2 \qquad [1.16]$$

In order to reduce the number of experiments required for optimization, this quadratic model is frequently approximated by a linear equation (50,57-63)

$$\ln k = A_0 + A_1 \phi_1 \qquad [1.17]$$

With this simplification, retention measurements at two solvent compositions are sufficient to describe the complete response surface. The linear approximation is accurate over a more limited range of solvent compositions than the quadratic model, and should not be extrapolated beyond the range of available experimental data. In addition, deviations from both linear and quadratic behavior may arise due to nonideal solute-solvent and solvent-solvent interactions, especially in polar solvents (64,65).

By extension of classical thermodynamics to non-interacting ternary solvent mixtures, the capacity factor can be described as a quadratic function of the volume fraction of each component

$$\ln k = A_0 + A_1\phi_1 + A_{11}\phi_1^2 + A_2\phi_2 + A_{22}\phi_2^2 + A_3\phi_3 + A_{33}\phi_3^2 + A_{12}\phi_1\phi_2 + A_{13}\phi_1\phi_3 + A_{23}\phi_2\phi_3 \quad [1.18]$$

If the volume fraction is a constrained parameter (e.g., $\phi_3 = 1 - \phi_1 - \phi_2$), this expression can be simplified as follows

$$\ln k = A_0 + A_1\phi_1 + A_{11}\phi_1^2 + A_2\phi_2 + A_{22}\phi_2^2 + A_{12}\phi_1\phi_2 \quad [1.19]$$

Alternatively, the semi-empirical expression proposed by Weyland *et al.* (66) can be obtained by neglect of the second-order terms in Equation [1.18] and inclusion of a term for first-order ternary solvent interactions

$$\ln k = A_0 + A_1\phi_1 + A_2\phi_2 + A_3\phi_3 + A_{12}\phi_1\phi_2 + A_{13}\phi_1\phi_3 + A_{23}\phi_2\phi_3 + A_{123}\phi_1\phi_2\phi_3 \quad [1.20]$$

This latter polynomial expression requires retention measurements at seven solvent compositions to describe the complete response surface.

The equations cited above have been widely and successfully applied for univariate optimization of mobile phase composition in normal- and reversed-phase chromatography, as well as in ion exchange, ion pair, and other chromatographic methods (1,2,20,26,49-51). Although there have been many noteworthy accomplishments, the most exemplary are those by Snyder, Dolan, *et al.* (50,59-63) for binary mobile phases and by Glajch, Kirkland, *et al.* (28,47) for ternary and quaternary mobile phases. In the latter work, a mixture-design statistical method is applied which combines the simultaneous method with regression techniques to optimize both selectivity and strength of the mobile phase. The mobile phases are chosen such that they exhibit the greatest possible difference in chemical interactions, including proton donor (methanol), proton acceptor (tetrahydrofuran), and dipole (acetonitrile) interactions (1). A minimum of seven preliminary experiments are performed, and the quality

criterion is evaluated by using the overlapping resolution mapping technique in order to locate the optimum ternary or quaternary mobile phase.

In addition to isocratic optimization, gradient mobile phases have also been optimized by a variety of methods (51,60-63,67-75). These methods involve optimization of the solvent selectivity, as discussed above, the strength of the initial and final solvent concentration, as well as the shape and duration of the gradient. The sequential simplex approach has been used by Watson and Carr (27), whereas regression techniques have been favored by Jandera, Churacek, *et al.* (69-73) and by Snyder, Dolan, *et al.* (51,60-63,68). Kirkland and Glajch (74) extended the mixture-design statistical method described above to gradient elution. Experimental data were acquired using a series of seven gradients with iso-eluotropic mobile phases of aqueous methanol, tetrahydrofuran, and acetonitrile. From these results, the quality criterion was evaluated by using the overlapping resolution mapping technique.

Stationary Phase Composition. In many cases, a single stationary phase is sufficient to achieve the desired chromatographic separation. Because it is a discrete parameter, the type of stationary phase is most often optimized by the simultaneous method (1,2,20). This approach is clearly illustrated in the work of Glajch *et al.* (52), who examined octyl-, cyano-, and phenethyl-modified silica stationary phases for the separation of phenylthiohydantoin derivatives of twenty common amino acids. They applied the mixture-design statistical method to optimize the mobile phase composition separately on each column. By comparison of the three overlapping resolution maps, the cyano-modified silica was identified as the optimal stationary phase.

When a single stationary phase is not sufficient, mixed or multimodal stationary phases have been used to combine dissimilar but compatible retention

mechanisms. Mixed phases that have been successfully used include reversed-phase with size exclusion (76-79), cation or anion exchange with size exclusion (79), reversed-phase with cation or anion exchange (80-84), and cation with anion exchange (83-85). These stationary phases may be combined in several ways: by incorporating or chemically bonding the stationary phases on the same particles (chemically mixed support), by incorporating the phases on different particles that are mixed within a single column (physically mixed support), or by incorporating the phases on different particles that are contained in separate columns connected in series (84).

Isaaq *et al.* (78) have investigated solute retention as a function of stationary phase composition for columns containing β-cyclodextrin- and octadecyl-modified silica. They observed that retention on chemically or physically mixed supports may not be predictable as a linear function of the stationary phase composition. This nonlinear additivity of solute retention may arise as a consequence of interactions between the stationary phases. On the other hand, retention on serially coupled columns is generally additive and predictable because the stationary phases are physically separated. Similar results were reported by Glajch *et al.* (52) for columns containing cyano- and phenethyl-modified silica. These investigations suggest that the regression technique may be used to optimize stationary phase composition for serially coupled columns.

Temperature. In comparison with mobile and stationary phase composition, temperature is less frequently used as an optimization parameter in liquid chromatography. The practical temperature range for most common solvents is somewhat limited, being constrained by the boiling point, freezing point, and viscosity. Nevertheless, temperature changes within this range have been

reported to have a significant influence on solute retention and selectivity as well as plate number (86-90).

Temperature optimization is commonly achieved by the simultaneous method. By comparing the quality criterion at several different temperatures, the optimum temperature may be readily identified (91-92). A more systematic approach has been adopted by using a regression method based on the classical thermodynamic relationship of van't Hoff (93,94). If the molar enthalpy and molar entropy are invariant with the absolute temperature (T), then

$$\ln k = A_0 + \frac{A_1}{T} \qquad [1.21]$$

By measuring retention at two or more temperatures, linear regression can be used to predict the capacity factor and, hence, the quality criterion at any other temperature by means of Equation [1.21]. The optimum temperature may be identified by the window diagram approach (95) or other graphical or numerical method. However, marked deviations from linearity have been observed for graphs of ln k *versus* 1/T for many solutes (18,96,97), thus reducing the accuracy of these optimization methods.

In addition to isothermal optimization, temperature programming has also been implemented in liquid chromatography. This is often accomplished by using microbore or capillary columns in order to minimize the effect of radial temperature gradients (98). Many workers have demonstrated that, under well-controlled experimental conditions, temperature programming may be comparable or advantageous to solvent programming (99-101). Although several applications of temperature programming in liquid chromatography have been reported, theoretical models that enable the prediction and optimization of solute retention are rare (101). The optimization is particularly complicated because

temperature influences both solute retention and band broadening during the separation, often in a manner that is not accurately predictable.

Other Parameters. In addition to the parameters discussed above, optimization techniques have also been developed for such physical parameters as particle size, column diameter, column length, flow rate, etc. Snyder, Dolan, *et al.* (50,51,59-63) have applied regression methods for particle size, and theoretical methods for column dimensions and flow rate. These methods are especially successful when combined with univariate optimization of the mobile phase composition in the DryLab I (isocratic) and DryLab G (gradient) programs (102).

1.6 Multivariate Optimization

If the optimum value of one parameter depends on and varies with the value of another, those parameters are mutually interacting. The optimization of interacting parameters is best achieved by concurrent, rather than independent, variation. All of the optimization procedures described previously, individually or in combination, may be used to implement multivariate optimization. However, the most widely used and successful methods for univariate optimization, simultaneous and regression methods, can become cumbersome and ineffective because the number of characterizing experiments increases rapidly with the number of parameters. In this section, the extension of these methods to multivariate optimization of important chromatographic parameters will be reviewed.

Multiple Mobile Phase Parameters. Two or more mobile phase parameters that are not constrained may be optimized by multivariate methods. A combination of the simultaneous and regression methods has been applied successfully for this purpose by Deming *et al.* (103,104). A factorial design with two parameters at three levels (3^2) was used to optimize the concentrations of an organic solvent (ϕ_1) and an ion-pairing agent (ϕ_2) in reversed-phase liquid chromatography. The resulting retention data were fitted by nonlinear least-squares to a semi-empirical relationship based on the combination of Equation [1.17] with a Freundlich isotherm

$$k = A_0 + A_4 \exp(-A_1 \phi_1) (1 + A_2 \phi_2^{1/A_3}) \qquad [1.22]$$

The selectivity factor of the least-resolved solute pair was used as the quality criterion to construct the response surface, from which the optimum mobile phase composition was determined. Under the optimum conditions, the experimental retention times for five substituted anilines were in close agreement with theoretically predicted values, having an average relative error of ±2.3%.

Otto and Wegscheider (105) also combined the simultaneous and regression techniques to optimize buffer type, pH, ionic strength, and organic solvent composition for the separation of simple organic acids, amino acids, and dipeptides. In preliminary experiments, the effects of buffer type and pH were examined simultaneously to select from among phosphate, citrate, acetate, tartrate, and glycine buffers (47 total experiments). A semi-empirical regression equation was used to relate the capacity factor to the hydrogen ion concentration and the dissociation constants of the buffer. Using the selectivity factor and the peak asymmetry as quality criteria, the citrate buffer was determined to be the most promising alternative. Next, a fractional factorial design ($3^2 \cdot 2^{1-1}$) was used

with a more complex regression equation to model retention as a function of the hydrogen ion concentration, the dissociation constants of the buffer, the ionic strength, and the solvent composition (18 total experiments). By using the selectivity of the least-resolved pair as the quality criterion, a response surface was generated to identify the optimum composition of the citrate buffer. The experimentally observed separation was in good agreement with the theoretical prediction, having an average relative error in capacity factor of ±3.8%. It is also noteworthy that the optimum composition, as well as the overall quality of the separation, predicted for the citrate buffer differed significantly from that for the phosphate buffer.

Mobile and Stationary Phases. Mobile and stationary phase compositions have been optimized concurrently by Glajch *et al.* (52) for the separation of phenylthiohydantoin derivatives of twenty common amino acids. In an extension of the univariate study described previously, the solute capacity factors were measured on three different columns containing octyl-, cyano-, and phenethyl-modified silica stationary phases using seven different ternary solvent compositions of methanol, acetonitrile, and tetrahydrofuran (21 total experiments). By using the regression model, a response surface was generated as a function of solvent composition for each solute on each column. In order to establish the optimum composition of the mobile and stationary phases, the solute retention on a mixed bed was assumed to be a linear combination of the retention on each individual stationary phase at the same mobile phase composition. Thus, the quality criterion was calculated for all possible combinations, from which the optimum stationary phase composition was predicted to be 28% cyano and 72% phenethyl and the optimum mobile phase composition was 9.2% methanol, 10.6% acetonitrile, 13% tetrahydrofuran, and

67.2% water with phosphoric acid at pH 2.1. This prediction was validated by using a single column containing a physically mixed bed as well as two serially coupled columns. A good separation of the amino acids was achieved that was similar, but not identical, in the two systems. Unfortunately, it was not possible to assess the predictive accuracy of these methods from the results presented by Glajch *et al.* (52).

Mobile Phase Composition and Temperature. The optimization of mobile phase composition and temperature has been accomplished by using a combination of the simultaneous and regression methods (101,106-108). Diasio and Wilburn (106) measured solute retention as a function of mobile phase composition and analyzed the results by linear regression. The optimum mobile phase composition was then used to measure solute retention at various temperatures, and the temperature that yielded the best quality criterion was identified as the optimum.

Jinno and Kuwajima (108) have used a similar approach to optimize mobile phase composition and temperature separately. Their method is distinctive because it attempts to generate regression equations that are based on physicochemical properties of the solutes and, hence, can potentially be applied to predict retention for solutes in the absence of experimental data. By using polynuclear aromatic hydrocarbons (PAH) as model solutes, the relevant size and shape parameters were calculated in various mobile phases and were incorporated as physicochemical constants into their model equation. The regression equations used linear relationships of the logarithm of capacity factor with the mobile phase composition (Equation [1.17]) and with the inverse temperature (Equation 1.21). By using this approach, the average relative error

67.2% water with phosphoric acid at pH 2.1. This prediction was validated by using a single column containing a physically mixed bed as well as two serially coupled columns. A good separation of the amino acids was achieved that was similar, but not identical, in the two systems. Unfortunately, it was not possible to assess the predictive accuracy of these methods from the results presented by Glajch *et al.* (52).

Mobile Phase Composition and Temperature. The optimization of mobile phase composition and temperature has been accomplished by using a combination of the simultaneous and regression methods (101,106-108). Diasio and Wilburn (106) measured solute retention as a function of mobile phase composition and analyzed the results by linear regression. The optimum mobile phase composition was then used to measure solute retention at various temperatures, and the temperature that yielded the best quality criterion was identified as the optimum.

Jinno and Kuwajima (108) have used a similar approach to optimize mobile phase composition and temperature separately. Their method is distinctive because it attempts to generate regression equations that are based on physicochemical properties of the solutes and, hence, can potentially be applied to predict retention for solutes in the absence of experimental data. By using polynuclear aromatic hydrocarbons (PAH) as model solutes, the relevant size and shape parameters were calculated in various mobile phases and were incorporated as physicochemical constants into their model equation. The regression equations used linear relationships of the logarithm of capacity factor with the mobile phase composition (Equation [1.17]) and with the inverse temperature (Equation 1.21). By using this approach, the average relative error

in the predicted capacity factor was ±4.4% for sixteen polynuclear aromatic hydrocarbons (PAH) in a standard reference material.

In the factorial design of Yoo *et al.* (101), solute retention was measured as a function of mobile phase composition at four different temperatures (20 total experiments), and then analyzed by linear regression. By using the resolution of the least-resolved solute pair as the quality criterion, the optimum mobile phase composition was identified by the window diagram approach at each temperature. These results were then used to optimize the separation of fourteen saturated and unsaturated fatty acids under temperature programming conditions. The optimum separation conditions enabled baseline resolution ($R_{i,i+1} \geq 1.5$) of the least-resolved solute pair, with reproducibility of retention time better than ±1.1%.

Because these simple approaches do not account for interaction between the parameters, others have adopted the use of regression methods to describe retention as a combined function of mobile phase composition and temperature. Melander and Horvath (109) have proposed the following analytical expression

$$\ln k = A_0 + \frac{A_1}{T} + A_2\phi\left(1 - \frac{T_c}{T}\right) \qquad [1.23]$$

where T_c is the compensation temperature, which was examined as a constant (625 °K) and an adjustable coefficient. This expression was later extended by Melander *et al.* (110) in order to improve the accuracy and precision of regression results

$$\ln k = A_0 + \frac{A_1}{T} + A_2\phi\left(1 - \frac{T_c}{T}\right) + A_3\phi \qquad [1.24]$$

Inherent in these equations is the assumption of linear relationships between the logarithm of capacity factor and mobile phase composition, and between the logarithm of capacity factor and inverse temperature. As a consequence of these assumptions, the average relative error in the predicted capacity factor was ±7.8% and ±6% for Equations [1.23] and [1.24], respectively, for 53 aromatic solutes.

Temperature and Flow Rate. The optimization of temperature and flow rate, as an alternative to mobile phase composition in adsorption chromatography, has been accomplished by Scott and Lawrence (111) using the simultaneous method. Methyl palmitate and dinonylphthalate were used as as models from among 11 aliphatic and aromatic solutes, and the resolution was examined as a function of linear velocity at six temperatures (26 total experiments). The optimum conditions were selected from among those studied, and the results were compared under constant (isothermal–isorheic) conditions as well as with gradient programming in both temperature and flow rate.

Moore and Synovec (112) used the regression method to optimize temperature and flow rate in a microbore LC column. In their approach, the mobile phase was heated before entrance to the column, and the flow rate was controlled to create an axial thermal gradient along the column. The average temperature within each column segment was estimated by using a two-dimensional distributed parameter model for cylindrical packed beds (113). The average capacity factor within each segment was determined as a function of the average temperature by the linear model given in Equation [1.21]. The overall solute capacity factor on the column was then calculated by summation of the capacity factor in each segment of the column. This approach was used to predict retention under conditions of both constant and gradient flow rate with

good results for the separation of dinitrophenylhydrazine derivatives of four aldehydes. Although the effect of temperature and flow rate on the plate height was also examined in this work, these effects were not included directly in the model equations in order to optimize resolution or other quality criterion.

Jinno and Yamagami (114) used the regression method to optimize temperature and flow rate concurrently under gradient programming conditions. In preliminary studies, a linear equation was used to relate the capacity factor of phenylthiohydantoin derivatives of five amino acids with a constant parameter that is characteristic of the physicochemical properties, shape, and structure. This equation enabled the estimation of capacity factor for other amino acids in the absence of experimental data, with average relative error of ±2.5%. Since capacity factor is independent of flow rate, this equation also allowed the prediction of retention time or volume under conditions of constant and gradient flow rate. In order to consider the effects of both flow rate and temperature programming simultaneously, a quadratic expression was included to relate the logarithm of capacity factor with temperature

$$\ln k = A_0 + \frac{A_1}{T} + \frac{A_2}{T^2} \qquad [1.25]$$

This approach was validated by optimizing the separation of the phenylthiohydantoin derivatives of twenty amino acids. The results show good agreement between the predicted and observed chromatograms with an average relative error in predicted retention time of ±1.7%.

1.7 Conclusion

A variety of methods has been used to optimize various parameters in liquid chromatography. Among these, regression methods have proven to be the most widely used and successful approach for univariate and multivariate optimization. The regression approach is attractive because, by using a simple linear or quadratic model, only a few initial experiments are necessary in order to characterize the response surface. While this approach can lead rapidly to the identification of the most promising experimental conditions, it requires that the model used to express the relationship between the parameter and the chromatographic property such as capacity factor, plate number, etc. be well defined. Unfortunately, deviations from ideal behavior frequently lead to nonlinear relationships for the parameters of interest in liquid chromatography, including mobile and stationary phase composition, temperature, and flow rate. Such deviations cannot be predicted *a priori* and, hence, serve to limit the accuracy with which the optimum conditions can be identified. This problem, which is detrimental in univariate optimization, becomes prohibitive when two or more parameters are to be optimized simultaneously.

In order to overcome this problem, a new approach has been developed for univariate and multivariate optimization called parametric modulation (115-119). The fundamental strategy of this approach is that chromatographic properties may be accurately predicted if the solute is constrained to undergo interactions independently within each mobile phase, stationary phase, and temperature environment. This strategy is implemented by maintaining each of these variables in discrete and separate zones along the chromatographic column, as illustrated schematically in Figure 1.4. The theoretical foundation and experimental verification of the parametric modulation technique is the subject of

Figure 1.4: Schematic illustration of the parametric modulation concept for n solvent zones in q serially coupled columns.

Figure 1.4

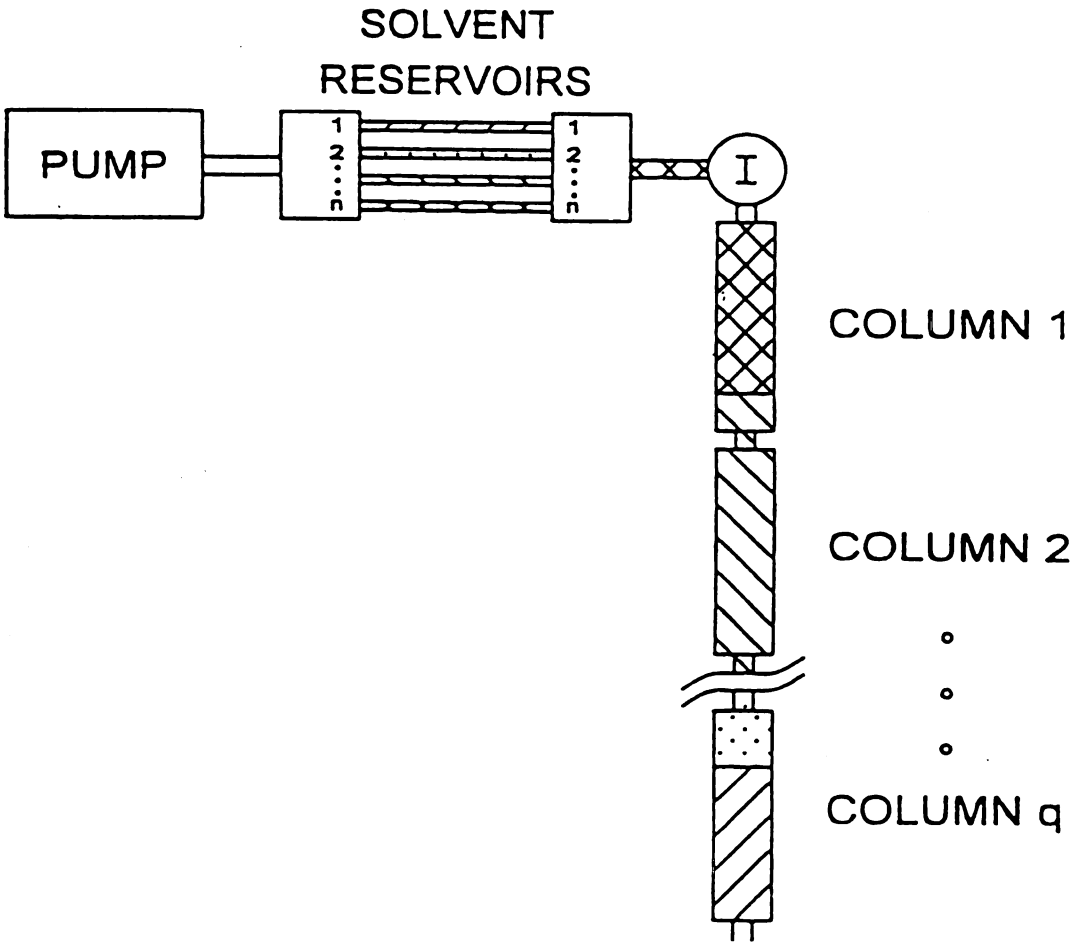

this dissertation. In Chapter 2, the concept of optimization by parametric modulation will be introduced and the theoretical basis of solute retention and dispersion established. Experimental verification of parametric modulation for univariate optimization of mobile phase and a comparison of the method with conventional premixed mobile phase is presented in Chapter 3. In Chapter 4, the multivariate optimization of both mobile and stationary phases is presented, and in Chapter 5 multivariate optimization of mobile phase and temperature is discussed. In the optimization of the separation of solutes, it is often assumed there is no significant interaction between solutes in a mixture. This assumption is investigated in Chapter 6, where a theoretical and experimental study of solute-solute interactions in liquid chromatography is presented. Finally, the work discussed in this dissertation is summarized and future work is proposed in Chapter 7.

1.8 References

1. L. R. Snyder and J. J. Kirkland, *Introduction to Modern Liquid Chromatography*, 2nd Edition (John Wiley-Interscience, New York, 1979).

2. P. J. Schoenmakers, *Optimization of Chromatographic Selectivity,* Journal of Chromatography Library, Volume 35 (Elsevier, Amsterdam, 1986).

3. S. Ahuja, *Selectivity and Detectability Optimization in HPLC,* John-Wiley and Sons, New York, Ch. 4

4. C. L. Deligny, M. C. Spanjer, J. C. Vanhouwelingen and H. M. Weesie, *J. Chromatogr.* **301**, 311 (1984)

5. S. Elchuk and R. M. Cassidy, *Anal. Chem.* **51**, 1434 (1979)

6. H. Miyagi, J. Miura, Y. Takata, S. Kamitake, S. Ganno and Y. Yamagata, *J. Chromatogr.* **239**, 733 (1982)

7. P. T. Kissinger, *Anal. Chem.* **49**, 883 (1979)

8. J. H. Knox and R. A. Hartwick, *J. Chromatogr.* **204**, 3 (1981)

9. W. W. Yau, J. J. Kirkland and D. D. Bly, *Modern Size Exclusion Chromatography,* Wiley-Interscience, New York, 1979

10. J. H. Hildebrand, R. L. Scott, *The Solubility of Nonelectrolytes*; Reinhold: New York, NY 1950; Chapter 23

11. A. F. M. Barton, *Chem. Rev.* **75**, 731 (1975)

12. W. Melander and C. Horvath, *In High performance Liquid Chromatography: Advances and Perspectives;* C. Horvath, Ed.; Academic press: New York, 1980, Vol. 2

13. C. Horvath and W. Melander and I. Molnar, *J. Chromatogr.* **125** 129 (1976)

14. D. E. Martire and R. E. Boehm, J. Chromatogr. **3**, 753 (1983)

15. D. E. Martire and R. E. Boehm, *J. Phy. Chem.* **87**, 1045 (1983)

16. K. A. Dill, *J. Phys. Chem.*, **91** 1987 (1988)

17. O. Sinanoglu and B. Pullman, *Molecular Association in Biology,* Academic Press, New York, 1968

18. L. A. Cole, J. G. Dorsey and K. A. Dill, *Anal. Chem.* **64**, 1324 (1992)

19. J. G. Dorsey and K. A. Dill, *Chem. Rev.,* **89** 331 (1989)

20. J. C. Berridge, *Techniques for the Automated Optimization of HPLC Separation* (John Wiley, New York, 1985).

21. J. L. Glajch and L. R. Snyder, *Computer-Assisted Method Development for High-Performance Liquid Chromatography* (Elsevier, Amsterdam, 1990).

22. R. E. Kaiser, *Gas Chromatographie* (Portig, Leipzig, 1960), p. 33.

23. S. N. Deming and M. L. H. Turoff, *Anal. Chem.* **50**, 546 (1978).

24. P. Jones and C. A. Wellington, *J. Chromatogr.* **213**, 357 (1981).

25. P. J. Schoenmakers, A. C. J. H. Drouen, H. A. H. Billiet, and L. de Galan, *Chromatographia* **15**, 48 (1982).

26. H. A. H. Billiet and L. de Galan, *J. Chromatogr.* **485**, 27 (1989).

27. M. W. Watson and P. W. Carr, *Anal. Chem.* **51**, 1835 (1979).

28. J. L. Glajch, J. J. Kirkland, K. M. Squire, and J. M. Minor, *J. Chromatogr.* **199**, 57 (1980).

29. J. Vajda and L. Leisztner, in *New Approaches in Liquid Chromatography*, H. Kalasz, Editor, Analytical Symposium Series, Volume 16 (Elsevier, Amsterdam, 1982), p. 103.

30. T. D. Schlabach and J. L. Excoffier, *J. Chromatogr.* **439**, 173 (1988).

31. H. J. G. Debets, B. L. Bajema, and D. A. Doornbos, *Anal. Chim. Acta* **151**, 131 (1983).

32. J. W. Weyland, C. H. P. Bruins, H. J. G. Debets, B. L. Bajema, and D. A. Doornbos, *Anal. Chim. Acta* **153**, 93 (1983).

33. A. Peeters, L. Buydens, D. L. Massart, and P. J. Schoenmakers, *Chromatographia* **26**, 101 (1988).

34. R. Cela, C. G. Barroso, and J. A. Perez-Bustamante, *J. Chromatogr.* **485**, 477 (1989).

35. S. N. Deming and S. L. Morgan, *Experimental Design: A Chemometric Approach* (Elsevier, Amsterdam, 1987).

36. J. C. Miller and J. N. Miller, *Statistics for Analytical Chemists*, 3rd Edition (Ellis Horwood Ltd., Chichester, England, 1993), Chapter 7.

37. T. F. Edgar and D. M. Himmelblau, *Optimization of Chemical Processes* (McGraw-Hill, New York, 1988), Chapter 6.

38. W. Spendley, G. R. Hext, and F. R. Hinsworth, *Technometrics* **4**, 44 (1962).

39. J. A. Nelder and R. Mead, *Comput. J.* **7**, 308 (1965).

40. M. L. Raney and W. C. Purdy, *Anal. Chim. Acta* **93**, 211 (1977).

41. V. Svoboda, *J. Chromatogr.* **201**, 241 (1980).

42. D. M. Fast, P. H. Culbreth, and E. J. Sampson, *Clin. Chem.* **28**, 444 (1982).

43. J. C. Berridge, *J. Chromatogr.* **244**, 1 (1982).

44. R. J. Laub, *Int. Lab.*, May/June, 16 (1981).

45. R. J. Laub and J. H. Purnell, *J. Chromatogr.* **112**, 71 (1975).

46. R. J. Laub, in *Physical Methods in Modern Chemical Analysis*, Volume 3, T. Kuwana, Editor (Academic Press, New York, 1983), Chapter 5.

47. J. L. Glajch and J. J. Kirkland, *J. Chromatogr.* **485**, 51 (1989).

48. E. R. Tufte, *The Visual Display of Quantitative Information* (Graphics Press, Cheshire, Connecticut, 1983).

49. S. N. Deming, J. G. Bower, and K. D. Bower, *Adv. Chromatogr.* **24**, 35 (1984).

50. L. R. Snyder, J. W. Dolan, and D. C. Lommen, *J. Chromatogr.* **485**, 65, (1989).

51. J. W. Dolan, D. C. Lommen, and L. R. Snyder, *J. Chromatogr.* **485**, 91 (1989).

52. J. L. Glajch, J. C. Gluckman, J. G. Charikofsky, J. M. Minor, and J. J. Kirkland, *J. Chromatogr.* **318**, 23 (1985).

53. M. T. W. Hearn, *Ion-Pair Chromatography* (Marcel Dekker, New York, 1985).

54. P. J. Schoenmakers, H. A. H. Billiet, and L. de Galan, *J. Chromatogr.* **282**, 107 (1983).

55. P. J. Schoenmakers, A. C. J. H. Drouen, H. A. H. Billiet, and L. de Galan, *Chromatographia* **15**, 688 (1982).

56. A. C. J. H. Drouen, H. A. H. Billiet, P. J. Schoenmakers, and L. de Galan, *Chromatographia* **16**, 48 (1982).

57. L. R. Snyder, *Anal. Chem.* **46**, 1384 (1974).

58. P. J. Schoenmakers, H. A. H. Billiet, and L. de Galan, *J. Chromatogr.* **185**, 179 (1979).

59. M. A. Quarry, R. L. Grob, L. R. Snyder, J. W. Dolan, and M. P. Rigney, *J. Chromatogr.* **384**, 163 (1987).

60. M. A. Quarry, R. L. Grob, and L. R. Snyder, *J. Chromatogr.* **285**, 1 (1984).

61. M. A. Quarry, R. L. Grob, and L. R. Snyder, *J. Chromatogr.* **285**, 19 (1984).

62. M. A. Quarry, R. L. Grob, and L. R. Snyder, *Anal. Chem.* **58**, 907 (1986).

63. L. R. Snyder, M. A. Quarry, and J. L. Glajch, *Chromatographia* **24**, 33 (1987).

64. H. Colin, G. Guiochon, and P. Jandera, *Anal. Chem.* **55**, 442 (1983).

65. A. C. J. H. Drouen, H. A. H. Billiet, and L. de Galan, *J. Chromatogr.* **352**, 127 (1986).

66. J. W. Weyland, C. H. P. Bruins, and D. A. Doornbos, *J. Chromatogr. Sci.* **22**, 31 (1984).

67. P. Jandera and J. Churacek, *J. Chromatogr.* **170**, 1 (1979).

68. J. W. Dolan, J. R. Gant, and L. R. Snyder, *J. Chromatogr.* **165**, 31 (1979).

69. P. Jandera and J. Churacek, *J. Chromatogr.* **192**, 1 (1980).

70. P. Jandera and J. Churacek, *J. Chromatogr.* **192**, 19 (1980).

71. P. Jandera, J. Churacek, and H. Colin, *J. Chromatogr.* **214**, 35 (1981).

72. P. Jandera and J. Churacek, *Gradient Elution in Column Liquid Chromatography - Theory and Practice* (Elsevier, Amsterdam, 1985).

73. P. Jandera, *J. Chromatogr.* **485**, 113 (1989).

74. J. J. Kirkland and J. L. Glajch, *J. Chromatogr.* **255**, 27 (1983).

75. J. L. Glajch and J. J. Kirkland, *J. Chromatogr. Sci.* **25**, 4 (1987).

76. I. H. Hagestam and T. C. Pinkerton, *Anal. Chem.* **57**, 1757 (1985).

77. C. P. Desilets, M. A. Rounds, and F. E. Regnier, *J. Chromatogr.* **544**, 25 (1991).

78. H. J. Issaq, D. W. Mellini, and T. E. Beesley, *J. Liq. Chromatogr.* **11**, 333 (1988).

79. B. Feibush and C. T. Santasania, *J. Chromatogr.* **544**, 41 (1991).

80. J. B. Crowther and R. A. Hartwick, *Chromatographia* **16**, 349 (1982).

81. R. Bischoff and L. W. McLaughlin, *J. Chromatogr.* **270**, 117 (1983).

82. L. A. Kennedy, W. Kopaciewicz, and F. E. Regnier, *J. Chromatogr.* **359**, 73 (1986).

83. Z. El Rassi and C. Horvath, *J. Chromatogr.* **359**, 255 (1986).

84. H. J. Issaq and J. Gutierrez, *J. Liq. Chromatogr.* **11**, 2851 (1988).

85. D. J. Pietrzyk, S. M. Senne, and D. M. Brown, *J. Chromatogr.* **546**, 101 (1991).

86. L. R. Snyder, *J. Chromatogr.* **179**, 167 (1979).

87. H. Colin, J. C. Diez-Masa, G. Guiochon, T. Czajkowska, and I. Miedziak, *J. Chromatogr.* **167**, 41 (1978).

88. R. B. Diasio and M. E. Wilburn, *J. Chromatogr. Sci.* **17**, 245 (1979).

89. J. Chmielowiec and H. Sawatzky, *J. Chromatogr.* **17**, 245 (1979).

90. K. B. Sentell and A. N. Henderson, *Anal. Chim. Acta* **246**, 139 (1991).

91. S. U. Sheikh and J. C. Touchstone, *Anal. Chem.* **509**, 1472 (1987).

92. L. C. Sander and S. A. Wise, *Anal. Chem.* **61**, 1749 (1989).

93. W. R. Melander, D. E. Campbell, and C. Horvath, *J. Chromatogr.* **158**, 215 (1978).

94. W. R. Melander, D. E. Campbell, and C. Horvath, *J. Chromatogr.* **185**, 99 (1979).

95. R. J. Laub and J. H. Purnell, *J. Chromatogr.* **161**, 49. (1978).

96. A. Nahum and C. Horvath, *J. Chromatogr.* **203**, 53 (1981).

97. W. E. Hammers and P. B. A. Verschoor, *J. Chromatogr.* **282**, 41 (1983).

98. H. M. McNair and J. Bowermaster, *J. High Resolut. Chromatogr. Chromatogr. Commun.* **10**, 27 (1987).

99. K. Jinno, J. B. Phillips, and D. P. Carne, *Anal. Chem.* **57**, 574 (1985).

100. G. Liu, N. M. Djordjevic, and F. Erni, *J. Chromatogr.* **592**, 239 (1992).

101. J. Yoo, J. T. Watson, and V. L. McGuffin, *J. Microcol. Sep.* **4**, 349 (1992).

102. L. R. Snyder and J. W. Dolan, *DryLab I User's Manual* and *DryLab G User's Manual* (LC Resources Inc., Lafayette, California, 1987).

103. B. Sachok, J. J. Stranahan, and S. N. Deming, *Anal. Chem.* **53**, 70 (1981).

104. B. Sachok, R. C. Konk, and S. N. Deming, *J. Chromatogr.* **199**, 317 (1980).

105. M. Otto and W. Wegscheider, *J. Liq. Chromatogr.* **6**, 685 (1983).

106. R. B. Diasio and M. E. Wilburn, *J. Chromatogr. Sci.* **17**, 565 (1979).

107. H. J. Issaq, S. D. Fox, K. Lindsey, J. H. McConnell, and D. E. Weiss, *J. Liq. Chromatogr.* **10**, 49 (1987).

108. K. Jinno and M. Kuwajima, *Chromatographia* **22**, 13 (1986).

109. W. R. Melander and C. Horvath, *Chromatographia* **18**, 353 (1984).

110. W. R. Melander, B. K. Chen, and C. Horvath, *J. Chromatogr.* **318**, 1 (1985).

111. R. P. W. Scott and J. G. Lawrence, *J. Chromatogr. Sci.* **7**, 65 (1969).

112. L. K. Moore and R. E. Synovec, *Anal. Chem.* **65**, 2663 (1993).

113. B. A. Finlayson, *Chem. Eng. Sci.* **26**, 1081 (1971).

114. K. Jinno and M. Yamagami, *Chromatographia* **27**, 417 (1988).

115. J. H. Wahl, C. G. Enke, and V. L. McGuffin, *Anal. Chem.* **62**, 1416 (1990).

116. J. H. Wahl, C. G. Enke, and V. L. McGuffin, *Anal. Chem.* **63**, 1118 (1991).

117. J. H. Wahl and V. L. McGuffin, *J. Chromatogr.* **485**, 541 (1989).

118. P. H. Lukulay and V. L. McGuffin, *J. Chromatogr.* **691**, 171 (1995).

119. P. H. Lukulay and V. L. McGuffin, *Anal. Chem.*, manuscript in preparation.

CHAPTER 2

THEORY OF PARAMETRIC MODULATION

In this chapter, the theoretical basis of solute retention and dispersion under the conditions of parametric modulation is introduced. The advantages of this method over existing popular methods are also presented. Although this discussion will be focused on liquid chromatography, the general concepts described herein are applicable to gas and supercritical fluid chromatography as well.

2.1 Theoretical Development

Theory of Solute Retention. In order to optimize separations under the conditions of parametric modulation, the theoretical basis of retention must be established. The inherent assumption underlying this theory is that solute retention is controlled independently within each solvent, stationary and temperature zone. In addition, it is assumed that the solute is able to achieve steady-state conditions rapidly after each change of environment. This latter requirement may restrict the selection of both mobile and stationary phases. The validity of these assumptions has been demonstrated previously for a single column (1-3).

The capacity factor (k_{ijp}), which is the thermodynamic measure of solute retention, may be expressed as follows:

$$k_{ijp} = \frac{t_{ijp}}{t_{ojp}} - 1 \qquad [2.1]$$

where t_{ijp} and t_{ojp} are the elution time of a retained and a nonretained solute, respectively, in solvent j and on column p. It may be readily shown (1,4) that the residence time of a solute in a solvent zone of length x_j is given by:

$$t_{ijp} = \frac{x_j}{u_p} \left(\frac{1+k_{ijp}}{k_{ijp}} \right) \qquad [2.2]$$

where u_p is the mobile-phase linear velocity on column p. The total retention time (t_i) of the solute is the summation of residence times in each solvent and on each column

$$t_i = \sum_{p=1}^{q} \sum_{j=0}^{n} t_{ijp} = \sum_{p=1}^{q} \sum_{j=0}^{n} \frac{x_j}{u_p} \left(\frac{1+k_{ijp}}{k_{ijp}} \right) \qquad [2.3]$$

Because the volumetric flow rate (F) of the mobile phase remains constant within the chromatographic system, the linear velocity on each column is related by

$$F = \pi r_p^2 \varepsilon_p u_p \qquad [2.4]$$

where r_p is the radius and ε_p is the total porosity of column p. By rearrangement of Equation [2.4] and substitution into Equation [2.3], the total retention time may be expressed in terms of the known column parameters

$$t_i = \sum_{p=1}^{q} \sum_{j=0}^{n} \frac{\pi r_p^2 \varepsilon_p x_j}{F} \left(\frac{1+k_{ijp}}{k_{ijp}} \right) \qquad [2.5]$$

The limit of the summation index (n), which represents the total number of solvent zones required to elute the solute from column p, is determined by evaluating the expression

$$\sum_{j=0}^{n} \frac{x_j}{k_{ijp}} = l_p \qquad [2.6]$$

If the limit has a noninteger value for the first column (p=1), the summation in Equation [2.5] is performed in the normal manner for the integer solvent zones 0 to n, and the fraction is treated as a multiplier for the last solvent zone. This solvent zone subsequently enters the second column, where the remainder is used as a multiplier for the first solvent zone (n=0) on the second column (p=2). The computation is performed in an analogous manner for all subsequent columns.

Theory of Solute Band Broadening. In order to optimize the separation of solutes under conditions of parametric modulation, the variance of the solute peak must be determined at the exit of the last environment. If the broadening arises primarily from the packed bed and is relatively independent of solute and solvent, the variance in length units $(\sigma_{ijp})_l^2$ can be expressed as:

$$(\sigma_{ijp})_l^2 = h_p \, d_p \, l_p \qquad [2.7]$$

where h_p is the reduced plate height, d_p is the particle diameter, and l_p is the length of column p. Since variances are only independent and additive in the time domain (4,5), the length variance within each solvent zone on each column must be converted to the corresponding temporal variance $(\sigma_{ijp})_t^2$

$$(\sigma_{ijp})_t^2 = \frac{(\sigma_{ijp})_l^2}{u_p^2} \left(\frac{t_{ijp}}{t_{ojp}} \right)^2 \qquad [2.8]$$

where the elution time of a retained solute is given by Equation [2.2] and the elution time of a nonretained solute (t_{ojp}) is given by

$$t_{ojp} = \frac{l_p}{u_p} \qquad [2.9]$$

By substitution of these expressions into Equation [2.8], the total temporal variance can be expressed as a summation of the contributions within all solvent zones and all columns

$$(\sigma_i)^2 = \sum_{p=1}^{q} \sum_{j=0}^{n} (\sigma_{ijp})^2 = \sum_{p=1}^{q} \frac{h_p\, d_p}{l_p} \left(\sum_{j=0}^{n} \frac{\pi\, r_p^2\, \varepsilon_p\, x_j}{F} \left(\frac{1+k_{ijp}}{k_{ijp}} \right) \right)^2 \qquad [2.10]$$

Finally, the effective number of theoretical plates (N) for the coupled column system under the conditions of solvent modulation is given by

$$N = \frac{t_i^2}{(\sigma_i)_t^2} \qquad [2.11]$$

where the total retention time and temporal variance are evaluated from Equations [2.5] and [2.10], respectively.

Theory of Solvent Zone Broadening. In order to ensure that solute retention is controlled independently within each solvent zone, it is necessary that the

zones exhibit minimal mixing at the boundaries. Such mixing will adversely influence the accuracy of predicting solute retention from the theoretical models. Moreover, distortion and even splitting of solute peaks may occur if they elute at or near the solvent zone boundary.

The zone purity can be expressed as the ratio of the lengths of the unmixed fraction of the final solvent zone to that of the original zone

$$\frac{x_j - \xi x_j}{x_j} = 1 - \xi \qquad [2.12]$$

When defined in this manner, the zone purity approaches unity when no intermixing occurs and approaches zero when the solvent zone is completely mixed by column broadening processes.

Determination of the zone purity by means of Equation [2.12] requires an estimation of the mixed fraction (ξ) of the solvent zone. This mixed fraction may be estimated by assuming that the initial solvent zone has an ideal rectangular profile of width x_j and that column broadening processes are adequately described by a Gaussian profile with variance given by Equation [2.7], as illustrated schematically in Figure 2.1. The mixed fraction is then calculated, with a statistical accuracy of 95%, by presuming that mixing extends $2(\sigma_o)_l$ at each boundary of the solvent zone, so that the total mixed region is $4(\sigma_o)_l$. The mixed fraction is, thus, given by

$$\xi = \frac{4(\sigma_o)_l}{x_j} \qquad [2.13]$$

where the total variance for a nonretained solvent zone $(\sigma_o)_l^2$ in length units is

Figure 2.1 Schematic illustration of solvent zone broadening ($1 - \xi = 0.95$).

Figure 2.1

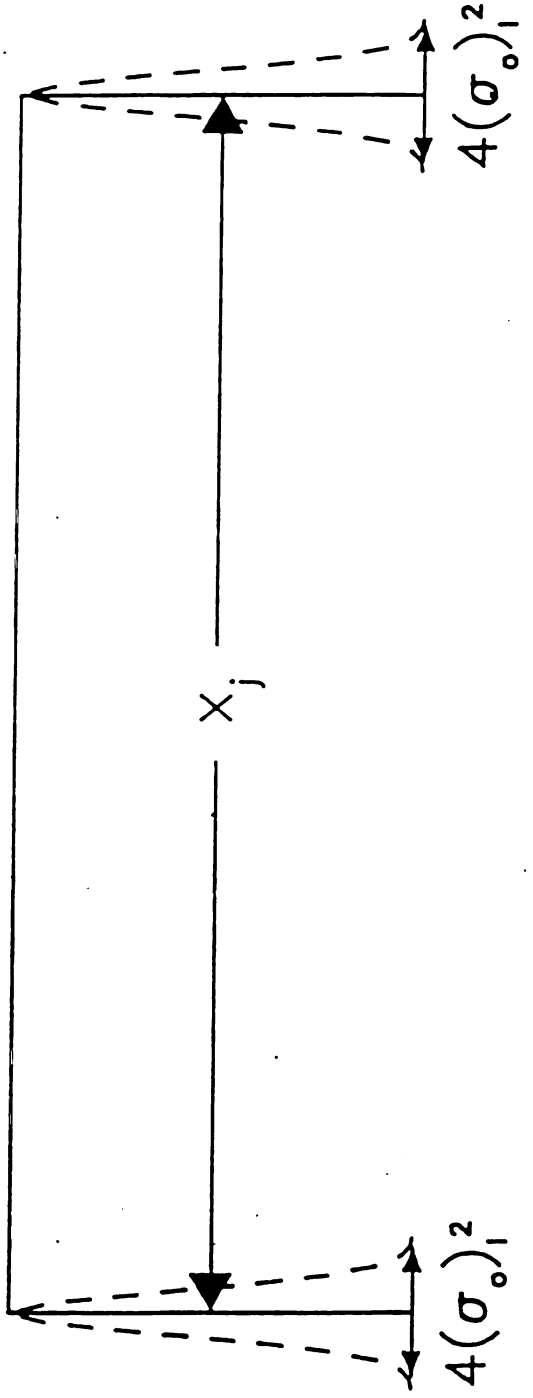

$$(\sigma_o)_l^2 = \frac{\left(\sum_{p=1}^{q} l_p\right)^2 \left(\sum_{p=1}^{q} h_p \; d_p \; l_p \; r_p^4 \; \varepsilon_p^2\right)}{\left(\sum_{p=1}^{q} l_p \; r_p^2 \; \varepsilon_p\right)^2} \qquad [2.14]$$

The effect of solvent zone length on the calculated zone purity is shown in Figure 2.2. It is apparent that the reduction of particle diameter and column length is important to maintain the integrity of the solvent zone. If the minimum acceptable value for the zone purity is arbitrarily defined to be 95%, as illustrated in Figure 2.1, the requisite solvent zone length may be determined from Equation [2.13] as follows

$$x_j = 80(\sigma_o)_l \qquad [2.15]$$

For example, a solvent zone length greater than 12.7 cm would be required to maintain 95% purity for a column with 5 μm particle diameter and 25 cm length. The limiting zone length given by Equation [2.15] is the minimum value that may be used with confidence under the conditions of solvent modulation in order to ensure adherence to the assumptions of the theoretical models.

2.2 Optimization Strategy

The strategy for optimizing separations requires preliminary measurement of the solute capacity factors in each solvent system on each column to be employed. From these measurements, the retention time and variance can then be predicted by using Equations [2.5] and [2.10], respectively, for any given

Figure 2.2A Effect of solvent zone length on zone purity according to Equations 2.12 – 2.14. Constant particle diameter (5 μm) with varying column lengths of 10 cm (—), 25 cm (–), and 100 cm (-).

Figure 2.2A

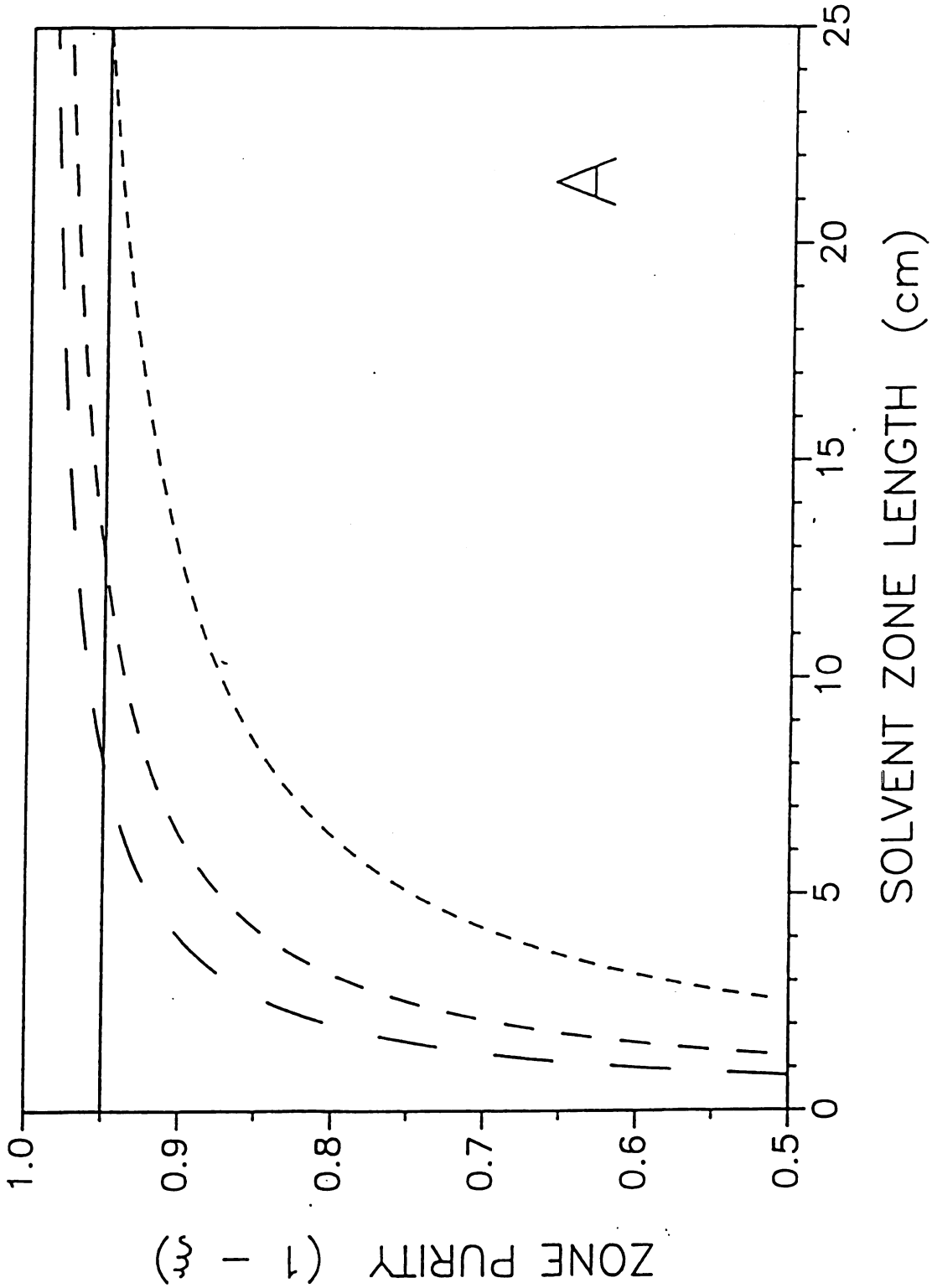
A
ZONE PURITY (1 − ξ)
1.0
0.9
0.8
0.7
0.6
0.5
0
5
10
15
20
25
SOLVENT ZONE LENGTH (cm)

Figure 2.2B Effect of solvent zone length on zone purity according to Equations 2.12 – 2.14. Constant column length (25 cm) with varying particle diameters of 3 μm (—), 5 μm (–), and 10 μm (-).

Figure 2.2B

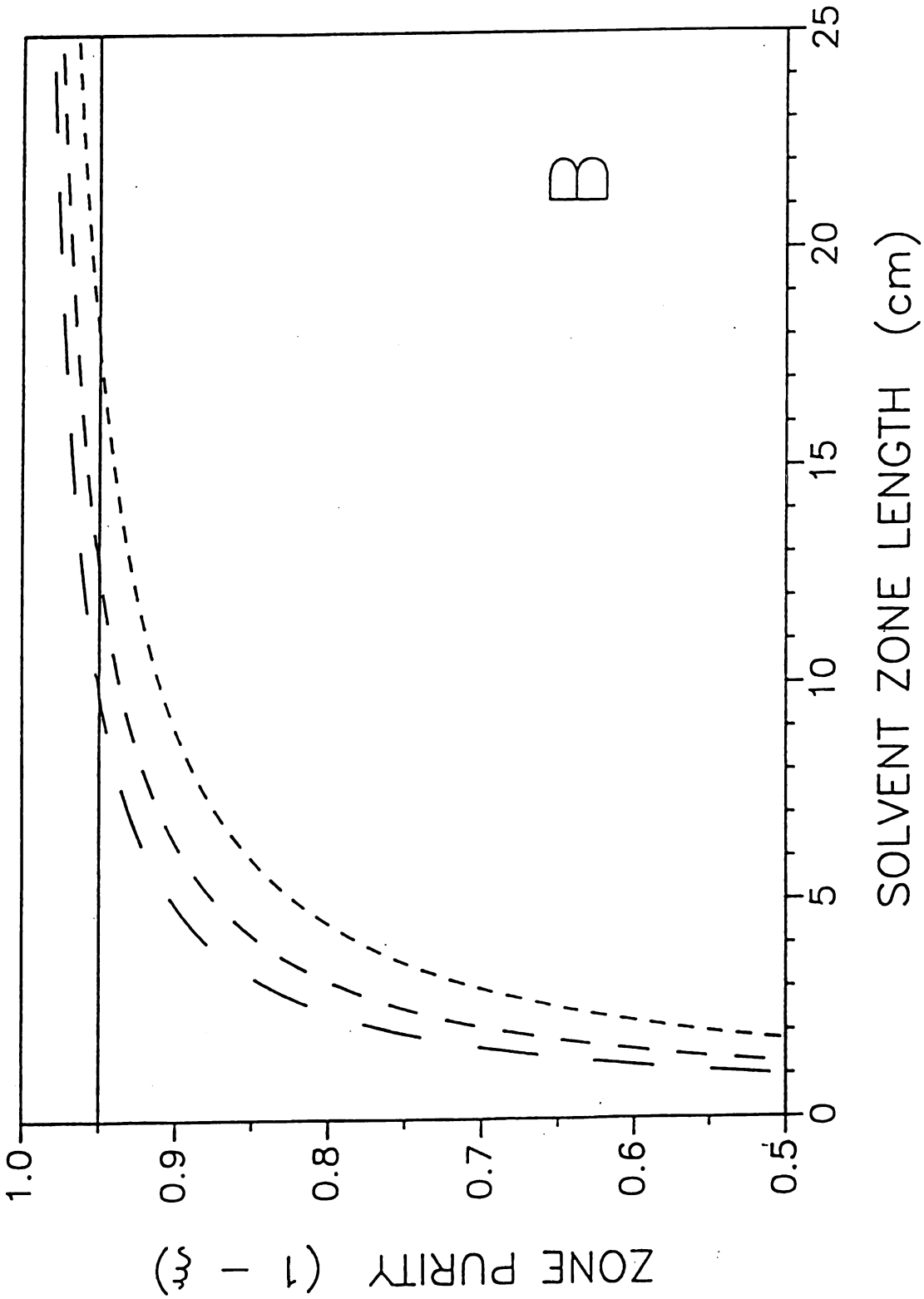
B
ZONE PURITY (1 − ξ)
1.0
0.9
0.8
0.7
0.6
0.5
0
5
10
15
20
25
SOLVENT ZONE LENGTH (cm)

solvent zone length and column length in any sequence. After the retention time and variance are calculated for each solute, the extent of separation between adjacent solutes is given by the resolution ($R_{i,i+1}$)

$$R_{i,i+1} = \frac{(t_{i+1}-t_i)}{2[(\sigma_{i+1})_t + (\sigma_i)_t]} \qquad [2.16]$$

The quality of the overall separation is then assessed using a modified form of the multivariate function developed by Schlabach and Excoffier (6), known as the Chromatographic Resolution Statistic (CRS)

$$CRS = \left(\sum_{i=1}^{m-1} \left(\frac{R_{i,i+1}-R_{opt}}{R_{i,i+1}-R_{min}} \right)^2 \frac{1}{R_{i,i+1}} + \sum_{i=1}^{m-1} \frac{(R_{i,i+1})^2}{(m-1)\, R_{avg}^2} \right) \frac{t_f}{m} \qquad [2.17]$$

where m is the total number of solutes, t_f is the elution time of the final solute, R_{opt} is the optimum or desired resolution, R_{min} is the minimum acceptable resolution, and R_{avg} is the average resolution which is given by

$$R_{avg} = \frac{1}{m} \sum_{i=1}^{m} R_{i,i+1} \qquad [2.18]$$

The first term of the CRS function is a measure of the extent of separation between each pair of adjacent solutes in the chromatogram. This term approaches zero when the individual resolution elements approach the optimum value, and approaches infinity when the individual resolution elements approach the minimum value. The second term of the CRS function reflects the uniformity of spacing between solutes, and approaches a minimum value of unity when the individual resolution elements are equal to the average value. The final term of

the CRS function is intended to minimize the analysis time, and may be neglected if this is not a primary goal of the optimization.

In the original expression defined by Schlabach and Excoffier (6), $(R_{i,i+1} - R_{opt})^2$ passes through a minimum and $1/(R_{i,i+1} - R_{min})^2$ passes through a maximum as $R_{i,i+1}$ increases. As a result, whenever any individual value of $R_{i,i+1}$ approaches R_{min}, the CRS value becomes extremely high and may no longer be representative of the overall separation quality. More importantly, however, values of $R_{i,i+1}$ that are equidistant from R_{min}, whether higher or lower in magnitude, are ranked equally. The detrimental consequence is that deceptively low CRS values may be assigned when an individual resolution element approaches zero (7). This problem may be addressed by altering the form of the CRS function such that, if $R_{i,i+1}$ is less than or equal to $R_{min} + 0.01$, the first term in Equation [2.17] is replaced by the constant term

$$\left(\frac{R_{opt} - R_{min}}{0.01}\right)^2 \frac{1}{R_{min}} \qquad [2.19]$$

In order to optimize the separation, the experimental conditions that yield the minimum value of the CRS function must be determined. The optimum conditions may be determined in two ways: (1) by varying the sequence and length of the solvent zones and columns in a systematic manner to construct a complete CRS response surface, from which the optimum is identified by visual inspection, or (2) by using an iterative search routine such as the simplex method (8,9).

2.3 Conclusion

The theoretical basis of the parametric modulation method has been developed for univariate and multivariate optimization. This approach has several advantages over traditional methods of chromatographic optimization. First, the predicted retention is inherently more accurate because it is calculated by summation of the known and measured behavior in discrete environments rather than by numerical regression in unknown or poorly characterized mixed environments. Second, the number of preliminary experiments necessary to fully characterize the chromatographic system is dramatically reduced in comparison with traditional methods. For a system composed of n mobile phases, q stationary phases, and t temperature zones, only $n \cdot q \cdot t$ retention measurements are necessary for each solute. From these preliminary measurements, the solute retention time and variance for any combination, sequence, and length of the zones may be calculated. Other physical parameters of interest given in Equations [2.5] and [2.10], such as particle size, column dimensions, and flow rate, may be optimized simultaneously with no addition experimental measurements. Thus, a complete multivariate response surface may be systematically generated and the optimum may be identified by visual inspection or by computer-assisted search methods.

The potential limitations of this approach arise from the assumptions inherent in development of the theoretical equations. First, it is assumed that solute retention is controlled independently within each individual environment. This requires that the zones for each mobile phase, stationary phase, and temperature exhibit minimal mixing at the boundaries. A statistical treatment may be used to estimate the minimum zone length required to maintain an acceptable level of zone purity (1,2,8,10). This approach also requires that the solute be

able to achieve steady-state conditions rapidly after each change in environment. This may limit the selection of mobile and stationary phases to those exhibiting rapid kinetics and linear isotherms for the solutes of interest. The validity of these assumptions has been examined for both univariate and multivariate optimization (1,2,10).

2.4 References

1. J.H. Wahl, C.G. Enke, and V.L. McGuffin, *Anal. Chem.* **62**, 1416 (1990).
2. J.H. Wahl, C.G. Enke, and V.L. McGuffin, *Anal. Chem.* **63**, 1118 (1991).
3. J.H. Wahl, *Ph.D. Dissertation*, Michigan State University, 1991.
4. J.C. Giddings, *Dynamics of Chromatography*, Marcel Dekker, New York, 1965.
5. J.C. Sternberg, *Adv. Chromatogr.* 2, 205 (1966).
6. T.D. Schlabach and J.L. Excoffier, *J. Chromatogr.* **439**, 173 (1988).
7. M.F.M. Tavares and V.L. McGuffin, *Anal. Chem.*, accepted for publication.
8. J.H. Wahl and V.L. McGuffin, *J. Chromatogr.* **485**, 541 (1989).
9. S.N. Deming and S.L. Morgan, *Anal. Chem.* **45**, 278A (1973).
10. P. H. Lukulay and V. L. McGuffin, *J. Chromatogr.* **691**, 171 (1995).

CHAPTER 3

UNIVARIATE OPTIMIZATION OF MOBILE PHASE BY PARAMETRIC MODULATION

3.1 Introduction

In this chapter, the specific case of mobile phase optimization by parametric modulation (solvent modulation) is discussed. Experimental verification of this technique is provided and compared with premixed mobile phases for the separation of corticosteroids. The separation is achieved on an octadecylsilica column using aqueous methanol and acetonitrile mobile phases. Based on these results the optimization methods are compared with respect to accuracy, total analysis time, critical resolution, and the overall quality of the separation.

3.2 Theoretical Concepts and Optimization Strategies

Premixed Solvents. In reversed-phase liquid chromatography, a mixture of aqueous and organic solvents is often employed to affect the separation of solutes. Various approaches have been utilized to optimize the composition of these mixed solvents (1-3), among which the commercially available optimization program known as DryLab I™ is one of the most popular and successful (4-9). By using the regression approach, this program combines semi-empirical models of chromatographic retention and dispersion with a few initial experiments for the

CHAPTER 3

UNIVARIATE OPTIMIZATION OF MOBILE PHASE BY PARAMETRIC MODULATION

3.1 Introduction

In this chapter, the specific case of mobile phase optimization by parametric modulation (solvent modulation) is discussed. Experimental verification of this technique is provided and compared with premixed mobile phases for the separation of corticosteroids. The separation is achieved on an octadecylsilica column using aqueous methanol and acetonitrile mobile phases. Based on these results the optimization methods are compared with respect to accuracy, total analysis time, critical resolution, and the overall quality of the separation.

3.2 Theoretical Concepts and Optimization Strategies

Premixed Solvents. In reversed-phase liquid chromatography, a mixture of aqueous and organic solvents is often employed to affect the separation of solutes. Various approaches have been utilized to optimize the composition of these mixed solvents (1-3), among which the commercially available optimization program known as DryLab I™ is one of the most popular and successful (4-9). By using the regression approach, this program combines semi-empirical models of chromatographic retention and dispersion with a few initial experiments for the

solutes of interest in order to optimize their separation. In this approach, a linear model is employed to relate the solute capacity factor (k) and the mobile phase composition (ϕ)

$$\log k = \log k_w - s\phi \qquad [3.1]$$

where the slope (s) is a constant that is characteristic of each solute within the chromatographic system, and the intercept ($\log k_w$) is the logarithm of the solute capacity factor using pure water as mobile phase. The solute capacity factor is calculated from the experimental data as

$$k = \frac{(t_r - t_o)}{t_o} \qquad [3.2]$$

where t_r and t_o are the elution times of a retained and nonretained solute, respectively.

Practical application of this technique requires that solute retention be measured by using at least two solvent compositions. This enables the estimation of the coefficients s and k_w for each solute by linear regression. Based on the values of these coefficients, the solute capacity factor can be predicted at other mobile phase compositions by means of Equation [3.1]. From the predicted capacity factors, the resolution between adjacent solutes can be calculated as follows

$$R_s = \frac{N^{1/2}}{4} \left(\frac{\alpha - 1}{\alpha}\right) \left(\frac{k'}{1+k'}\right) \qquad [3.3]$$

where N is the number of theoretical plates, α is the selectivity factor, and k' is the average capacity factor. The quality of the separation is evaluated by means of the resolution between the least-resolved solute pair, called the critical resolution (R_{crit}). In order to optimize the separation, the critical resolution is

mapped as a function of the solvent composition (8, 10,11). From this resolution map, the mobile phase composition that yields the highest value of the critical resolution can be determined by visual inspection.

Solvent Modulation. The general concept and theory of solvent modulation have been discussed previously in Chapter 2. In this technique, the overall retention of solute i is given by (1,2)

$$k_i = \frac{\sum_{j=0}^{n} x_j \left(\frac{1+k_{ij}}{k_{ij}} \right)}{L} - 1 \qquad [3.4]$$

where k_{ij} is the capacity factor of solute i in solvent j, x_j is the solvent zone length, and the limit of summation n represents the number of solvent zones required to elute the solute from a column of length L. Thus, in solvent modulation, the overall retention is varied by means of the type, sequence, and length of the solvent zones applied to the column.

The strategy for optimization by this technique requires preliminary measurement of solute capacity factor in each solvent of interest. Based on these measurements, the overall capacity factor under the conditions of solvent modulation can be estimated by means of Equation [3.4]. Next, the resolution between adjacent solutes i and i+1 is calculated using the form of the resolution equation below

$$R_{i,i+1} = \frac{N^{1/2}}{2} \left(\frac{k_{i+1} - k_i}{2+k_i + k_{i+1}} \right) \qquad [3.5]$$

The quality of the separation is then assessed by using a modified form of the multivariate function known as the Chromatographic Resolution Statistic (CRS) developed by Schlabach and Excoffier (12)

$$CRS = \left(\sum_{i=1}^{m-1} \left(\frac{R_{i,i+1} - R_{opt}}{R_{i,i+1} - R_{min}} \right)^2 \frac{1}{R_{i,i+1}} + \sum_{i=1}^{m-1} \frac{(R_{i,i+1})^2}{(m-1)\, R_{avg}^2} \right) \frac{t_f}{m} \qquad [3.6]$$

where m is the total number of solutes, t_f is the elution time of the final solute, R_{opt} is the optimum or desired resolution, R_{min} is the minimum acceptable resolution, and R_{avg} is the average resolution calculated according to Equation [2.18].

In order to optimize the separation, the solvent zone lengths which yield the minimum value of the CRS function must be determined. This minimum CRS value may be determined in two ways: 1) by varying the length of each solvent zone systematically to produce the complete response surface from which the optimum is determined by visual inspection, or 2) by using an sequential search routine such as the simplex method (13,14). The former method is time consuming, but provides a detailed view of the complete response surface. The latter method is more efficient but, because the surface may contain many local maxima and minima, care must be taken to ensure that the global optimum is identified. Consequently, a combination of these approaches is desirable.

3.3 Experimental Methods

Materials and Methods. The following corticosteroids are utilized in this investigation: cortisone (17α,21-dihydroxy-pregn-4-ene-3,11,20-trione), hydrocortisone (11β,17α,21-trihydroxy-pregn-4-ene-3,20-di-one), tetrahydrocortisone (3α,17α,21-tri-hydroxy-5β-pregnane-11,20-dione), tetrahydrocortisol (3α,11β,17α,21-tetrahydroxy-5β-pregnane-20-one), prednisone (17α,21-dihydroxy-pregna-1,4-diene-3,11,20-trione), prednisolone (11β,17α,21-trihydroxy-pregna-1,4-diene-3,20-dione), methylprednisolone (11β,17α,21-trihydroxy-6α-methyl-pregna-1,4-diene-3,20-dione), and dehydrocorticosterone (21-hydroxy-pregn-4-ene-3,11,20-trione). These corticosteroids shown in Figure 3.1 are obtained from the Sigma Chemical Company (St. Louis, MO, USA) and are used without further purification. Standard solutions are prepared in methanol at 10^{-3} M concentration for tetrahydrocortisone and tetrahydrocortisol, and at 10^{-6} M concentration for all other corticosteroids. Organic solvents are high-purity, distilled-in-glass grade (Baxter Healthcare, Burdick & Jackson Division, Muskegon, MI, USA); water is deionized and double distilled in glass (Model MP-3A, Corning Glass Works, Corning, NY, USA).

Experimental System. A chromatographic pump equipped with two 40-mL syringes (Model 140, Applied Biosystems, Foster City, CA, USA) is used to deliver the mobile phase at 0.5 mL/min. Sample introduction is achieved by using a 10-μL injection valve (Model EQ 60, Valco Instruments Co., Houston, TX, USA). The chromatographic column (47 cm × 0.46 cm i.d.) is packed with octadecylsilica material (Spheri-5 RP-18, 5 μm, Applied Biosystems) to have a total plate number (N) of approximately 10,000 for the solutes of interest. Solute detection is accomplished by using a variable-wavelength UV-visible absorbance

Figure 3.1 Structures of corticosteroids.

Figure 3.1

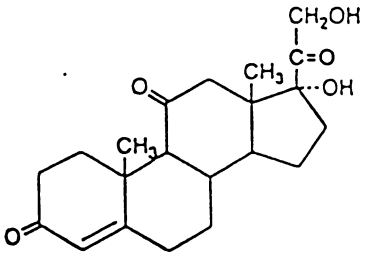

CORTISONE

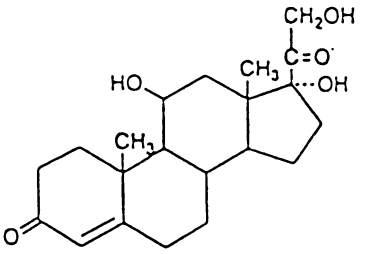

HYDROCORTISONE

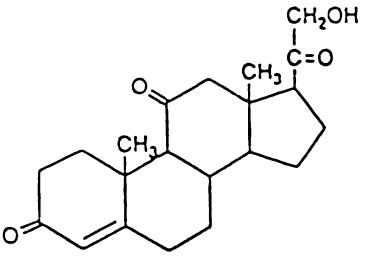

DEHYDROCORTICOSTERONE

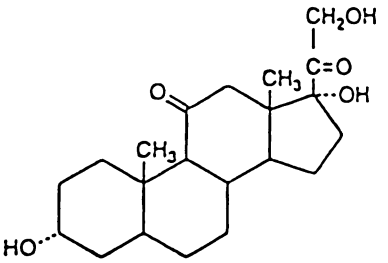

TETRAHYDROCORTISONE

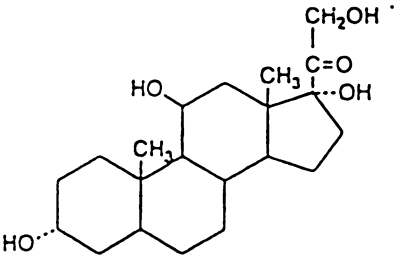

TETRAHYDROCORTISOL

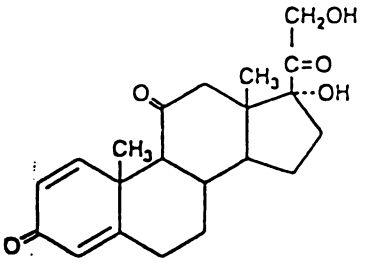

PREDNISONE

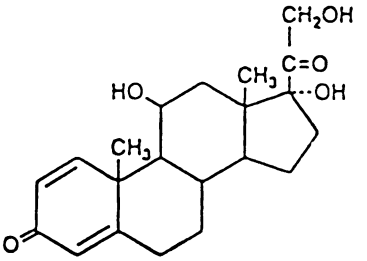

PREDNISOLONE

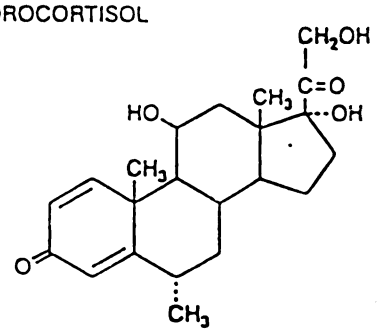

METHYLPREDNISOLONE

detector (240 nm, 0.005 AUFS, Model 166, Beckman Instruments, San Ramon, CA, USA).

Computer-Assisted Optimization Programs. The optimization program for premixed mobile phases, DryLab I™ Isocratic HPLC Simulation/Optimization Program (LC Resources Inc., Lafayette, CA, USA), is executed on an IBM-compatible computer with 80486 microprocessor. From the initial measurements of solute retention times, this program uses linear regression to calculate the capacity factor as a function of the mobile phase composition. In addition, the total analysis time, selectivity factor, and critical resolution are calculated from Equations [3.1] to [3.3], assuming a plate number of 10,000. The optimum conditions are identified from a graph of the critical resolution as a function of mobile phase composition (11).

The optimization program for solvent modulation is written in the Fortran 77 language and executed on a VAX Station 3200 computer (Digital Equipment, Maynard, MA, USA) (15-17). From initial measurements of solute capacity factors, the overall capacity factor of each solute is calculated for the conditions of solvent modulation by using Equation [3.4]. The resolution of each solute pair is calculated by using Equation [3.5], and the overall quality of the separation is assessed by means of the CRS function in Equation [3.6], where the selected values for the optimum and minimum acceptable resolutions are 1.5 and 0.5, respectively. The optimum conditions are identified by two methods (18). In the topographic mapping method, these calculations are performed while systematically incrementing each solvent zone length within a prescribed range. By graphing the resulting CRS values as a function of the solvent zone length, a complete response surface is constructed. The minimum CRS value is then located by visual inspection of this response surface (17). In the sequential

search method, the modified simplex algorithm of Nelder and Mead (14) is employed. This algorithm permits expansion and contraction of the simplex during the search and will converge at the optimum position. In order to ensure the identification of the global optimum, both the size and the location of the initial simplex are varied systematically in 200 independent searches (17). For each initial simplex, the calculations are performed according to Equations [3.4] to [3.6] at each successive vertex, and the best conditions are continuously updated and stored in a file (18). This file contains the solvent zone lengths, the solute elution order, the predicted capacity factors, the predicted resolutions, and the corresponding CRS value for the separation.

3.4 Results and Discussion

In this work, solvent modulation and premixed solvents are compared by using computer-assisted optimization programs to optimize the separation of eight corticosteroids. The practical utility of both techniques requires that solute retention be measured in solvents of different compositions, from which the optimum conditions for the separation can be predicted. The capacity factor of each corticosteroid was measured on an octadecylsilica column using 60% and 75% methanol as well as 35% and 50% acetonitrile. Table 3.1 summarizes the retention measurements for the corticosteroids. In the methanol mobile phases, all of the corticosteroids are well separated except for prednisolone and hydrocortisone. On the other hand, in the acetonitrile mobile phases, the corticosteroids are separated with the exceptions of prednisone and

Table 3.1 Capacity Factors for Corticosteroids on Octadecylsilica Stationary Phase using Methanol and Acetonitrile Mobile Phases

CORTICOSTEROIDS	CAPACITY FACTOR (k)			
	Methanol–Water		Acetonitrile–Water	
	60%	75%	35%	50%
Prednisone	1.57	0.41	1.66	0.50
Cortisone	1.73	0.48	1.83	0.58
Prednisolone	2.14	0.55	1.40	0.41
Hydrocortisone	2.18	0.56	1.69	0.50
Dehydrocorticosterone	2.97	0.69	4.09	1.39
Methylprednisolone	3.79	0.86	2.53	0.70
Tetrahydrocortisol	4.29	0.96	1.94	0.50
Tetrahydrocortisone	5.17	1.08	2.53	0.63

hydrocortisone as well as methylprednisolone and tetrahydrocortisone. Thus, the least-resolved solute pairs vary with the type of organic modifier.

Premixed Solvents. To optimize the separation of corticosteroids using premixed solvents, the DryLab I™ program is utilized. Based on the preliminary measurements of the capacity factors in Table 3.1, this program calculates the retention of the corticosteroids at other solvent compositions according to Equation [3.1]. In order to determine the optimum solvent composition, the critical resolution of the least-resolved solute pair is mapped as a function of the mobile phase composition. The resolution maps for the aqueous acetonitrile and methanol mixtures are shown in Figures 3.2 and 3.3, respectively. For the acetonitrile mixtures, the composition of 30% acetonitrile is predicted to yield the highest value of the critical resolution. The least-resolved solutes are prednisone and hydrocortisone, with a predicted resolution of 0.3. Because this region of the resolution map is irregular, slight variations in the mobile phase composition may result in a large change in the critical resolution. For the methanol mixtures, however, a more rugged optimum region is observed between 55% and 60% methanol. The least-resolved solutes are prednisolone and hydrocortisone, with a predicted resolution of 0.3. Because this region is relatively broad and flat, slight variations in the mobile phase composition will not be as detrimental. Thus, 56% methanol was chosen as the optimum mobile phase composition and was used to obtain the separation shown in Figure 3.4. From this chromatogram, it is apparent that prednisolone and hydrocortisone are completely overlapped ($R_s \approx 0.3$), whereas all other solutes are fully resolved. The experimentally measured capacity factors are in good agreement with the theoretically predicted values from Equation [3.1], as summarized in Table 3.2, with an average relative error of ±3.22%.

Figure 3.2 Critical resolution as a function of the mobile phase composition for aqueous acetonitrile mixtures. Column: 47 × 0.46 cm i.d., packed with octadecylsilica material. Solutes: (1) prednisone, (2) cortisone, (3) prednisolone, (4) hydrocortisone, (5) dehydrocorticosterone, (6) methyl-prednisolone, (7) tetrahydrocortisol, (8) tetrahydrocortisone.

Figure 3.2

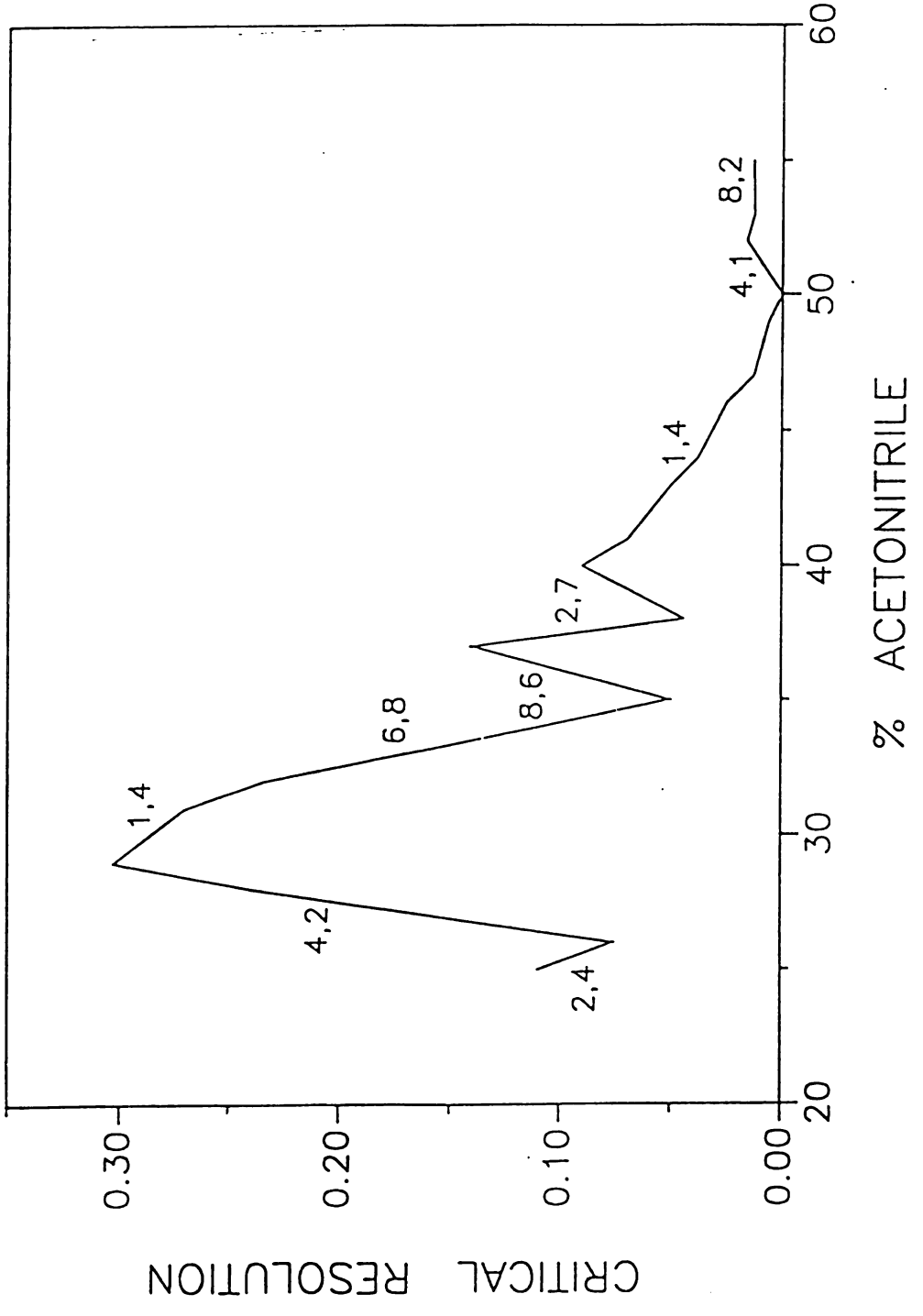
CRITICAL RESOLUTION
0.30
0.20
0.10
0.00
20
30
40
50
60
% ACETONITRILE
1,4
4,2
2,4
6,8
8,6
2,7
1,4
4,1
8,2

Figure 3.3 Critical resolution as a function of the mobile phase composition for aqueous methanol mixtures. Experimental conditions as given in Figure 3.2

Figure 3.3

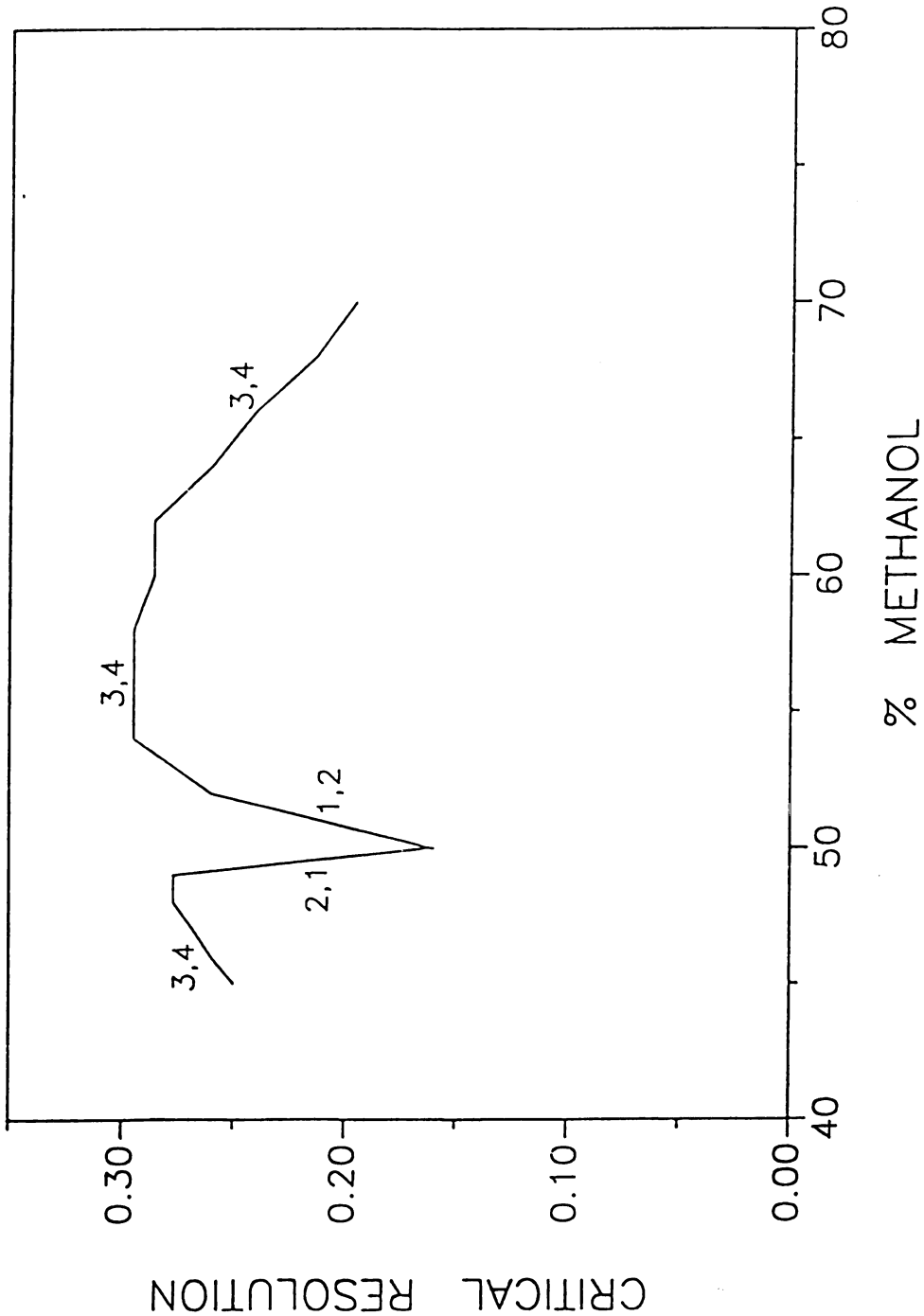
CRITICAL RESOLUTION
0.30
0.20
0.10
0.00
40
50
60
70
80
% METHANOL
3,4
2,1
1,2
3,4
3,4

Figure 3.4 Experimental chromatogram of corticosteroids obtained under the predicted optimum conditions for premixed mobile phases. Column: 47 × 0.46 cm i.d., packed with octadecylsilica material. Mobile phase: 56% methanol, 0.5 mL/min. Detector: UV-visible absorbance detector, 240 nm, 0.005 AUFS. Solutes: (1) prednisone, (2) cortisone, (3) prednisolone, (4) hydrocortisone, (5) dehydrocorticosterone, (6) methylprednisolone, (7) tetrahydrocortisol, (8) tetrahydrocortisone.

Figure 3.4

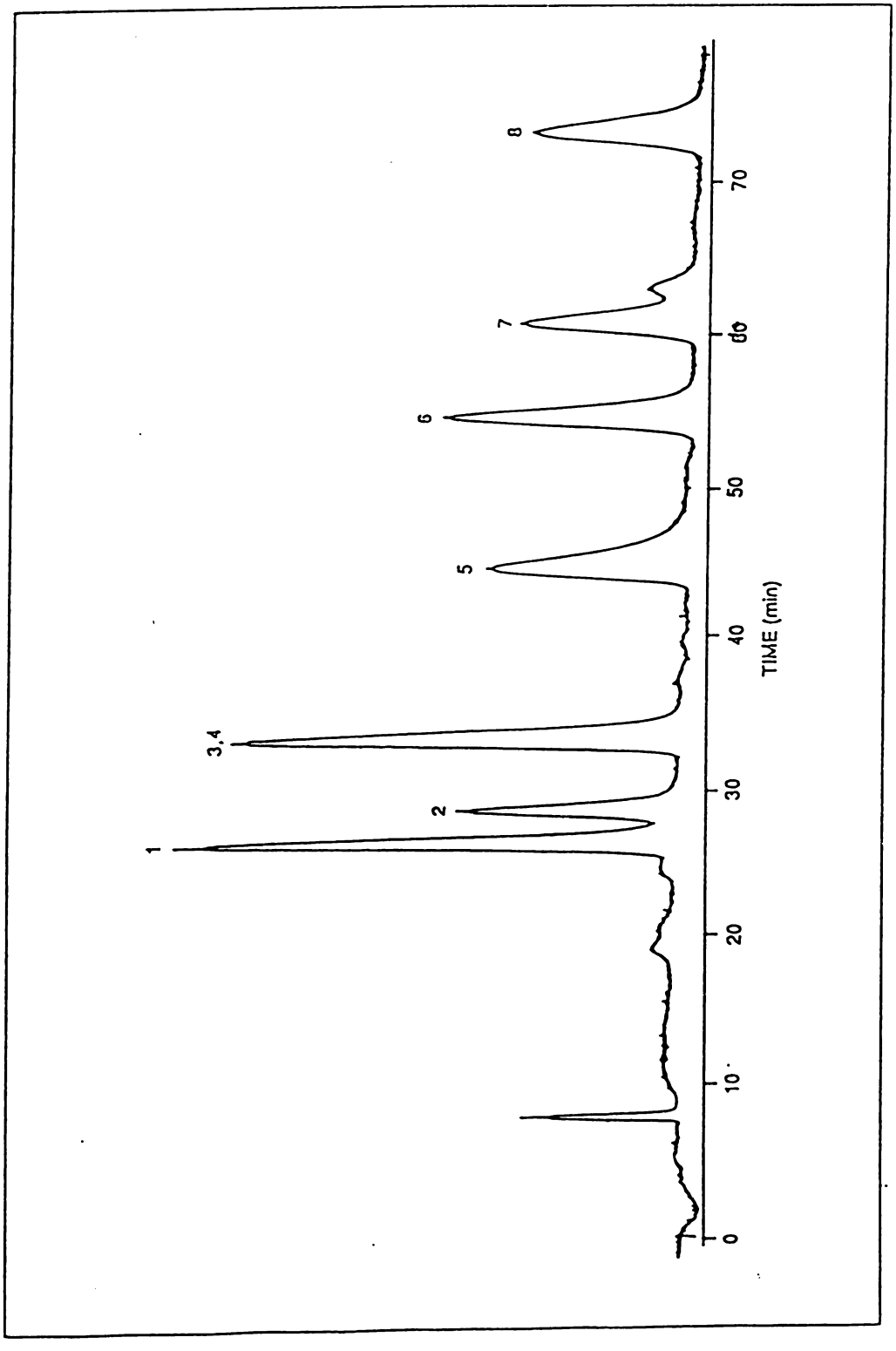

Table 3.2 Comparison of Experimental and Theoretical Capacity Factors under the Predicted Optimum Conditions for Premixed Mobile Phases

CORTICOSTEROIDS	CAPACITY FACTOR (k)		
	Theory†	Experiment	Relative Error (%)‡
Prednisone	2.46	2.25	–8.54
Cortisone	2.60	2.54	–2.31
Prednisolone	3.27	3.11	–4.89
Hydrocortisone	3.32	3.11	–6.32
Dehydrocorticosterone	4.62	4.55	–1.52
Methylprednisolone	5.84	5.80	–0.68
Tetrahydrocortisol	6.61	6.60	–0.15
Tetrahydrocortisone	8.08	8.19	1.36
Average			±3.22

† Calculated by using Equation [3.1].
‡ Calculated as 100 x (Experiment – Theory)/Theory.

Solvent Modulation. To optimize the separation of corticosteroids using solvent modulation, the four solvent systems shown in Table 3.1 are utilized. Although there are twelve possible permutations of a two-solvent modulation sequence, the computer-assisted search routines provide a rapid and effective means to identify the most promising permutation. For each permutation, the sequential simplex method is used to determine the minimum CRS value on the complete response surface. The results of this preliminary search are summarized in Table 3.3. From these results, the most promising solvent modulation sequence is identified to be 50% acetonitrile followed by 60% methanol (CRS_{min} = 1.9). The least-resolved solutes are cortisone and hydrocortisone, with a predicted resolution of 1.30. Although this permutation initially appears to be very promising, a more detailed inspection by the topographic mapping method reveals that the response surface is highly irregular. Variations in the solvent zone length as small as ±1.0 cm alter the identity of the least-resolved solute pair and cause a significant change in the critical resolution. As a consequence of this limitation, the next most promising permutation of 35% acetonitrile followed by 60% methanol (CRS_{min} = 3.6) is selected for further study. The chromatograms corresponding to each of these solvents are shown in Figure 3.5. The least-resolved solutes in 35% acetonitrile are methylprednisolone and tetrahydrocortisone, whereas those in 60% methanol are prednisolone and hydrocortisone. Although the separation of all solutes is not achievable in either of these solvents individually, the results in Table 3.3 suggest that the modulation of these solvents may provide a more beneficial separation. In order to determine the optimum conditions for solvent modulation, the complete response surface was constructed by the mapping method. The topographic and contour maps of the CRS response surface are shown in Figure 3.6 as a function of the solvent zone length. When expressed in terms of the

Table 3.3 Evaluation of the Permutations for a Two-Solvent Modulation Sequence

Solvent 1	Solvent 2	t_f (min)	R_{crit}	CRS_{min}
60% Methanol	75% Methanol	29.3	0.20	95
75% Methanol	60% Methanol	28.8	0.19	96
35% Acetonitrile	50% Acetonitrile	32.3	0.15	113
50% Acetonitrile	35% Acetonitrile	33.9	0.15	104
60% Methanol	35% Acetonitrile	50.3	0.72	26
35% Acetonitrile	60% Methanol	51.9	0.99	3.6
60% Methanol	50% Acetonitrile	30.3	0.86	8.1
50% Acetonitrile	60% Methanol	31.1	1.30	1.9
75% Methanol	35% Acetonitrile	18.9	0.20	97
35% Acetonitrile	75% Methanol	19.3	0.18	98
75% Methanol	50% Acetonitrile	18.6	0.18	100
50% Acetonitrile	75% Methanol	18.6	0.18	101

Figure 3.5 Separation of corticosteroids in individual mobile phases for solvent modulation. Mobile phase: (A) 60% methanol, (B) 35% acetonitrile, 0.5 mL/min. All other experimental conditions as given in Figure 3.4.

Figure 3.5

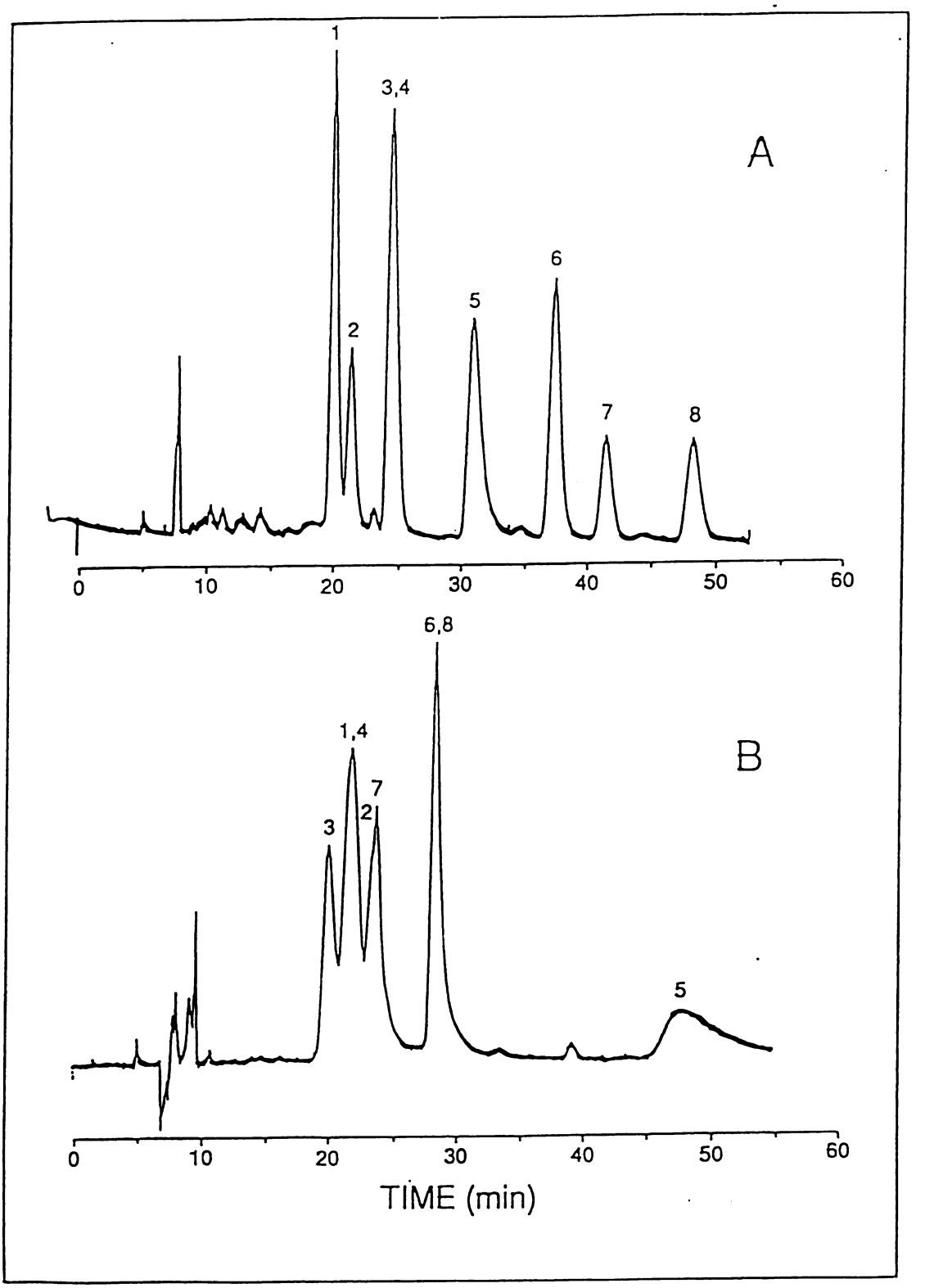
1
3,4
A
6
5
2
7
8
0
10
20
30
40
50
60
6,8
1,4
B
7
2
3
5
0
10
20
30
40
50
60
TIME (min)

Figure 3.5 Separation of corticosteroids in individual mobile phases for solvent modulation. Mobile phase: (A) 60% methanol, (B) 35% acetonitrile, 0.5 mL/min. All other experimental conditions as given in Figure 3.4.

Figure 3.5

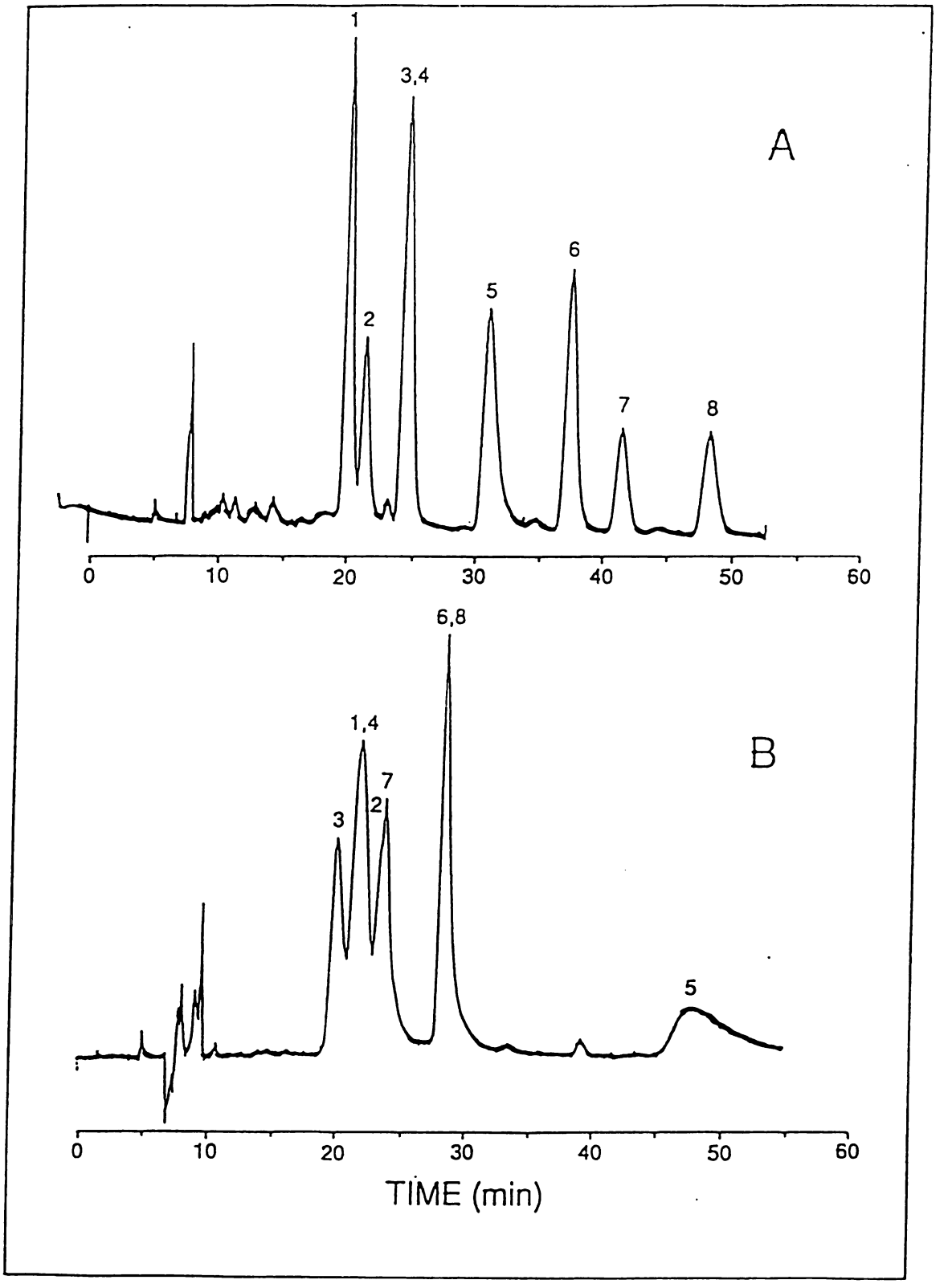
A
1
2
3,4
5
6
7
8
0
10
20
30
40
50
60
B
3
1,4
7
2
6,8
5
0
10
20
30
40
50
60
TIME (min)

Figure 3.6A Topographic map of the CRS response surface as a function of the fractional zone lengths for 35% acetonitrile and 60% methanol.

FIGURE 3.6B Contour map of the CRS response surface as a function of the fractional zone lengths for 35% acetonitrile and 60% methanol.

Figure 3.6B

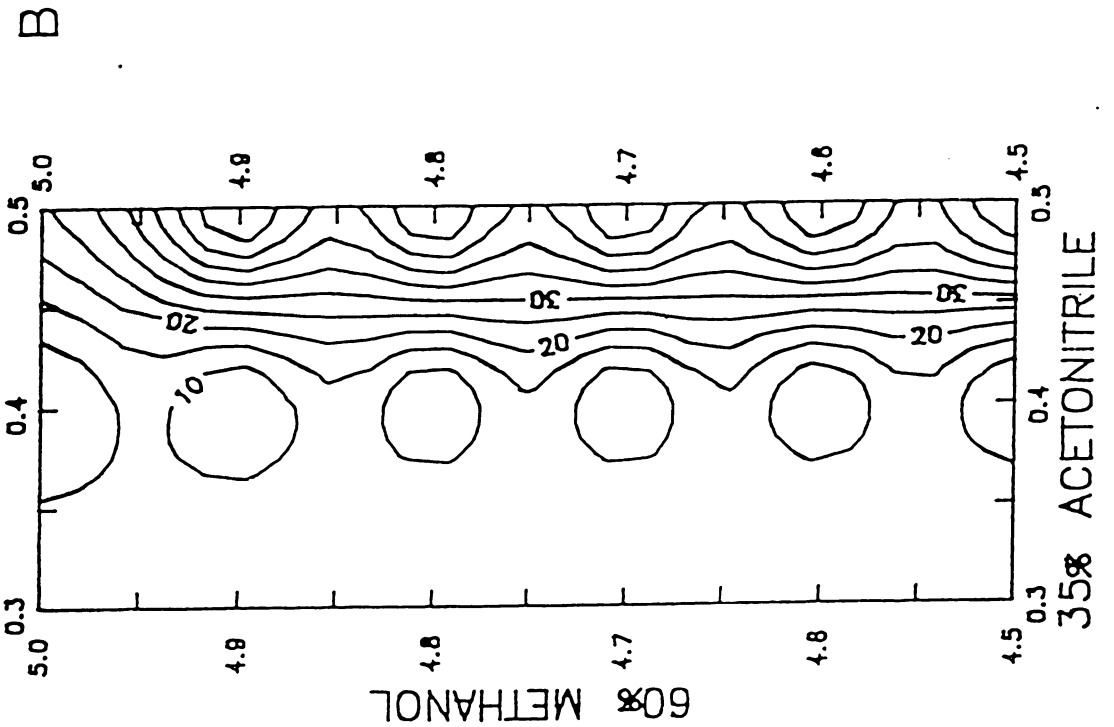

fractional length (x_j/L), these maps may be used to determine the optimum conditions independent of the column length. From these maps, the minimum CRS is predicted for zones of 35% acetonitrile and 60% methanol in fractional lengths of 0.4 and 4.8, respectively, which correspond to absolute lengths of 19 and 226 cm, respectively, for the 47 cm column utilized in this study.

The experimental chromatogram in Figure 3.7 shows good separation of all corticosteroids with the exception of the least-resolved solute pair, prednisolone and hydrocortisone ($R_{crit} \approx 0.7$). The experimentally measured capacity factors agree well with the theoretically predicted values from Equation [3.4], as summarized in Table 3.4, with an average relative error of ±2.70%.

Comparison of Solvent Modulation and Premixed Solvents. The optimization methods used in this work may be compared on the basis of the following criteria: average relative error in predicted capacity factor, total analysis time, critical resolution, and overall quality of the separation assessed by the CRS function. The average relative error is ±2.70% for the solvent modulation technique, compared with ±3.22% for premixed solvents. When optimized with solvent modulation, the corticosteroid separation is achieved experimentally in 52 minutes with a critical resolution of 0.7, and a CRS value of approximately 26. When optimized with premixed solvents by DryLab I™, the corticosteroid separation is achieved experimentally in 73 minutes with a critical resolution of 0.3, and a CRS value of approximately 146. On the basis of these criteria, the separation achieved by using solvent modulation is at least comparable to and, in some respects, significantly better than that achieved by using premixed solvents.

Figure 3.7 Experimental chromatogram of corticosteroids obtained under the predicted optimum conditions for solvent modulation. Mobile phase: solvent modulation sequence of 35% acetonitrile and 60% methanol in fractional zone lengths of 0.4 and 4.8, respectively, 0.5 mL/min. All other experimental conditions as given in Figure 3.4.

Figure 3.7

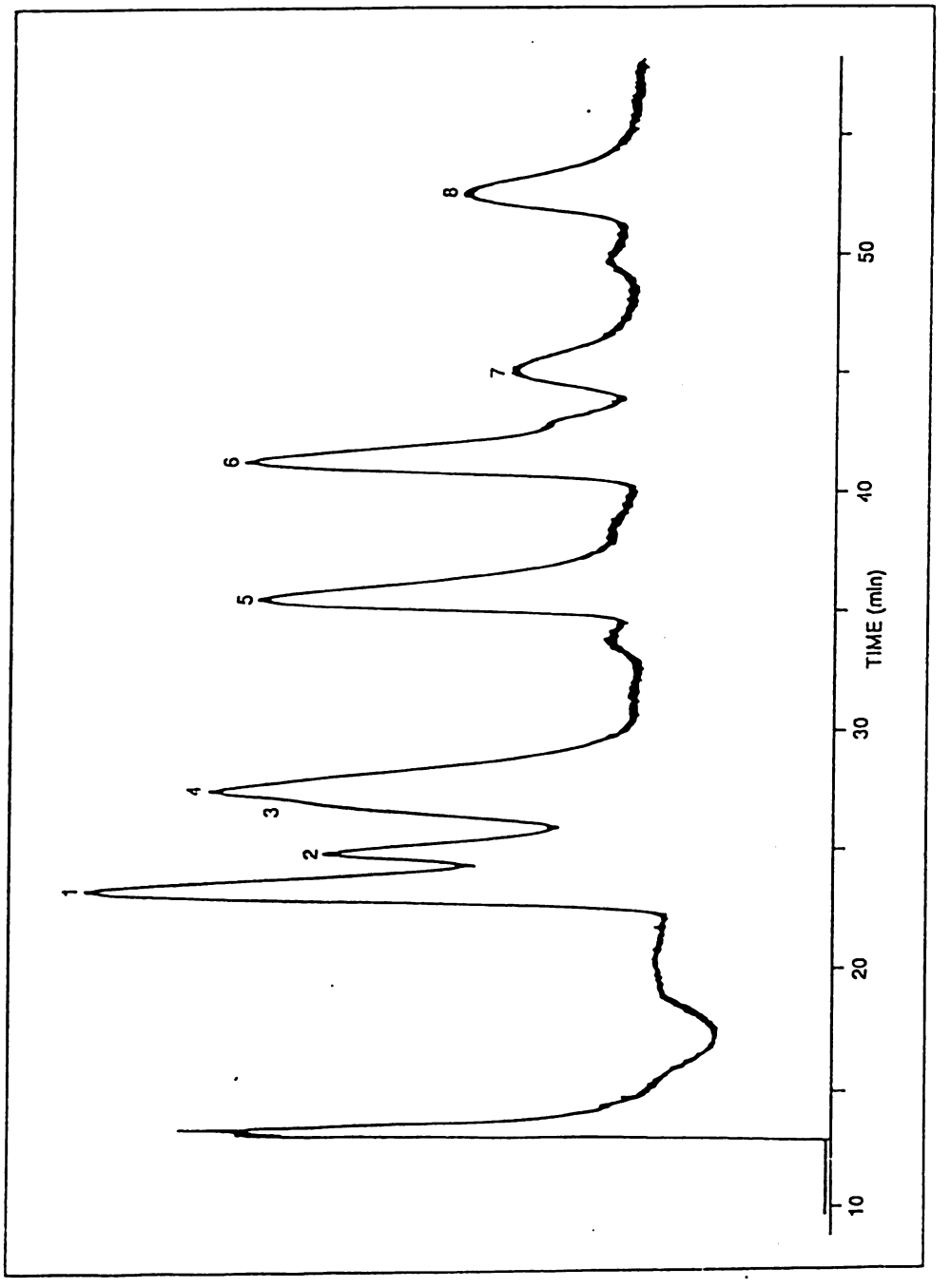

Figure 3.7 Experimental chromatogram of corticosteroids obtained under the predicted optimum conditions for solvent modulation. Mobile phase: solvent modulation sequence of 35% acetonitrile and 60% methanol in fractional zone lengths of 0.4 and 4.8, respectively, 0.5 mL/min. All other experimental conditions as given in Figure 3.4.

Figure 3.7

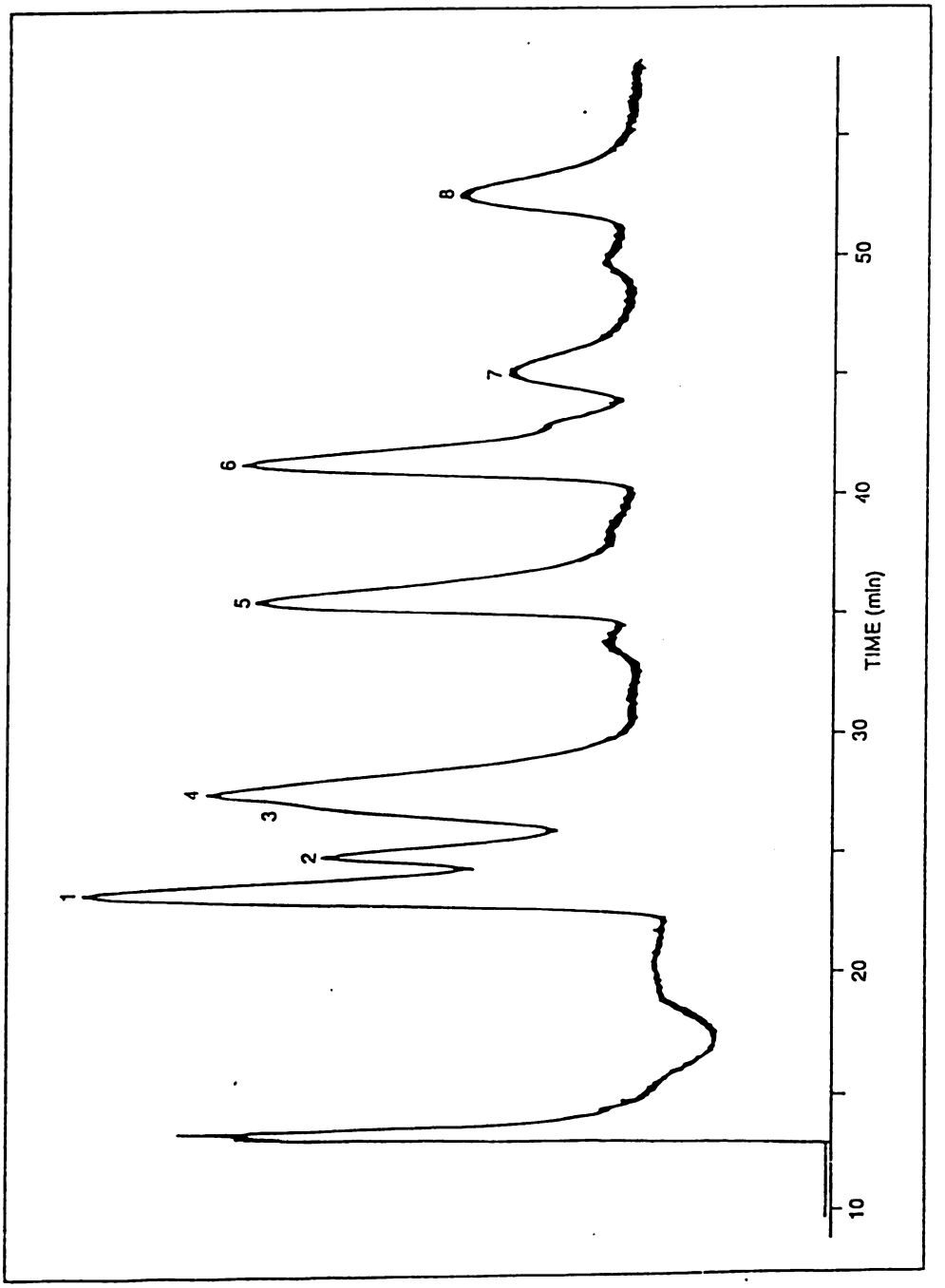

Table 3.4 Comparison of Experimental and Theoretical Capacity Factors under the Predicted Optimum Conditions for Solvent Modulation

CORTICOSTEROIDS	CAPACITY FACTOR (k)		
	Theory†	Experiment	Relative Error (%)‡
Prednisone	1.59	1.58	–0.63
Cortisone	1.76	1.78	1.14
Prednisolone	1.93	2.08	7.77
Hydrocortisone	2.06	2.10	1.94
Dehydrocorticosterone	3.08	2.97	–3.57
Methylprednisolone	3.59	3.60	0.28
Tetrahydrocortisol	3.82	4.01	4.97
Tetrahydrocortisone	4.76	4.82	1.26
Average			±2.70

† Calculated by using Equation [3.4].
‡ Calculated as 100 x (Experiment – Theory)/Theory.

3.5 Conclusions

Solvent modulation is a practical alternative to premixed mobile phases in liquid chromatography. Because the solvent zones are spatially and temporally separated from one another, solute retention is a simple time-weighted average of the retention in each individual solvent. Consequently, optimization of the separation is more accurate and requires fewer preliminary experiments with solvent modulation than with premixed solvents. In this study, the separation of corticosteroids was optimized by each technique and compared with respect to accuracy, total analysis time, critical resolution, and overall quality of the separation. The solvent modulation approach compares favorably in all of these respects and, hence, is demonstrated to be a very promising optimization strategy.

3.6 References

1. H. A. H. Billiet, L. de Galan, *J. Chromatogr.* **485**, 27 (1989)
2. J. L. Glajch, L. R. Snyder, *Computer-Assisted Method Development for High Performance Liquid Chromatography,* Elsevier, Amsterdam, 1990
3. L. R. Snyder, J. J. Kirkland, *Introduction to Modern liquid Chromatography,* 2nd ed., John-Wiley, New York, 1979
4. M. A. Quarry, R. L. Grob, L. R. Snyder, *J. Chromatogr.* **285**, 1 (1984)
5. M. A. Quarry, R. L. Grob, L. R. Snyder, *J. Chromatogr.* **285**, 19 (1984)
6. M. A. Quarry, R. L. Grob, L. R. Snyder, *Anal. Chem.* **58**, 907 (1986)
7. L. R. Snyder, M. A. Quarry, J. L. Glajch, *Chromatographia* **24**, 33 (1987)
8. L. R. Snyder, J. W. Dolan, D. C. Lommen, *J. Chromatogr.* **485**, 65 (1989)
9. J. W. Dolan, D. C. Lommen, L. R. Snyder, *J. Chromatogr.* **485**, 91 (1989)
10. R. J. Laub, J. H. Purnell, *J. Chromatogr.* **112**, 71 (1975)
11. L. R. Snyder, J. W. Dolan, *DryLab I User's Manual,* LC Resources Inc., Lafayette, CA, 1987
12. T. D. Schlabach, J. L. Excoffier, *J. Chromatogr.* **439**, 173 (1988)
13. W. Spendly, G. R. Hext, F. R. Hinsworth, *Technometrics* **4**, 44 (1962)
14. J. A. Nelder, R. Mead, *Comput. J.* **7**, 308 (1968)
15 J. H. Wahl, C. G. Enke, V. L. McGuffin, *Anal. Chem.* **62**, 1416 (1990)
16. J. H. Wahl, C. G. Enke, V. L. McGuffin, *Anal. Chem.* **63**, 1118 (1991)
17. J. H. Wahl, V. L. McGuffin, *J. Chromatogr.* **485**, 541 (1989)
18. J.H. Wahl, *Ph.D. Dissertation*, Michigan State University, 1991.

CHAPTER 4

MULTIVARIATE OPTIMIZATION OF MOBILE AND STATIONARY PHASES BY PARAMETRIC MODULATION

4.1 Introduction

The subject of this chapter is the experimental verification of multivariate optimization by the parametric modulation approach. In the work described herein, the use of serially coupled columns and solvent modulation is investigated as a viable strategy for the optimization of both stationary and mobile phases. By maintaining the stationary phases in separate columns and the mobile phases as separate zones, the solute will interact independently in each environment (Figure 1.4). Thus, overall solute retention will be a simple, predictable function of the capacity factor weighted by the time that the solute is exposed to each stationary and mobile phase. This approach should allow accurate prediction of solute retention and, hence, allow optimization of multidimensional separations with a minimum number of preliminary experiments.

4.2 Theoretical Development

The optimization of the separation requires that the overall retention time (t_i) be calculated when the solute is exposed to each stationary phase and

mobile phase. This is accomplished by summing retention within each individual environment as shown below

$$t_i = \sum_{p=1}^{q} \sum_{j=0}^{n} \frac{\pi r_p^2 \ \varepsilon_p \ x_j}{F} \left(\frac{1+k_{ijp}}{k_{ijp}} \right) \qquad [4.1]$$

where k_{ijp} is the capacity factor of solute i in solvent j on column p, r_p and ε_p are the radius and total porosity of column p, respectively, x_j is the length of solvent zone j, F is the volumetric flow rate, n and q are the limits of summation of number of solvent zones and columns, respectively.

In a similar manner, the variance (σ_i^2) of the solute zone in temporal units is calculated by independent summation as

$$(\sigma_i)^2 = \sum_{p=1}^{q} \sum_{j=0}^{n} (\sigma_{ijp})^2 = \sum_{p=1}^{q} \frac{h_p \, d_p}{l_p} \left(\sum_{j=0}^{n} \frac{\pi r_p^2 \ \varepsilon_p \ x_j}{F} \left(\frac{1+k_{ijp}}{k_{ijp}} \right) \right)^2 \qquad [4.2]$$

where h_p is the reduced plate height, d_p is the particle diameter, and l_p is the length of column p.

The resolution between adjacent solute zones ($R_{i,i+1}$) is then calculated by substitution of Equations [4.1] and [4.2] in the following expression

$$R_{i,i+1} = \frac{(t_{i+1} - t_i)}{2[(\sigma_{i+1})_t + (\sigma_i)_t]} \qquad [4.3]$$

Finally, a criterion such as the chromatographic resolution statistic (CRS) (1) shown below is used to evaluate the overall quality of the separation

$$CRS = \left(\sum_{i=1}^{m-1} \left(\frac{R_{i,i+1} - R_{opt}}{R_{i,i+1} - R_{min}} \right)^2 \frac{1}{R_{i,i+1}} + \sum_{i=1}^{m-1} \frac{(R_{i,i+1})^2}{(m-1)\, R_{avg}^2} \right) \frac{t_f}{m} \qquad [4.4]$$

where R_{opt} and R_{min} are the optimum and minimum resolution, respectively, R_{avg} is the average resolution, t_f is the total analysis time, and m is the number of solutes.

The computer program used to accomplish these calculations is given in Appendix [A1.2].

4.3 Experimental Methods

Materials and Methods. Reagent-grade polynuclear aromatic hydrocarbons (PAH) are obtained from Sigma Chemicals (St. Louis, MO, USA). Standard solutions are prepared at 10^{-4} M by dissolution of the PAH in spectroscopic-grade methanol. Organic solvents are high purity distilled-in-glass grade (Baxter Healthcare, Burdick and Jackson Division, Muskegon, MI, USA); water is deionized and doubly distilled in glass (Model MP-3A, Corning Glass Works, Corning, NY, USA).

Experimental System. The chromatographic system consists of a dual syringe pump (Model 140, Applied Biosystems, San Jose, CA, USA), which is programmed to deliver solvent zones for a specified time period at a nominal flow rate of 1 µL/min. Sample introduction is achieved by using a 1.0 µL injection valve (Model ECI4W1, Valco Instruments, Houston, TX, USA), after which the effluent stream is split (75:1) and applied to the chromatographic column. The

microcolumns are prepared from fused-silica capillary tubing (200 μm I.D., Polymicro Technologies, Phoenix, AZ, USA), whose length can be readily adjusted, and terminated with a quartz wool frit. The microcolumns are packed with octadecylsilica and β-cyclodextrinsilica materials (5 μm diameter, Advanced Separation Technologies, Whippany, NJ, USA) according to the slurry packing procedure described previously (2). The octadecylsilica and β-cyclodextrinsilica columns, respectively, have total porosity (ε_p) of 0.81 and 0.80, separation impedance (ϕ_p) of 890 and 720, and reduced plate height (h_p) of 3.2 and 12.9 using pyrene as a model solute under standard test conditions (2).

The polynuclear aromatic hydrocarbon solutes are detected using both laser-induced fluorescence and UV-visible absorbance in a 75 μm I.D. fused-silica capillary flow cell. In the fluorescence detection system [37,38], a helium-cadmium laser (325 nm, 25 mW, Model 3074-40M, Omnichrome, Chino, CA, USA) is reflected by a dielectric mirror and focussed on the capillary with a quartz lens. The fluorescence emission is collected perpendicular and coplanar to the excitation beam with another quartz lens, spectrally isolated with a bandpass interference filter (420 nm, S10-420-F, Corion, Holliston, MA, USA), and focussed onto a photomultiplier tube (Model Centronic Q4249B, Bailey Instruments, Saddle Brook, NJ, USA). The photocurrent is amplified and converted to voltage by a picoammeter (Model 480, Keithley Instruments, Cleveland, OH, USA). A variable-wavelength UV-absorbance detector (Model Uvidec 100-V, Japan Spectroscopic Co., Tokyo, Japan), operated at 254 nm, is placed in series after the fluorescence detector. Data are acquired simultaneously from both detectors using an analog-to-digital converter (Model DT2805-5716, Data Translation, Marlborough, MA, USA) together with a personal computer (Model ZMF-248-40, Zenith Data Systems, St. Joseph, MI, USA). The data acquisition programs are written in the Forth-based

programming language ASYST (Version 2.1, Keithley Asyst, Rochester, NY, USA).

Computer-Assisted Optimization Program. The computer optimization program is written in the FORTRAN 77 language to be executed on a VAXstation 3200 computer (Digital Equipment, Maynard, MA, USA). This program generates a complete CRS response surface by using a systematic mapping procedure. The lengths of each column and solvent zone are varied independently within prescribed limits; column lengths are varied from 0 to 75 cm and solvent zones are varied from the minimum length that maintains 95% purity (Equation [2.15]) to the maximum length required to elute all solutes. For each combination of column and solvent lengths, the total retention time and variance of each solute peak are calculated by means of Equations [4.1] and [4.2], respectively. The resolution between each pair of adjacent solute peaks is calculated by using Equation [4.3]. Finally, the overall quality of the separation is assessed by means of the modified CRS function (Equations [4.4] and [2.19]), using selected values for the optimum and minimum acceptable resolution of 1.5 and 0.3, respectively. By graphing the CRS value as a function of the column and solvent zone lengths, a complete multidimensional response surface can be constructed. The minimum CRS value is then identified by visual inspection of the response surface. To assist in identifying the minimum CRS value, the five best conditions are continuously updated and stored in a file by the computer program.

4.4 Results and Discussion

The goal of these preliminary studies is to demonstrate the conceptual basis and to test the theoretical models of solvent modulation using serially coupled columns. To facilitate these goals, the stationary phases were selected for their dissimilar retention mechanisms, but compatible mobile phase requirements. Octadecylsilica retains solutes predominantly by a partition mechanism, whereas β-cyclodextrinsilica forms inclusion complexes based on the size and shape of the solute. Although both of these phases interact with solutes by van der Waals forces, monomeric octadecylsilica is dominated by enthalpic effects while β-cyclodextrinsilica has a significant entropic contribution. This difference in retention mechanisms may be advantageous for the separation of isomeric four- and five-ring polynuclear aromatic hydrocarbons (PAH), whose structures are shown in Figure 4.1.

The capacity factors for each PAH were measured on the octadecylsilica and β-cyclodextrinsilica stationary phases using mobile phases with compositions of 80% and 90% aqueous methanol as well as 50% and 70% aqueous acetonitrile. On the octadecylsilica phase (Table 4.1), many of the isomeric four- and five-ring compounds are well separated. However, there are several critical pairs that are difficult to resolve in all mobile phases, most notably chrysene and benz[a]anthracene, as well as benzo[e]pyrene and perylene.

Although PAH molecules are reported to form inclusion complexes with β-cyclodextrinsilica (3-7), the capacity factors are very small under all experimental conditions examined herein (Table 4.2). Only by using the weakest mobile phases is the PAH retention measurable and the resolution partially achieved. Although methanol mobile phases show no selectivity based on either solute size or shape, the acetonitrile mobile phases appear to be able to discriminate

Figure 4.1 Structures of isomeric four- and five-ring polynuclear aromatic hydrocarbons.

Figure 4.1

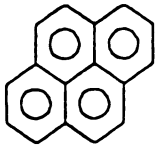

PYRENE

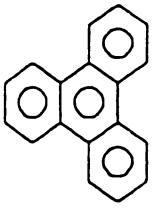

TRIPHENYLENE

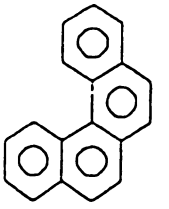

BENZO[c]PHENANTHRENE

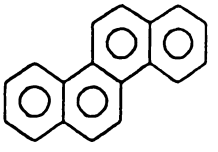

CHRYSENE

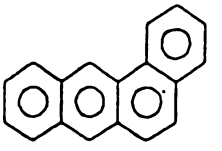

BENZ[a]ANTHRACENE

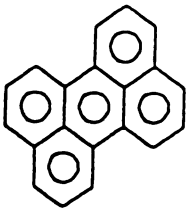

PERYLENE

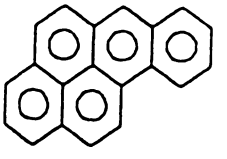

BENZO[a]PYRENE

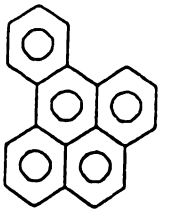

BENZO[e]PYRENE

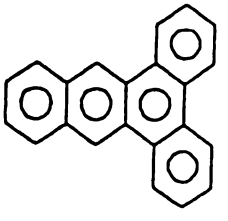

DIBENZ[a,c]ANTHRACENE

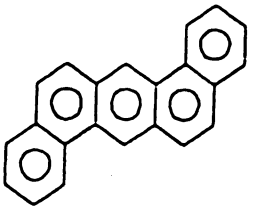

DIBENZ[a,h]ANTHRACENE

Table 4.1 Capacity factors (k_{ijp}) for polynuclear aromatic hydrocarbons on octadecylsilica stationary phase using aqueous methanol and acetonitrile mobile phases.

POLYNUCLEAR AROMATIC HYDROCARBONS	CAPACITY FACTOR (k_{ijp})			
	METHANOL		ACETONITRILE	
	80%	90%	50%	70%
PYRENE	4.65	1.93	14.5	4.12
TRIPHENYLENE	5.90	2.39	18.7	5.01
BENZO[c]PHENANTHRENE	6.23	2.69	20.9	5.37
CHRYSENE	6.91	2.61	22.6	5.52
BENZ[a]ANTHRACENE	7.00	2.61	23.0	5.64
BENZO[e]PYRENE	10.5	3.78	31.8	8.16
PERYLENE	10.8	3.74	32.0	8.18
BENZO[a]PYRENE	13.0	4.01	39.3	9.45
DIBENZ[a,c]ANTHRACENE	15.0	4.64	49.0	10.6
DIBENZ[a,h]ANTHRACENE	17.6	5.45	56.4	11.7

Table 4.2 Capacity factors (k_{ijp}) for polynuclear aromatic hydrocarbons on β-cyclodextrinsilica stationary phase using aqueous methanol and acetonitrile mobile phases.

POLYNUCLEAR AROMATIC HYDROCARBONS	CAPACITY FACTOR (k_{ijp})			
	METHANOL		ACETONITRILE	
	80%	90%	50%	70%
PYRENE	0.09	0.06	0.18	0.08
TRIPHENYLENE	0.11	0.06	0.16	0.08
BENZO[c]PHENANTHRENE	0.13	0.06	0.18	0.07
CHRYSENE	0.15	0.07	0.17	0 08
BENZ[a]ANTHRACENE	0.15	0.06	0.19	0.09
BENZO[e]PYRENE	0.12	0.06	0.25	0.14
PERYLENE	0.18	0.14	0.36	0.17
BENZO[a]PYRENE	0.15	0.07	0.26	0.15
DIBENZ[a,c]ANTHRACENE	0.16	0.08	0.35	0.16
DIBENZ[a,h]ANTHRACENE	0.18	0.08	0.37	0.17

between the four- and five-ring classes. The most noteworthy and useful result is that perylene may be readily separated from both benzopyrene isomers on the β-cyclodextrinsilica phase.

Based on these results, it seems reasonable to expect that resolution of the PAH can be achieved by serial coupling of the octadecylsilica and β-cyclodextrinsilica columns. However, there are 64 possible permutations for the columns and solvents examined in this study: 8 one-column/one-solvent systems, 24 one-column/two-solvent systems, 8 two-column/one-solvent systems, and 24 two-column/two-solvent systems. It would clearly be nearly impossible to examine all of these possibilities by time-consuming, trial-and-error experimental measurements. However, the computer program described previously provides a rapid and effective means to identify the most promising permutation. The individual capacity factors (k_{ijp}) for the PAH solutes shown in Tables 4.1 and 4.2 are used to calculate the retention time and variance according to Equations [4.1] and [4.2], respectively. The resolution of each adjacent pair of solutes is calculated from Equation [4.3], and the overall quality of the separation is assessed by the CRS function in Equation [4.4]. For each possible combination and sequence of columns and solvents, the minimum CRS values are stored in a file and are used to identify the most promising permutation for further study. The results of these preliminary simulations are summarized in Table 4.3 for the permutations of a two-column/two-solvent chromatographic system. If the minimum CRS value is used as the criterion for evaluation, then the best column sequence is predicted to be octadecylsilica followed by β-cyclodextrinsilica, and the best solvent sequence is 80% methanol followed by 50% acetonitrile. These conditions should provide a minimum resolution of 0.97 with a total analysis time of 113 minutes.

Table 4.3 Evaluation of the permutations of a two-column/two-solvent chromatographic system for the separation of polynuclear aromatic hydrocarbons. The columns are octadecylsilica (ODS) and β-cyclodextrinsilica (β-CD); the solvents are aqueous mixtures of methanol (CH_3OH) and acetonitrile (CH_3CN) as given in Tables 4.1 and 4.2. The analysis time (t_f), minimum resolution ($(R_{i,i+1})_{min}$) and minimum Chromatographic Resolution Statistic (CRS_{min}) function corresponding to the optimum conditions are given.

COLUMN 1	COLUMN 2	SOLVENT 1	SOLVENT 2	t_f (min)	$(R_{i,i+1})_{min}$	CRS_{min}
ODS	β-CD	80% CH_3OH	90% CH_3OH	326	0.61	520
ODS	β-CD	90% CH_3OH	80% CH_3OH	373	0.61	590
ODS	β-CD	50% CH_3CN	70% CH_3CN	349	0.71	250
ODS	β-CD	70% CH_3CN	50% CH_3CN	344	0.72	250
ODS	β-CD	80% CH_3OH	50% CH_3CN	113	0.97	33
ODS	β-CD	50% CH_3CN	80% CH_3OH	159	0.99	43
ODS	β-CD	80% CH_3OH	70% CH_3CN	326	0.85	160
ODS	β-CD	70% CH_3CN	80% CH_3OH	318	0.87	160
ODS	β-CD	90% CH_3OH	50% CH_3CN	282	0.59	530
ODS	β-CD	50% CH_3CN	90% CH_3OH	259	0.59	480
ODS	β-CD	90% CH_3OH	70% CH_3CN	241	0.46	3,100
ODS	β-CD	70% CH_3CN	90% CH_3OH	209	0.48	2,500

If resolution and not analysis time is considered to be the primary goal, the final term may be neglected in evaluation of the CRS function in Equation [4.4]. Under these conditions, the results for the permutations of a two-column/two-solvent chromatographic system are summarized in Table 4.4. In some cases, the optimum separation is virtually identical to that identified in Table 4.3; in other cases, a significant increase in resolution is achieved, usually at the expense of an increase in analysis time. Again, the most promising choice for column sequence is octadecylsilica followed by β-cyclodextrinsilica, and the most promising solvent sequence is 80% methanol followed by 50% acetonitrile. This permutation will be evaluated in further detail below.

In order to identify the most favorable experimental conditions, the computer program is used first to determine the optimum lengths of the octadecylsilica and β-cyclodextrinsilica columns. The topographic and contour maps of the CRS response surface are shown in Figure 4.2 as a function of the column length. It is apparent that the overall quality of the separation improves dramatically with increasing length of the octadecylsilica column. Although the extent of the improvement after 25 cm is relatively small, the minimum CRS value is achieved for a column length of 75 cm. In contrast, the β-cyclodextrinsilica column has no beneficial effect upon the separation and, thus, has an optimal column length of 0 cm.

The computer program is used next to determine the optimum lengths of the 80% methanol and 50% acetonitrile solvent zones. The topographic and contour maps of the CRS response surface are shown in Figure 4.3 as a function of the solvent zone length. There are several regions that yield low values for the CRS function; the overall minimum value is observed for solvent lengths of 167 cm of 80% methanol and 318 cm of 50% acetonitrile.

Table 4.4 Evaluation of the permutations of a two-column/two-solvent chromatographic system for the separation of polynuclear aromatic hydrocarbons. The columns are octadecylsilica (ODS) and β-cyclodextrinsilica (β-CD); the solvents are aqueous mixtures of methanol (CH_3OH) and acetonitrile (CH_3CN) as given in Tables 4.1 and 4.2. The analysis time (t_f), minimum resolution ($(R_{i,i+1})_{min}$) and minimum Chromatographic Resolution Statistic (CRS_{min}) function corresponding to the optimum conditions are given, when analysis time is not considered to be a goal of the optimization.

COLUMN 1	COLUMN 2	SOLVENT 1	SOLVENT 2	t_f (min)	$(R_{i,i+1})_{min}$	CRS_{min}
ODS	β-CD	80% CH_3OH	90% CH_3OH	374	0.61	16
ODS	β-CD	90% CH_3OH	80% CH_3OH	373	0.61	16
ODS	β-CD	50% CH_3CN	70% CH_3CN	349	0.71	7.3
ODS	β-CD	70% CH_3CN	50% CH_3CN	344	0.72	7.2
ODS	β-CD	80% CH_3OH	50% CH_3CN	666	1.39	1.9
ODS	β-CD	50% CH_3CN	80% CH_3OH	586	1.37	2.0
ODS	β-CD	80% CH_3OH	70% CH_3CN	326	0.85	5.0
ODS	β-CD	70% CH_3CN	80% CH_3OH	322	0.87	5.0
ODS	β-CD	90% CH_3OH	50% CH_3CN	427	0.70	15
ODS	β-CD	50% CH_3CN	90% CH_3OH	386	0.70	15
ODS	β-CD	90% CH_3OH	70% CH_3CN	241	0.46	130
ODS	β-CD	70% CH_3CN	90% CH_3OH	209	0.48	120

Figure 4.2A Topographic map of the CRS response surface as a function of the column length (cm) for octadecylsilica and β-cyclodextrinsilica.

Figure 4.2A

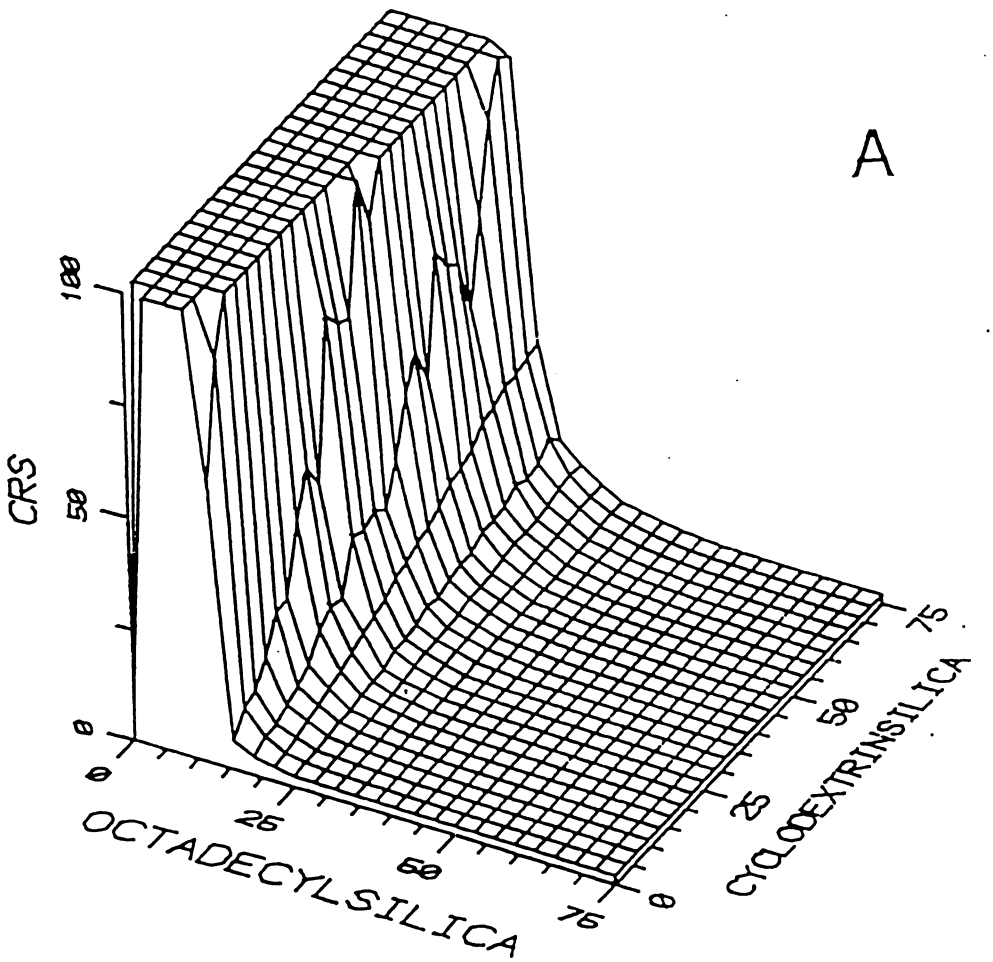
A
CRS
100
50
0
0
25
50
75
OCTADECYLSILICA
0
25
50
75
CYCLODEXTRINSILICA

Figure 4.2B Contour map of the CRS response surface as a function of the column length (cm) for octadecylsilica and β-cyclodextrinsilica.

Figure 4.2B

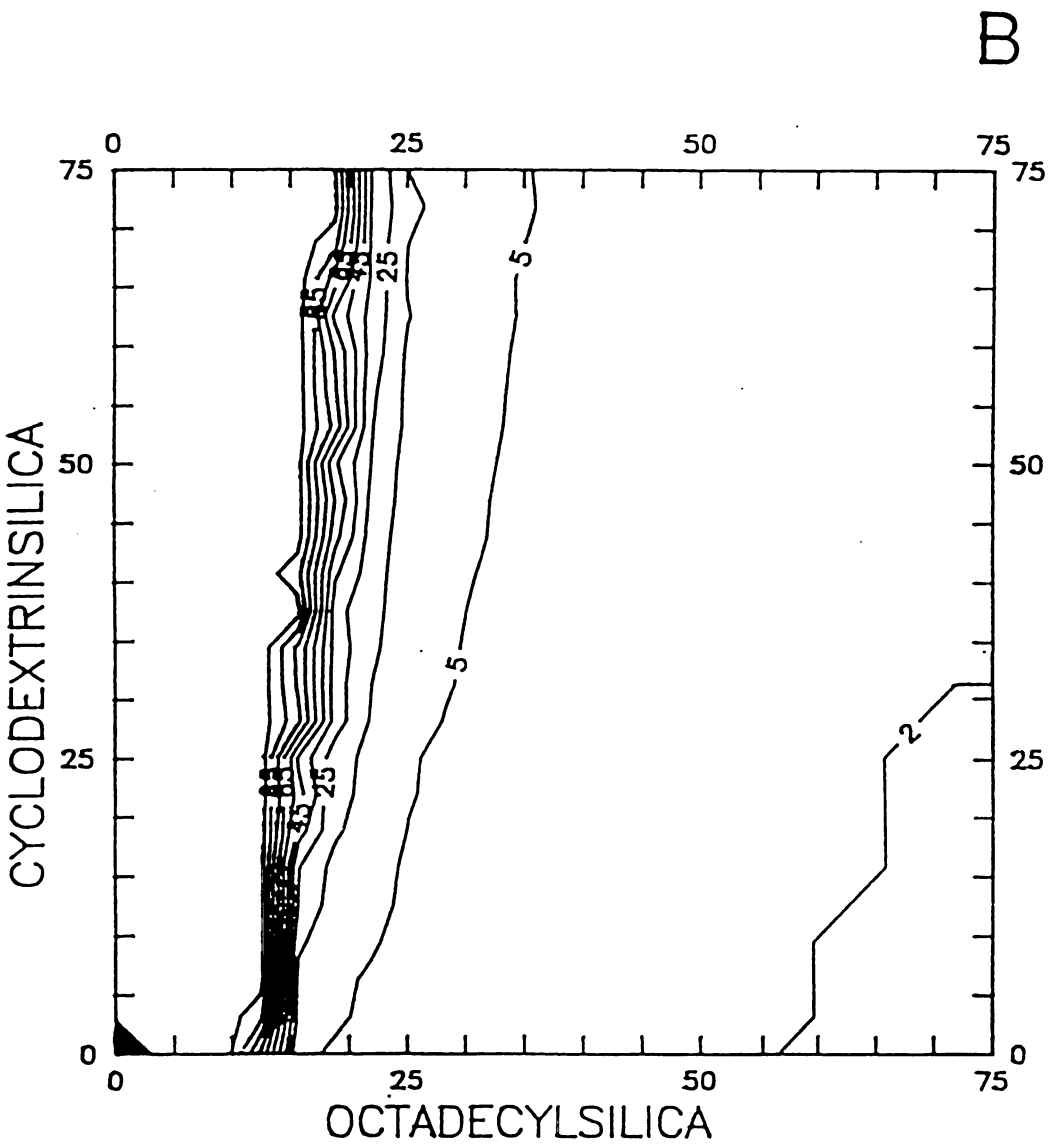

Figure 4.3A Topographic map of the CRS response surface as a function of the solvent zone length (cm) for 80% methanol and 50% acetonitrile.

Figure 4.3A

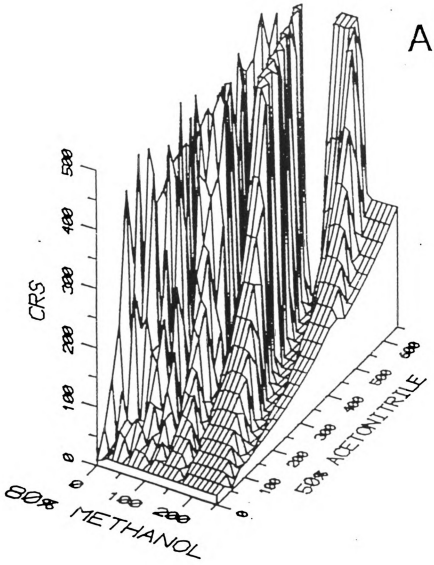
A
CRS
0
100
200
300
400
500
80% METHANOL
0
100
200
50% ACETONITRILE
0
100
200
300
400
500
600

Figure 4.3B Contour map of the CRS response surface as a function of the solvent zone length (cm) for 80% methanol and 50% acetonitrile.

Figure 4.3B

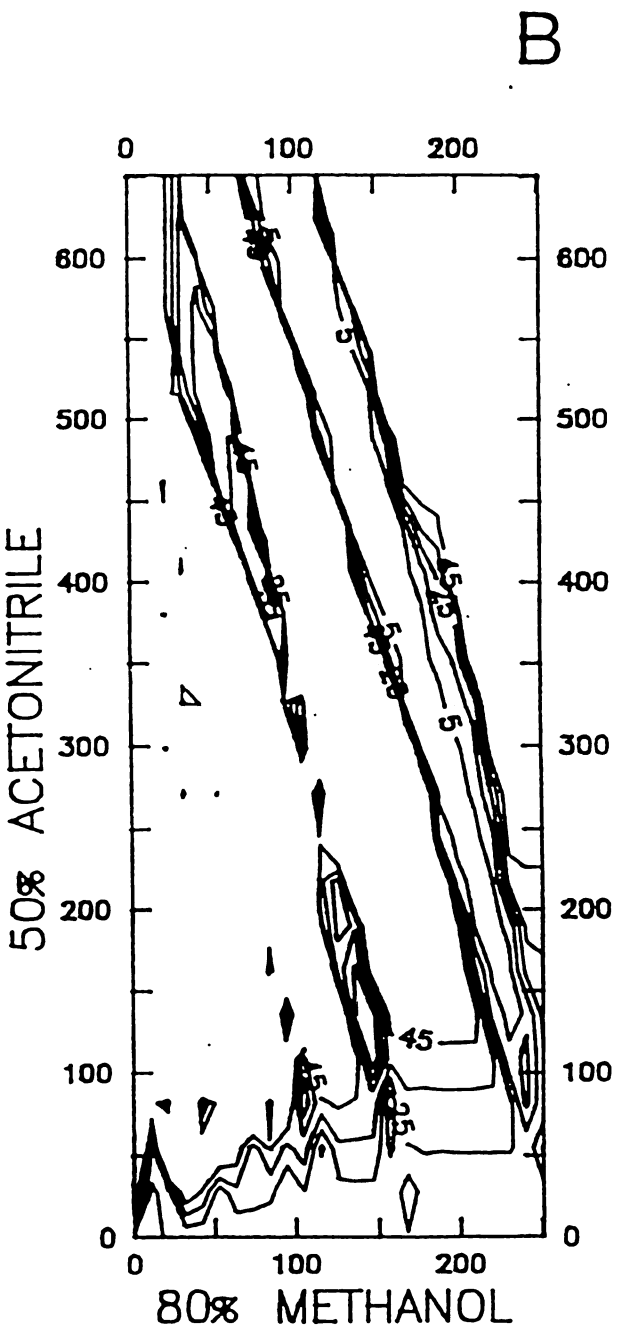
B
0
100
200
600
500
400
300
200
100
0
50% ACETONITRILE
80% METHANOL
45
25
5

The predicted separation of the isomeric four- and five-ring PAH with a 75 cm octadecylsilica column is shown in Figure 4.4. The optimal solvent modulation sequence of 80% methanol and 50% acetonitrile in zones of 167 and 318 cm length, respectively, provides a good overall separation (CRS = 1.9) with an analysis time of 666 min. Under these conditions, the critical solute pair is chrysene and benz[a]anthracene ($R_{i,i+1}$ = 1.39). All other solute pairs have resolution greater than the optimum value (1.5), which is desirable for accurate qualitative and quantitative analysis.

Although this optimized separation initially appears to be very promising, a more detailed examination of the CRS response surfaces is warranted. In the immediate vicinity of the optimum conditions shown in Figure 4.3, the CRS function is found to vary in a significant and abrupt manner. For example, as the solvent zone length of 80% methanol changes by ±5 cm, the CRS value increases by approximately two orders of magnitude. Thus, small variations in the experimental conditions may have a highly detrimental effect upon the quality of the separation. The next most favorable permutation identified from Table 4.4, in which the column sequence is octadecylsilica followed by β-cyclodextrinsilica and the solvent sequence is 70% acetonitrile followed by 80% methanol, does not suffer from this limitation. This permutation will be evaluated in further detail below.

The topographic and contour maps of the CRS response surface are shown in Figure 4.5 as a function of the column length. The overall quality of the separation improves continuously with increasing length of the octadecylsilica column, up to the limit of 75 cm. As noted for the previous case, β-cyclodextrinsilica is relatively ineffectual and, thus, has an optimal length of 0 cm.

The topographic and contour maps of the CRS response surface are shown in Figure 4.6 as a function of the solvent zone length. There is a broad

Figure 4.4 Predicted chromatogram for the isomeric PAH with a 75 cm octadecylsilica column using the optimal solvent modulation sequence of 80% methanol and 50% acetonitrile in zones of 167 and 318 cm length, respectively. Solutes: (1) pyrene, (2) triphenylene, (3) benzo[c]phenanthrene, (4) chrysene, (5) benz[a]anthracene, (6) benzo[e]pyrene, (7) perylene, (8) benzo[a]pyrene, (9) dibenz[a,c]anthracene, (10) dibenz[a,h]anthracene.

Figure 4.4

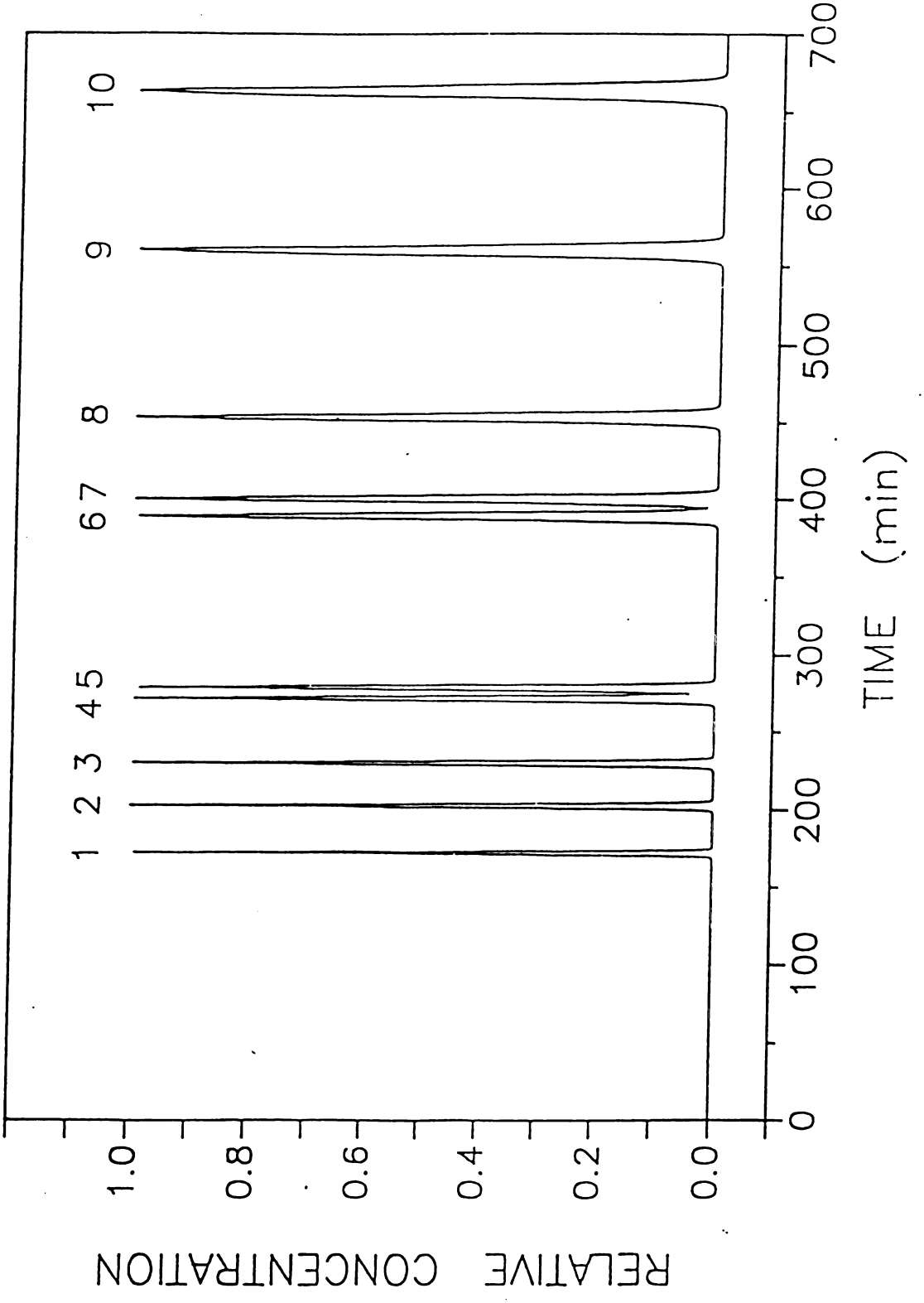
1
2
3
4
5
6
7
8
9
10
0
100
200
300
400
500
600
700
TIME (min)
1.0
0.8
0.6
0.4
0.2
0.0
RELATIVE CONCENTRATION

Figure 4.5A Topographic map of the CRS response surface as a function of the column length (cm) for octadecylsilica and β-cyclodextrinsilica.

Figure 4.5A

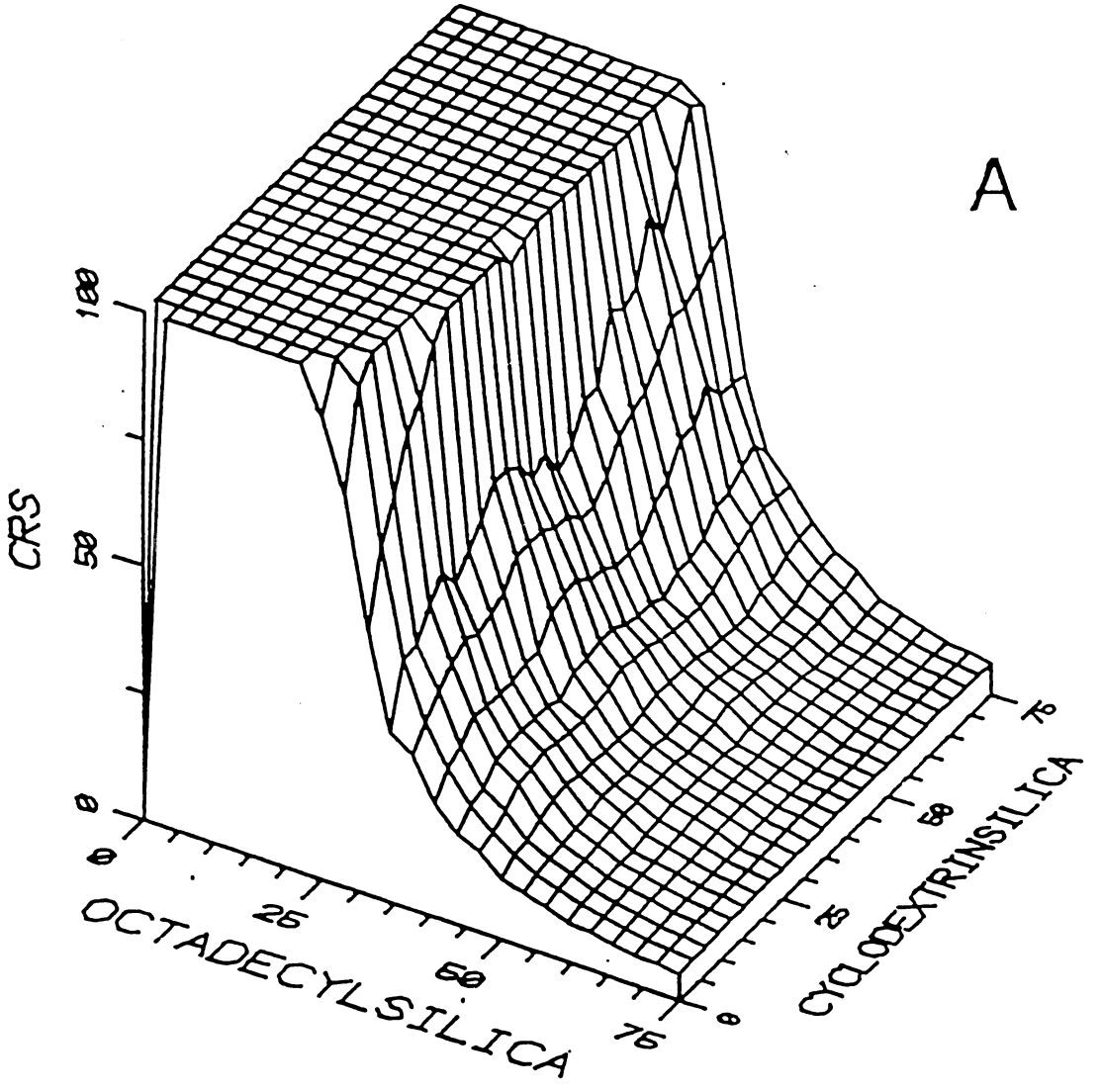
A
CRS
100
50
0
0
25
50
75
OCTADECYLSILICA
0
25
50
75
CYCLODEXTRINSILICA

Figure 4.5B Contour map of the CRS response surface as a function of the column length (cm) for octadecylsilica and β-cyclodextrinsilica.

Figure 4.5B

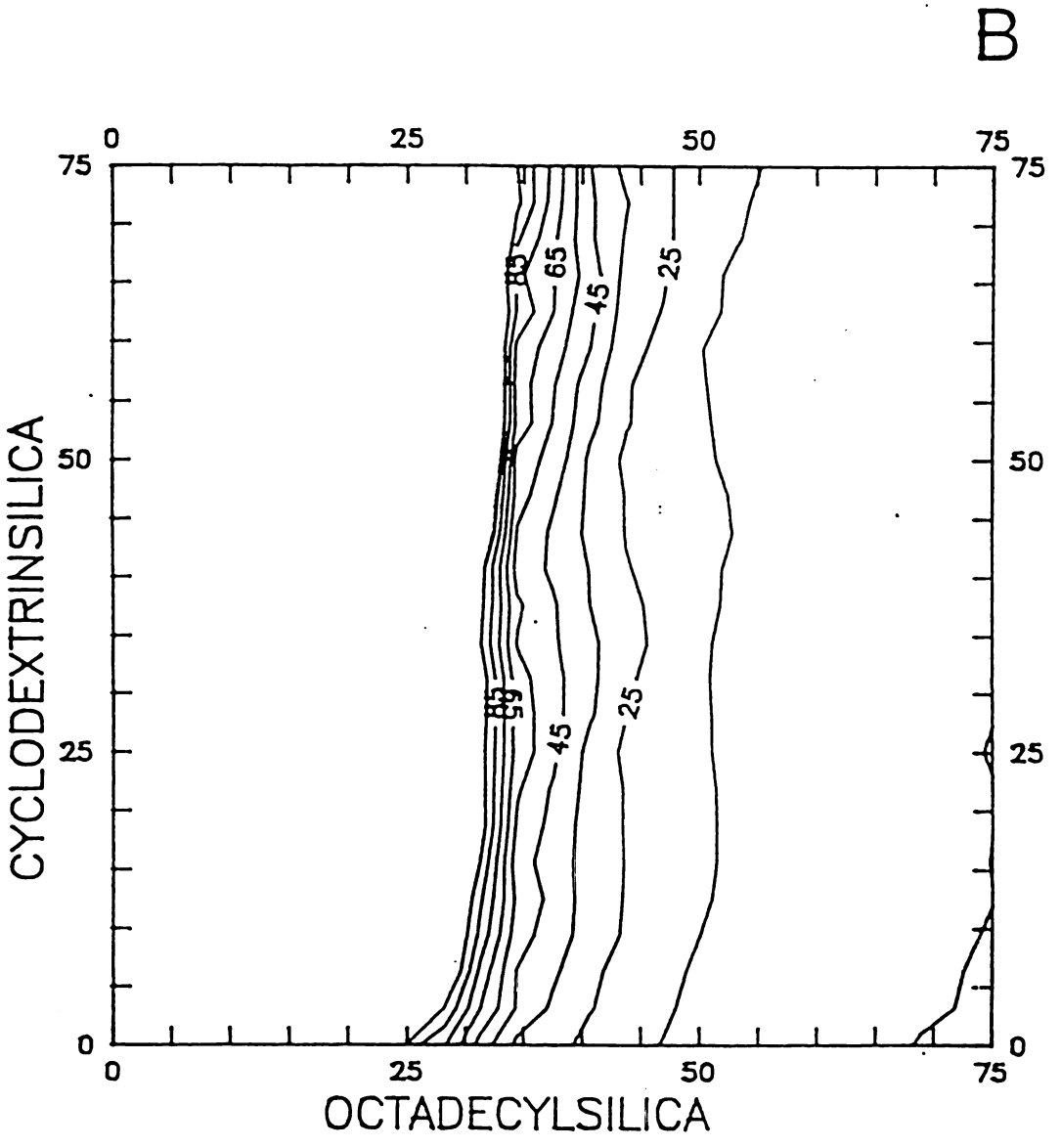

Figure 4.5B Contour map of the CRS response surface as a function of the column length (cm) for octadecylsilica and β-cyclodextrinsilica.

Figure 4.5B

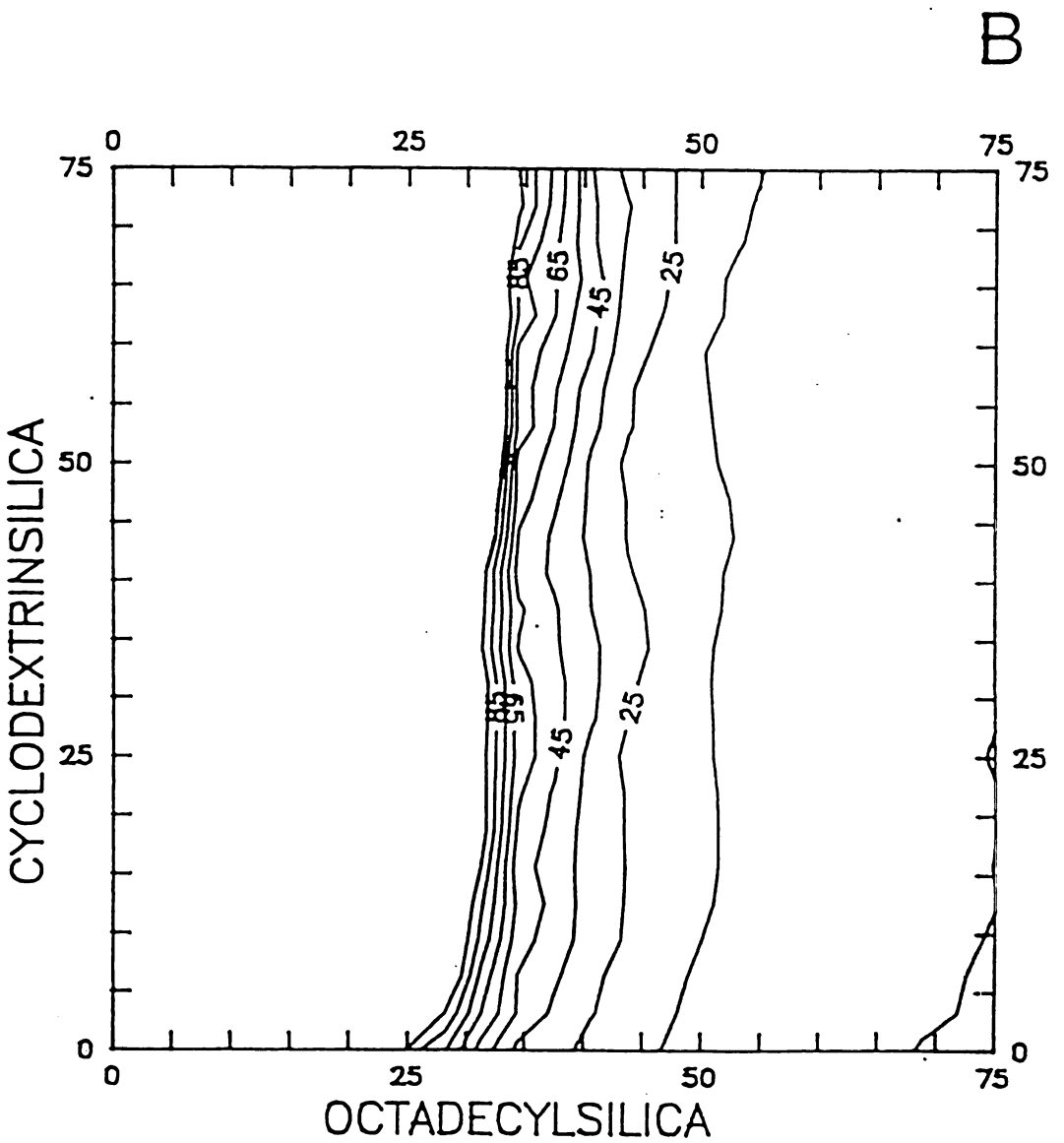

Figure 4.6A Topographic map of the CRS response surface as a function of the solvent zone length (cm) for 70% acetonitrile and 80% methanol.

Figure 4.6A

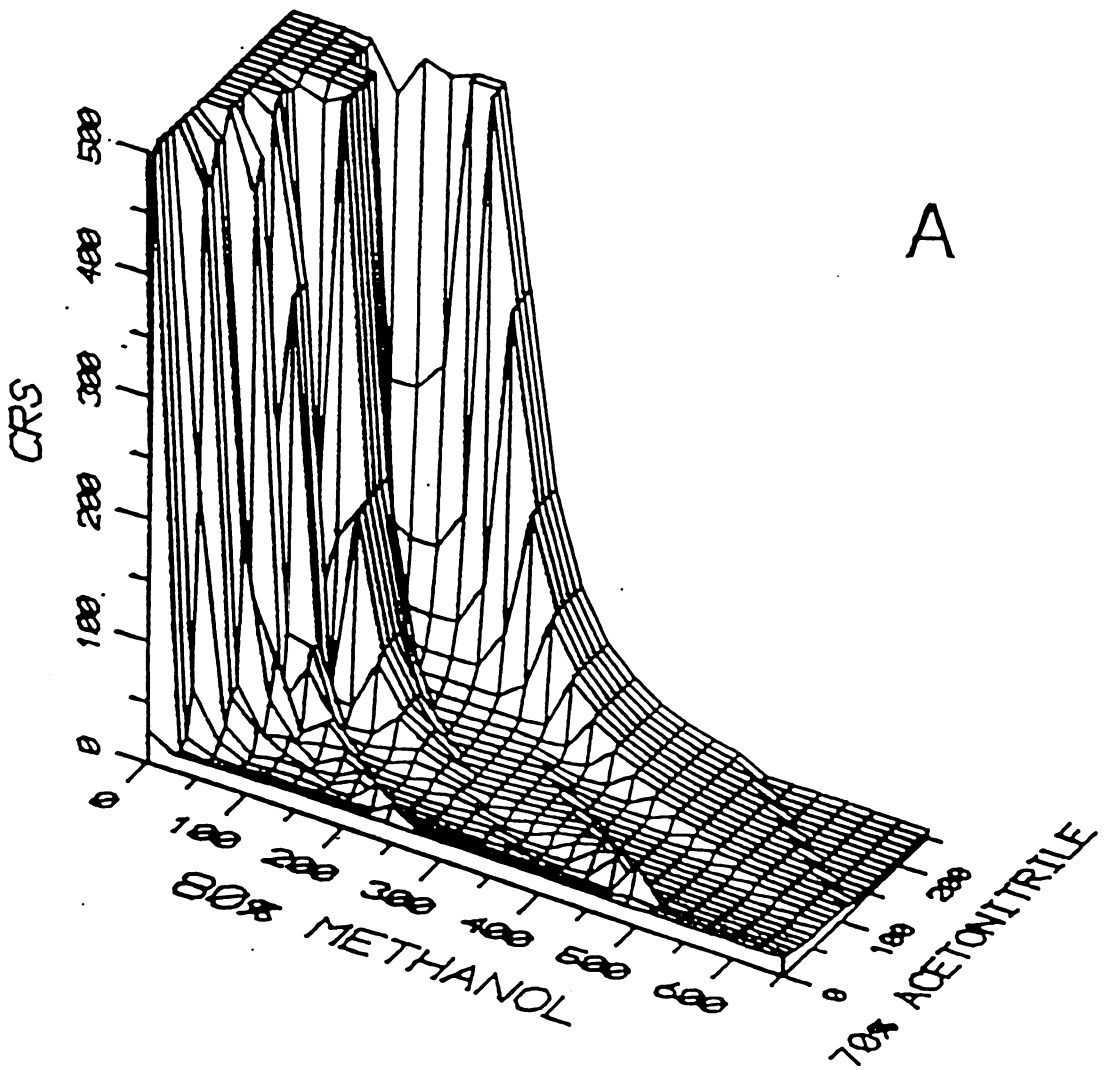
A
CRS
0
100
200
300
400
500
0
100
200
300
400
500
600
80% METHANOL
0
100
200
70% ACETONITRILE

Figure 4.6B Contour map of the CRS response surface as a function of the solvent zone length (cm) for 70% acetonitrile and 80% methanol.

Figure 4.6B

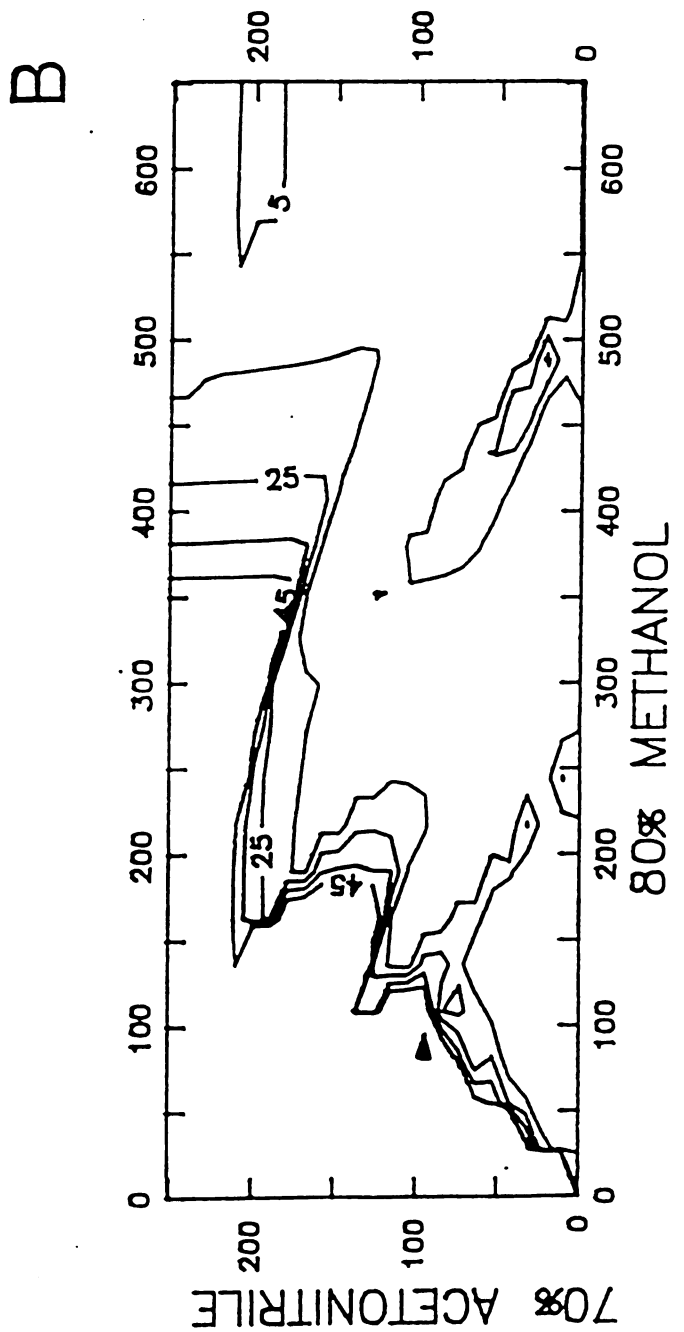

region of the surface having relatively low values for the CRS function; the minimum value is achieved for solvent lengths of 203 cm of 70% acetonitrile and 634 cm of 80% methanol.

The predicted separation of the isomeric PAH with a 75 cm octadecylsilica column is shown in Figure 4.7. The optimal solvent modulation sequence of 70% acetonitrile and 80% methanol in zones of 203 and 634 cm length, respectively, provides an excellent separation (CRS = 5.0) with an analysis time of 319 min. All solute pairs have resolution greater than the minimum acceptable value (0.3), whereas two pairs have resolution less than the optimum value (1.5). These critical solute pairs are chrysene and benz[a]anthracene ($R_{i,i+1}$ = 0.88), as well as benzo[e]pyrene and perylene ($R_{i,i+1}$ = 0.88). Because the CRS response surfaces shown in Figures 4.5 and 4.6 are relatively flat in the vicinity of the optimum, small discrepancies in column length and solvent zone length should have little effect upon the quality of the separation. Thus, the analytical method should be relatively reproducible and rugged.

In order to demonstrate the practical application of this method, the separation of the isomeric four- and five-ring PAH was performed under the predicted optimum conditions. The experimental chromatogram (Figure 4.8) shows excellent separation of all PAH standards with resolution comparable to that in the predicted chromatogram (Figure 4.7). The experimental retention time and peak width for each PAH standard agree well with the theoretically predicted values from Equations [4.1] and [4.2], respectively, as summarized in Table 4.5. The average relative error is ±3.5% for retention time and ±21% for peak width. Thus, the theoretical models developed herein can accurately predict the experimental results for solvent modulation in serially coupled columns.

Figure 4.7 Predicted chromatogram for the isomeric PAH with a 75 cm octadecylsilica column using the optimal solvent modulation sequence of 70% acetonitrile and 80% methanol in zones of 203 and 634 cm length, respectively. Solutes as given in Figure 4.4.

Figure 4.7

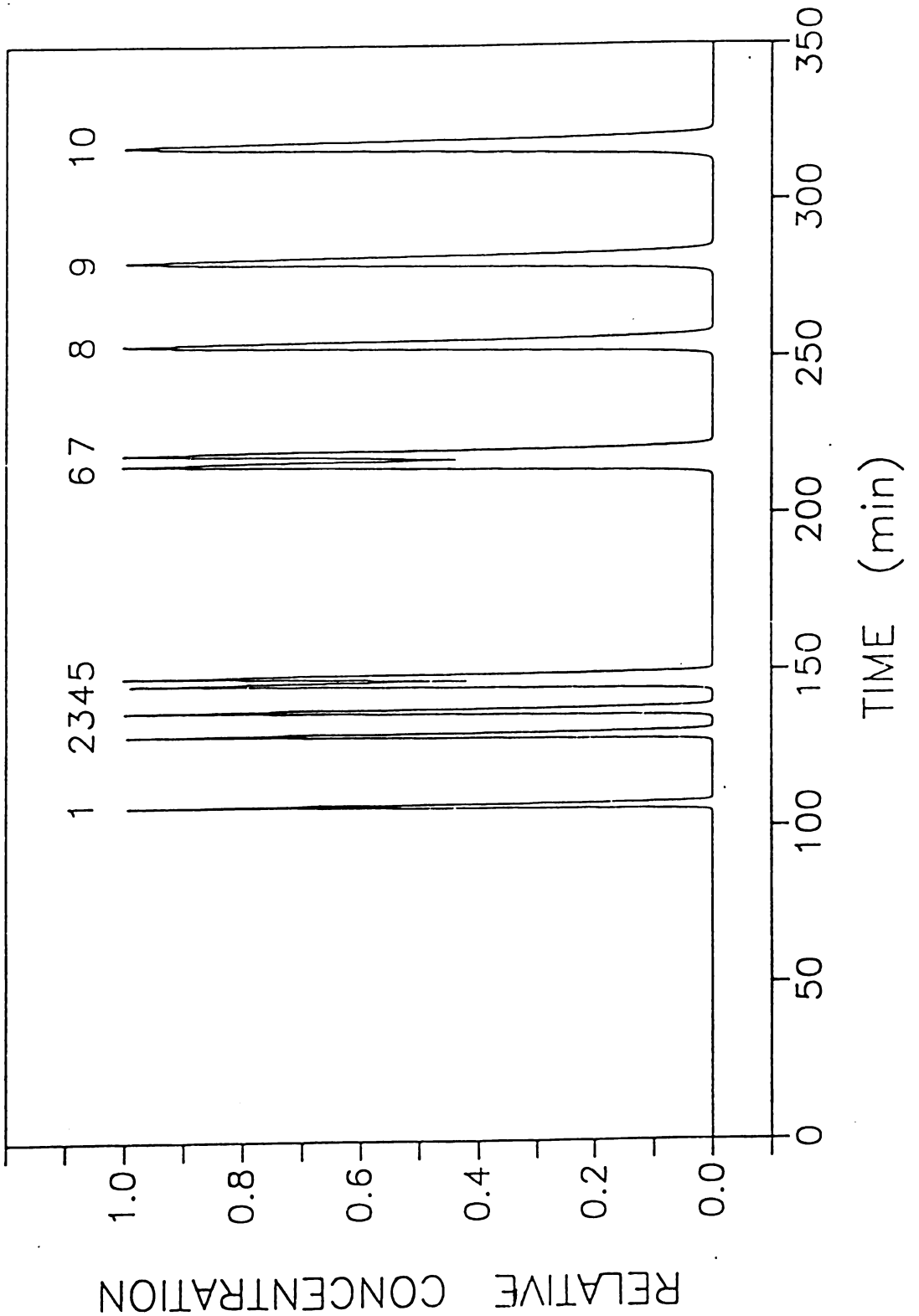
1
2345
67
8
9
10
0
50
100
150
200
250
300
350
TIME (min)
1.0
0.8
0.6
0.4
0.2
0.0
RELATIVE CONCENTRATION

Figure 4.8 Experimental chromatogram obtained under the predicted optimum conditions. Column: 200 µm I.D. x 75 cm fused silica capillary, packed with 5 µm octadecylsilica. Mobile phase: solvent modulation sequence of 70% acetonitrile and 80% methanol in zones of 203 and 634 cm length, respectively, 0.95 µL/min. Detectors: (A) UV-visible absorbance at 254 nm to indicate solvent modulation sequence, (B) Laser-induced fluorescence with excitation at 325 nm and emission at 420 nm to indicate solute retention. Solutes: (0) injection solvent, (1) pyrene, (2) triphenylene, (3) benzo[c]phenanthrene, (4) chrysene, (5) benz[a]anthracene, (6) benzo[e]pyrene, (7) perylene, (8) benzo[a]pyrene, (9) dibenz[a,c]anthracene, (10) dibenz[a,h]anthracene.

Figure 4.8

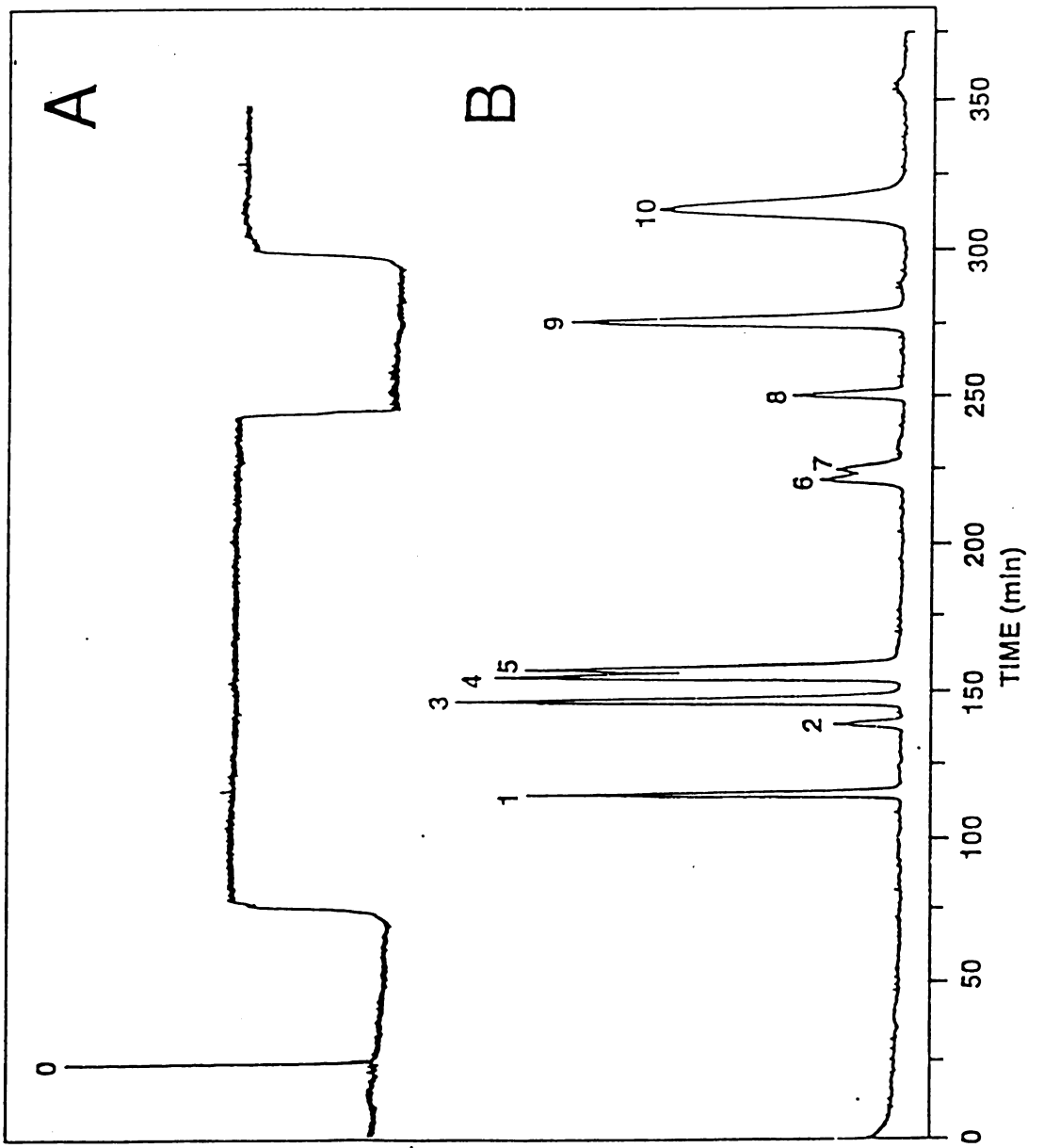

Table 4.5 Comparison of experimental (EXPT) and theoretical (THEORY) retention time and peak width under the predicted optimum conditions illustrated in Figures 4.7 and 4.8.

POLYNUCLEAR AROMATIC HYDROCARBONS	RETENTION TIME (min)			WIDTH (min)		
	EXPT	THEORY[a]	% ERROR[b]	EXPT	THEORY[c]	% ERROR[b]
PYRENE	112	107	4.7	2.3	2.0	15
TRIPHENYLENE	136	129	5.4	2.8	2.4	17
BENZO[c]PHENANTHRENE	143	137	4.4	3.0	2.5	20
CHRYSENE	151	146	3.4	3.1	2.7	15
BENZ[a]ANTHRACENE	154	148	4.1	3.1	2.7	15
BENZO[e]PYRENE	218	217	0.5	3.2	4.0	−20
PERYLENE	221	220	0.5	3.2	4.1	−22
BENZO[a]PYRENE	247	257	−3.9	4.1	4.8	−15
DIBENZ[a,c]ANTHRACENE	271	284	−4.6	5.1	5.2	−6.0
DIBENZ[a,h]ANTHRACENE	310	320	−3.1	9.9	5.9	68
AVERAGE			±3.5			±21

[a] Calculated from Equation (4.1).
[b] % ERROR = 100 (EXPT − THEORY)/THEORY
[c] Calculated from Equation (4.2), assuming a peak width of 4 $(\sigma_i)_t$.

4.5 Conclusion

The complete optimization of separations in multimodal or multidimensional liquid chromatography is a nontrivial task due, in part, to the large number of variable parameters and, in part, to deviations from ideal retention behavior. The computer program developed in this work appears to present a promising approach for examining all possible permutations of parameters, such as stationary and mobile phases, that may be used in multidimensional optimization. Because the individual stationary and mobile phases are spatially separated from one another, solute retention is a simple, time-weighted average of each environment to which the solute is exposed. For a system comprised of q columns and n solvents, only q x n measurements of the solute capacity factor are necessary. From these measurements, retention may be accurately predicted for any sequence and length of the stationary and mobile phases. This approach was demonstrated for the separation of isomeric polynuclear aromatic hydrocarbons using octadecylsilica and β-cyclodextrinsilica stationary phases with aqueous methanol and acetonitrile mobile phases. Based on these results, this approach appears to be a viable strategy for the simultaneous optimization of stationary and mobile phase environments.

4.6 References

1. J.H. Wahl, *Ph.D. Dissertation*, Michigan State University, 1991.

2. J.C. Gluckman, A. Hirose, V.L. McGuffin, and M. Novotny, *Chromatographia* **17**, 303 (1983).

3. H.J. Issaq, D.W. Mellini, and T.E. Beesley, *J. Liq. Chromatogr.* **11**, 333 (1988).

4. D.W. Armstrong, W. DeMond, A. Alak, W.L. Hinze, T.E. Riehl, and K.H. Bui, *Anal. Chem.* **57**, 234 (1985).

7. D.W. Armstrong, A. Alak, W. DeMond, W.L. Hinze, and T.E. Riehl, *J. Liq. Chromatogr.* **8**, 261 (1985).

8. M. Olsson, L.C. Sander, and S.A. Wise, *J. Chromatogr.* **477**, 277 (1989).

9. P.R. Fielden and A.J. Packham, *J. Chromatogr.* **516**, 355 (1990).

CHAPTER 5

MULTIVARIATE OPTIMIZATION OF MOBILE PHASE AND TEMPERATURE BY PARAMETRIC MODULATION

5.1 Introduction

The goal of this chapter is to present an experimental verification of the simultaneous optimization of mobile phase and temperature by the parametric modulation approach. By maintaining different portions of a polymeric octadecylsilica column at different temperatures and the mobile phases as separate zones, the solute will interact independently in each environment (Figure 5.1). Thus, the overall solute retention will be a simple, predictable function of the capacity factor weighted by the time that the solute is exposed to each temperature region and mobile phase. This approach should allow accurate prediction of solute retention and, hence, allow optimization of multidimensional separations with a minimum number of preliminary experiments.

5.2 Theoretical Development

The theoretical basis of solute retention and dispersion under conditions of parametric modulation has been established in Chapter 2. For the case of optimizing mobile phase and temperature, the technique requires that the overall

CHAPTER 5

MULTIVARIATE OPTIMIZATION OF MOBILE PHASE AND TEMPERATURE BY PARAMETRIC MODULATION

5.1 Introduction

The goal of this chapter is to present an experimental verification of the simultaneous optimization of mobile phase and temperature by the parametric modulation approach. By maintaining different portions of a polymeric octadecylsilica column at different temperatures and the mobile phases as separate zones, the solute will interact independently in each environment (Figure 5.1). Thus, the overall solute retention will be a simple, predictable function of the capacity factor weighted by the time that the solute is exposed to each temperature region and mobile phase. This approach should allow accurate prediction of solute retention and, hence, allow optimization of multidimensional separations with a minimum number of preliminary experiments.

5.2 Theoretical Development

The theoretical basis of solute retention and dispersion under conditions of parametric modulation has been established in Chapter 2. For the case of optimizing mobile phase and temperature, the technique requires that the overall

Figure 5.1 Schematic illustration of the parametric modulation concept for the simultaneous optimization of mobile phase and temperature

Figure 5.1

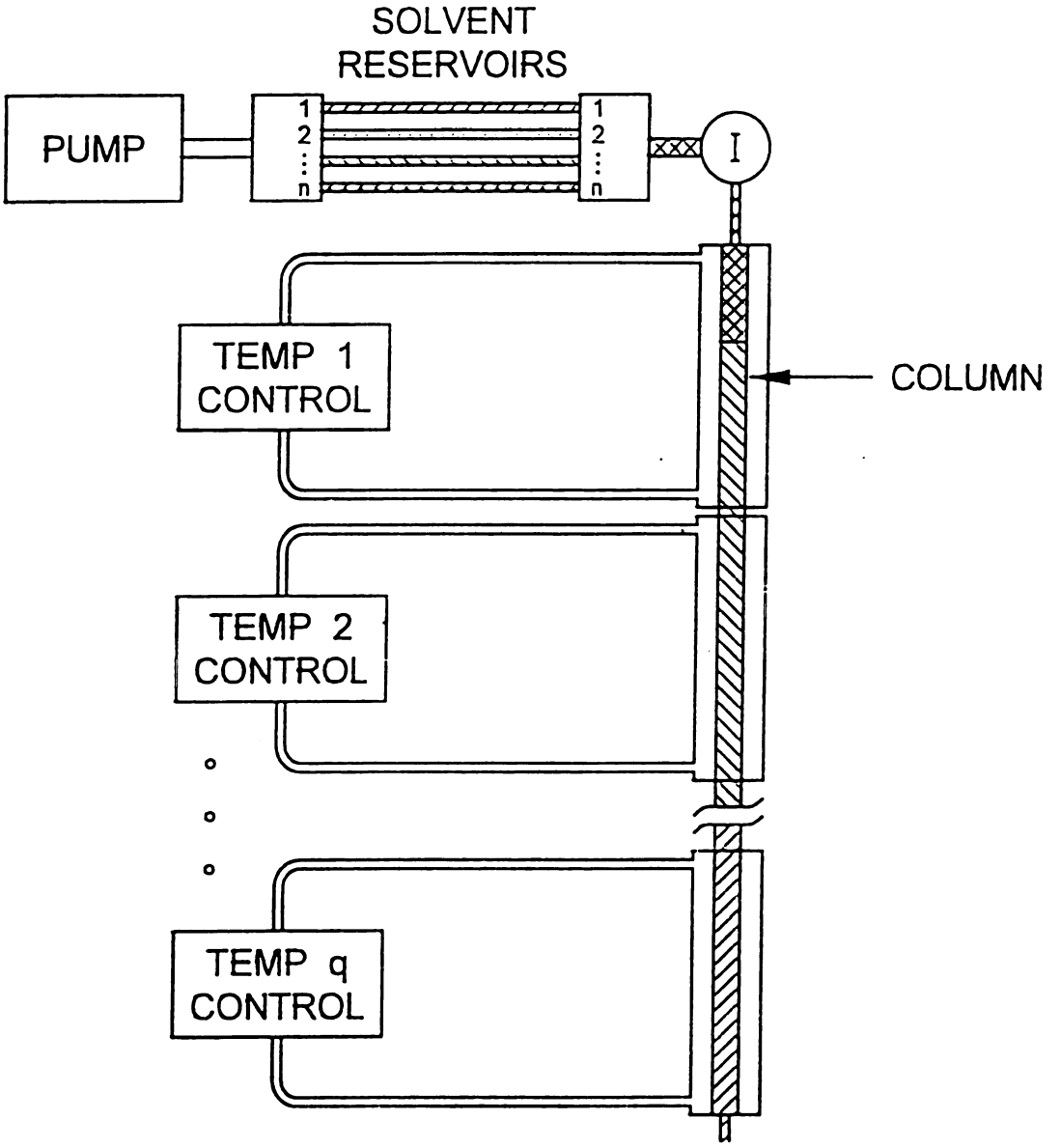
SOLVENT
RESERVOIRS
PUMP
1
2
n
1
2
n
I
TEMP 1
CONTROL
COLUMN
TEMP 2
CONTROL
TEMP q
CONTROL

retention time (t_i) be calculated when the solute is exposed to each mobile phase and temperature region. This is accomplished by summing retention within each individual environments as shown below

$$t_i = \sum_{p=1}^{q} \sum_{j=0}^{n} \frac{\pi r_p^2 \ \varepsilon_p \ x_j}{F} \left(\frac{1+k_{ijp}}{k_{ijp}} \right) \qquad [5.1]$$

where k_{ijp} is the capacity factor of solute i in mobile phase j on column at temperature p, r_p and ε_p are the radius and total porosity of column at temperature p, respectively, x_j is the length of solvent zone, F is the volumetric flow rate, n and q are the limits of summation of number of solvent and temperature zones, respectively.

In a similar manner, the variance (σ_i^2) of the solute zone in temporal units is calculated by independent summation as

$$(\sigma_i)^2 = \sum_{p=1}^{q} \sum_{j=0}^{n} (\sigma_{ijp})^2 = \sum_{p=1}^{q} \frac{h_p \, d_p}{l_p} \left(\sum_{j=0}^{n} \frac{\pi r_p^2 \ \varepsilon_p \ x_j}{F} \left(\frac{1+k_{ijp}}{k_{ijp}} \right) \right)^2 \qquad [5.2]$$

where h_p is the reduced plate height, d_p is the particle diameter, and l_p is the length of column at temperature p.

The resolution between adjacent solute zones ($R_{i,i+1}$) is then calculated by substitution of Equations [5.1] and [5.2] in the following expression

$$R_{i,i+1} = \frac{(t_{i+1} - t_i)}{2[(\sigma_{i+1})_t + (\sigma_i)_t]} \qquad [5.3]$$

Finally, a criterion such as the chromatographic resolution statistic (CRS) (1) shown below is used to evaluate the overall quality of the separation

$$CRS = \left(\sum_{i=1}^{m-1} \left(\frac{R_{i,i+1} - R_{opt}}{R_{i,i+1} - R_{min}} \right)^2 \frac{1}{R_{i,i+1}} + \sum_{i=1}^{m-1} \frac{(R_{i,i+1})^2}{(m-1)\, R_{avg}^2} \right) \frac{t_f}{m} \qquad [5.4]$$

where R_{opt} and R_{min} are the optimum and minimum resolution, respectively, R_{avg} is the average resolution, t_f is the analysis time and m is the number of solutes.

The computer program used to accomplish these calculations is given in Appendix [A1.2].

5.3 Experimental Methods

Chromatographic System. The experimental system is illustrated schematically in Figure 5.1. A dual syringe pump (Model 140, Applied Biosystems, San Jose, CA, USA) is programmed to deliver solvent zones for a specified time period. The sample is introduced by means of a 1.0 µL injection valve (Model ECI4W1, Valco Instruments, Houston, TX, USA), after which the effluent stream is split (75:1) to yield a nominal injection volume of 13 nL, and a nominal flow rate of 1.2 µL/min. In order to ensure rapid thermal transport and equilibration, the chromatographic column is prepared from fused silica tubing of capillary dimension (350 µm O.D., 200 µm I.D., Polymicro Technologies, Phoenix, AZ, USA) which is terminated at the desired length with a quartz wool frit. An irregular silica (5.5 µm IMPAQ 200, PQ Corporation, Conshohocken, PA, USA) with a polymeric octadecylsilica phase (5.4 µmol/m^2), is slurry packed

according to the procedure described previously (2). The resulting column has total porosity (ε_p) of 0.90, separation impedance (ϕ_p) of 450, and reduced plate height (h_p) of 3.7 at 45°C, 4.3°C at 40°C, 4.7 at 35°C and 4.5 at 23°C using pyrene as a model solute under standard test conditions (2). For independent control of each temperature zone, the column is enclosed in water jackets contructed of nylon tubing (0.32 cm O.D., 0.2 cm ID., Cole-Parmer, Niles, IL, USA) and fittings (Swagelok NY-200-3, Crawford Fitting Co., Solon, OH, USA). Water circulation is provided by thermostatically controlled baths (Model RTE 9B; Neslab Instruments, Portsmouth, NH, USA), with an operating range of -20 to 100 ° C (± 0.1° C).

The polynuclear aromatic hydrocarbon solutes are detected using both laser-induced fluorescence and UV-absorbance in a 75 µm I.D. fused-silica capillary flow cell. In the fluorescence detection system (3), a helium-cadmium laser (325 nm, 25 mW, Model 3074-40M, Omnichrome, Chino, CA, USA) is reflected by a dielectric mirror and is focussed on the capillary with a quartz lens. The fluorescence emission is collected perpendicular and coplanar to the excitation beam with another quartz lens, spectrally isolated with a bandpass interference filter (420 nm, S10-420-F, Corion, Holliston, MA, USA), and focussed onto a photomultiplier tube (Model Centronic Q4249B, Bailey Instruments, Saddle Brook, NJ, USA). The photocurrent is amplified and converted to voltage by a picoammeter (Model 480, Keithley Instruments, Cleveland, OH, USA). A variable-wavelength UV-absorbance detector (Model Uvidec 100-V, Japan Spectroscopic Co., Tokyo, Japan), operated at 254 nm, is placed in series after the fluorescence detector. Data from both detectors are displayed simultaneously by using a chart recorder (Model 585, Linear Instruments Corp., Reno, NV, USA)

Materials and Method. Reagent-grade chrysene, benz[a]anthracene, benzo[c]phenanthrene, pyrene, perylene, benzo[a]pyrene, and benzo[e]pyrene are obtained from Sigma Chemical Co. (St. Louis, MO USA). Tetrabenzonaphthalene and phenanthro[3,4-c]phenanthrene are obtained from the National Institute of Standards and Technology (Gaithersburg, MD, USA). Standard solutions of each polynuclear aromatic hydrocarbon (PAH) are prepared by dissolution in methanol at 10^{-4} M concentration. Organic solvents are high purity distilled-in-glass grade (Baxter Healthcare, Burdick and Jackson Division, Muskegon, MI, USA).

Computer-Assisted Optimization Program. The separation is optimized by means of the computer-assisted optimization routine discussed in Chapter 4. The program was executed on a VAXstation 3200 computer (Digital Equipment, Maynard, MA, USA). The program utilizes a systematic maping procedure in which the length of each parameter to be optimized is varied independently within prescribed limits. For the present study, temperature zone length is varied from 0 to 90 cm, and the solvent zone length is varied from 5 cm to the maximum length required to elute all solutes. For each combination of temperature and solvent zone length, the total retention time and variance of each solute are calculated by means of Equations [5.1] and [5.2], respectively. The resolution between each pair of adjacent solute peaks is calculated by using Equation [5.3]. Finally, the overall quality of the separation is assessed by means of the modified CRS function (Equation [5.4] and [2.19]), using selected values for the optimum and minimum acceptable resolution of 1.5 and 1.0, respectively. By graphing the CRS value as a function of temperature and solvent zone lengths, a complete multivariate response surface may be constructed. The minimum CRS value is

then identified by visual inspection or by computer search of the response surface.

5.4 Results and Discussion

The goals of this preliminary study are to demonstrate the conceptual and theoretical basis of parametric modulation, and to apply this strategy to the multivariate optimization of mobile phase and temperature. In preparation to meet these objectives, it is worthwhile to elucidate and to clarify the condition under which a spatial gradient in temperature will be most beneficial. In a spatial gradient, unlike a temporal gradient, all solutes will encounter all temperature zones in an analogous manner (Equation (5.1)). Solutes that exhibit a linear relationship between ln k and 1/T (Equation (1.21)) will spend the same fraction of their total retention time in each temperature zone. For these ideal solutes, there exists a single temperature that is exactly equivalent to the spatial temperature gradient, whether that gradient is discontinuous (as described herein) or continuous in nature (4). Consequently, a spatial temperature gradient can be utilized for all solutes but will only be superior to isothermal conditions for solutes that deviate from ideal thermodynamic behavior.

On the basis of this consideration, the chromatographic system and solutes chosen for these preliminary studies should exhibit a distinct change in the retention mechanism with temperature. Although there are a variety of chromatographic systems that meet this criterion, octadecylsilica has been chosen as the stationary phase because of its widespread use and general applicability in liquid chromatography. This type of stationary phase has been shown to undergo a phase transition, where the transition temperature is

dependent upon the bonding density of the alkyl group, the alkyl chain length, the mobile phase composition and other variables (5-7). Whereas the exact thermodynamic nature of this phase transition remains the subject of continued study and controversy, it is nevertheless apparent that a significant change in the structure and morphology occurs. These changes have been examined by a number of analytical techniques, including nuclear magnetic resonance spectroscopy (8-10), Fourier-transform infrared spectroscopy (11,12), thermal analysis, (13), as well as chromatographic methods. At temperatures above the transition point, the stationary phase appears to be randomly oriented and flexible, so that solute retention is dominated by enthalpic interactions. As temperature is decreased below the transition point, the stationary phase becomes progressively more rigid and ordered, so that solute retention acquires a correspondingly greater entropic contribution. Under "entropy dominated" conditions, there is a significant increase in the selectivity of octadecylsilica with respect to the size and shape of solute molecules (3). Throughout the phase transition, both ΔH and ΔS are temperature dependent, leading to substantial deviations from ideal behavior for many solutes.

For these studies, the model solutes consist of isomeric four-, five-, and six-ring polynuclear aromatic hydrocarbons (PAH), whose structures are shown in Figure 5.2. A polymeric octadecylsilica with a high bonding density of 5.4 $\mu mole/m^2$ is utilized as stationary phase. From previous studies (14), the transition temperature for this material is known to be approximately 45° C. Because of the progressive nature of the phase transition, however, it is not known where the most optimal variations in selectivity will occur for the model solutes. Thus, it is desirable to examine a broad range of temperatures in the vicinity of the transition temperature. Representative chromatograms of a

Figure 5.2 Structures of polynuclear aromatic hydrocarbons

Figure 5.2

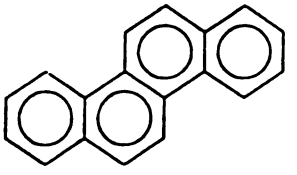

CHRYSENE

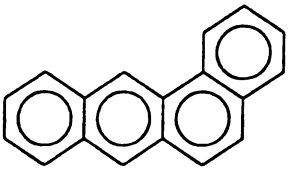

BENZ[a]ANTHRACENE

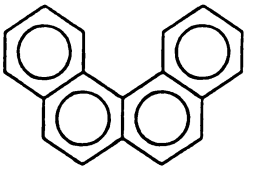

BENZO[c]PHENANTHRENE

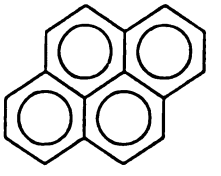

PYRENE

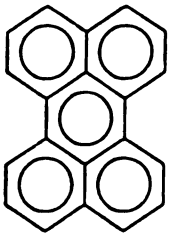

PERYLENE

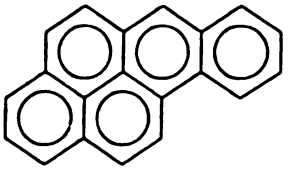

BENZO[a]PYRENE

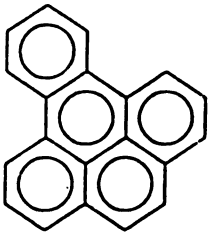

BENZO[e]PYRENE

TETRABENZONAPHTHALENE

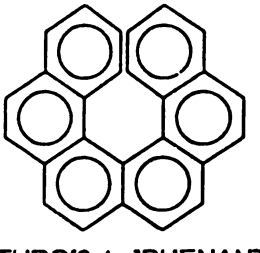

PHENANTHRO[3,4-c]PHENANTHRENE

mixture of the model solutes are shown Figure 5.3 at various temperatures in the range from 23 to 45° C.

The capacity factors of each PAH were measured at temperatures of 23, 35, 40, and 45° C using pure methanol (Table 5.1) and acetonitrile (Table 5.2) as mobile phases. In general, the capacity factors of the PAHs decrease with increasing temperature for both mobile phase. In the methanol mobile phase, a change in the elution order of chrysene and the tetrabenzonaphthalene occurred at about 35° C. In the acetonitrile mobile phase, a change in the elution order of phenanthro[3,4-c]phenanthrene and benz[a]anthracene occurred at around 35° C. In order to further examine the influence of temperature on the retention and selectivity of the solutes, a plot of ln k vs. 1/T was obtained (van't Hoff plot) for both mobile phases. Using methanol as the mobile phase (Figure 5.4), it is apparent that the logarithm of capacity factor increases linearly with temperature between 23° C and 35° C, but deviates from linearity at 35° C. This deviation is more clear with some solutes than with others. For example, tetrabenzonaphthalene and chrysene show greater deviations from linearity than the other solutes. This deviation from a linear trend of ln k vs 1/T at 35° C and change in elution order of solutes suggests a change in the retention mechanism of the stationary phase. A similar break in the linear trend of ln k versus 1/T was also observed when acetonitrile was used as the mobile phase (Figure 5.5).

Based on the results shown above, it seems reasonable to expect that resolution of the isomeric PAHs can be achieved by modulation of the mobile phase and temperature. However, there are 64 possible permutations for the solvents and temperatures examined in this study: 8 one-solvent/one-temperature systems, 24 one-solvent/two-temperature systems, 8 two-solvent/one-temperature systems, and 24 two-solvnt/two-temperature systems. It would be clearly impossible to examine all of these possibilities by

Figure 5.3 Effect of temperature on the selectivity of polynuclear aromatic hydrocarbons using 100% methanol as mobile phase. Column: 200 mm I.D. x 75 cm fused silica capillary, packed with 5.5 mm polymeric octadecylsilica. Mobile phase: 100% methanol at 1.2 µL/min. Detector: Laser-induced fluorescence with excitation at 325 nm and emission at 420 nm. Solutes: (1) Benzo[c]phenanthrene (2) pyrene (3) phenanthrophenanthrene (4) benz[a]anthracene (5) tetrabenzonaphthacene (6) chrysene (7) benzo[e]pyrene (8) perylene (9) benzo[a]pyrene.

Figure 5.3

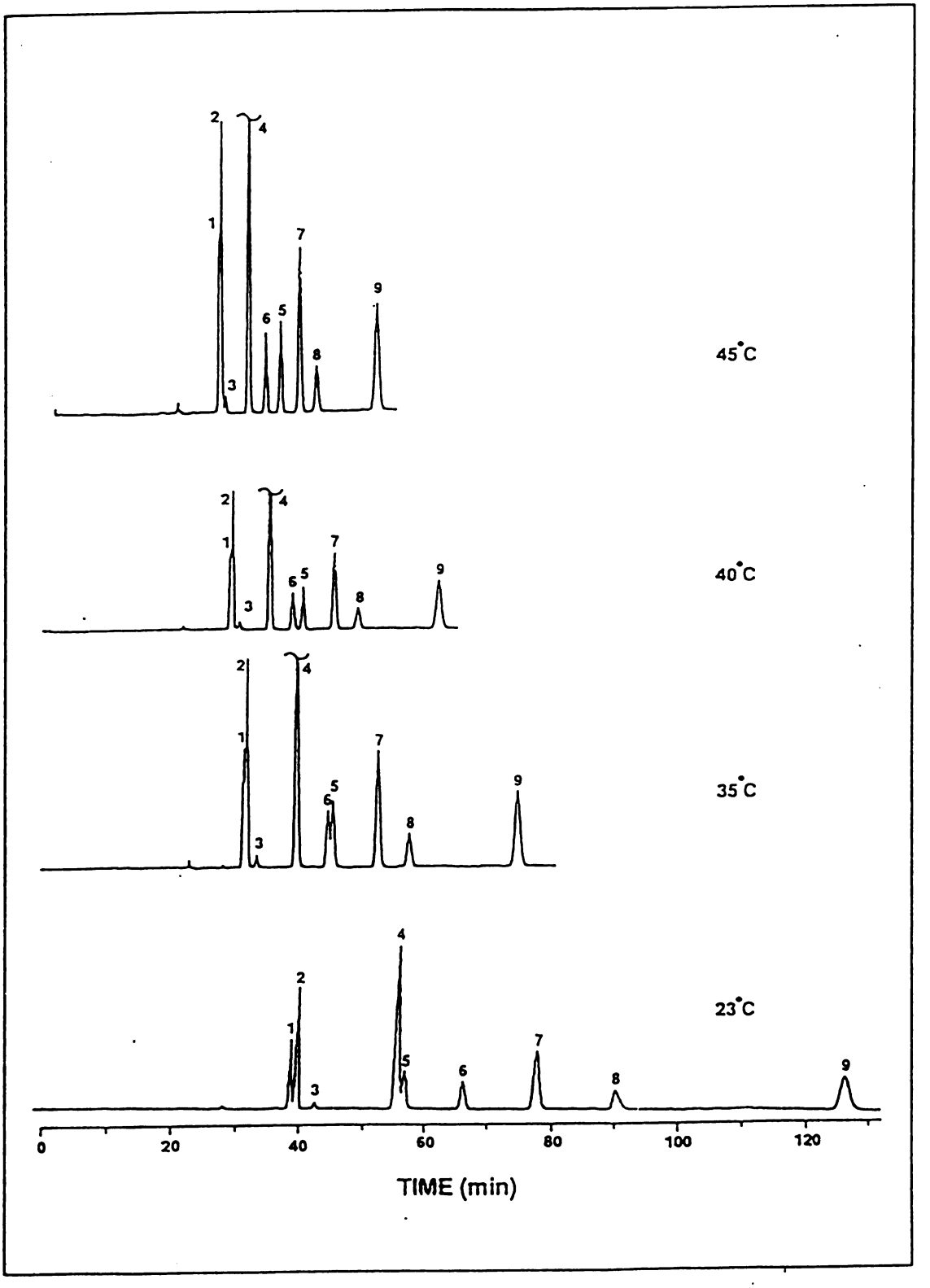

Table 5.1 Capacity factors (k_{ijp}) for polynuclear aromatic hydrocarbons on polymeric octadecylsilica stationary phase obtained at different temperatures using 100% methanol as mobile phase.

POLYNUCLEAR AROMATIC HYDROCARBONS	CAPACITY FACTOR (k_{ijp}) 100 % METHANOL			
	23 ° C	35 ° C	40 ° C	45 ° C
BENZO[c]PHENANTHRENE	0.77	0.63	0.58	0.52
PYRENE	0.82	0.65	0.61	0.53
PHENANTHROPHENANTHRENE	0.95	0.74	0.67	0.58
BENZ[a]ANTHRACENE	1.53	1.05	0.94	0.80
TETRABENZONAPHTHACENE	1.60	1.35	1.24	1.10
CHRYSENE	2.04	1.32	1.15	0.97
BENZO[e]PYRENE	2.57	1.72	1.53	1.28
PERYLENE	3.14	1.98	1.73	1.43
BENZO[a]PYRENE	4.79	2.85	2.46	2.00

Table 5.2 Capacity factors (k_{ijp}) for polynuclear aromatic hydrocarbons on polymeric octadecylsilica stationary phase obtained at different temperatures using 100% acetonitrile as mobile phase.

POLYNUCLEAR AROMATIC HYDROCARBONS	CAPACITY FACTOR (k_{ijp}) 100 % ACETONITRILE			
	23 ° C	35 ° C	40 ° C	45 ° C
BENZO[c]PHENANTHRENE	0.51	0.39	0.34	0.31
PYRENE	0.58	0.41	0.38	0.34
PHENANTHROPHENANTHRENE	0.77	0.56	0.48	0.40
BENZ[a]ANTHRACENE	0.83	0.55	0.48	0.41
TETRABENZONAPHTHACENE	1.06	0.84	0.71	0.61
CHRYSENE	1.04	0.64	0.54	0.45
BENZO[e]PYRENE	1.48	0.96	0.79	0.67
PERYLENE	1.68	1.00	0.85	0.71
BENZO[a]PYRENE	2.47	1.41	1.14	0.92

Figure 5.4 Effect of temperature on logarithm of capacity factor for polynuclear aromatic hydrocarbons using 100% methanol as mobile phase. Solutes: (Δ) Benzo[c]phenanthrene (●) pyrene (□) phenanthrophenanthrene (▲) benz[a]anthracene (◊) tetrabenzonaphthacene (■) chrysene (O) benzo[e]pyrene (♦) perylene (∇) benzo[a]pyrene.

Figure 5.4

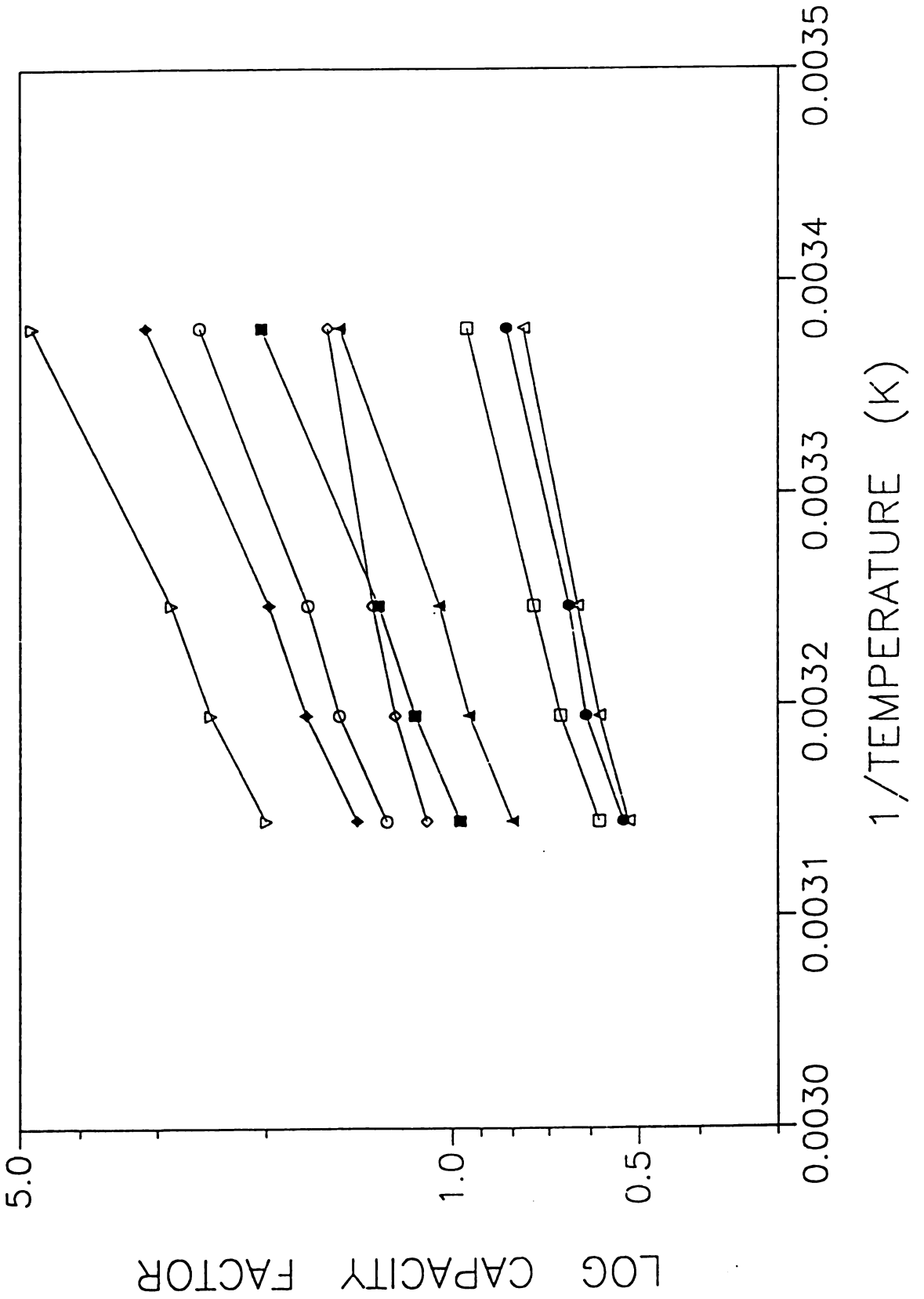
5.0
1.0
0.5
LOG CAPACITY FACTOR
0.0030
0.0031
0.0032
0.0033
0.0034
0.0035
1/TEMPERATURE (K)

Figure 5.5 Effect of temperature on logarithm of capacity factor for polynuclear aromatic hydrocarbons using 100% acetonitrile as mobile phase. Solutes: (Δ) Benzo[c]phenanthrene (●) pyrene (❑) phenanthrophenanthrene (▲) benz[a]anthracene (◊) tetrabenzonaphthacene (■) chrysene (O) benzo[e]pyrene (♦) perylene (∇) benzo[a]pyrene.

Figure 5.5

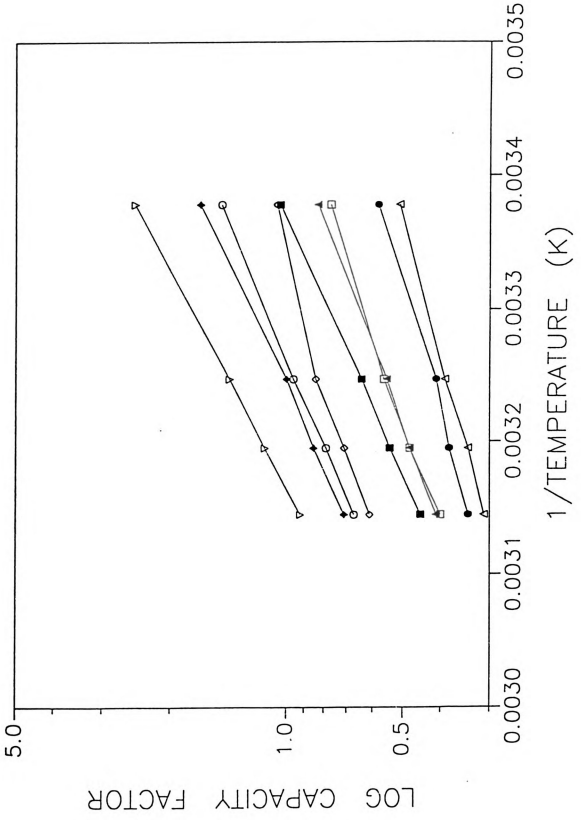
5.0
1.0
0.5
LOG CAPACITY FACTOR
0.0030
0.0031
0.0032
0.0033
0.0034
0.0035
1/TEMPERATURE (K)

time-consuming, trial-and-error experimental measurements. However, the computer program described previously provides a rapid and effective means to identify the most promising of these permutations.

In order to exploit the different selectivity of the stationary phase at different temperatures, the column should be maintained at more than one temperature. This was accomplished by maintaining different portions of the column at different temperatures as shown in Figure 5.1. By using the computer program described earlier, the optimum length of column maintained at each temperature and the length of solvent necessary for the total separation of all the solutes can be determined. This is achieved by systematically varying the length of column maintained at each temperature as well as the length of solvent zone. For each combination of column and solvent lengths, the total retention time and variance of each solute are calculated by means of Equations 5.1 and 5.2, respectively, using the individual capacity factors in Tables 5.1 and 5.2. The resolution between each pair of adjacent solute is calculated by means of Equation 5.3. Finally, the overall quality of the separation is assessed by means of the modified CRS function (15), using selected values of 1.5 and 1.0 for the optimum and minimum acceptable resolution.

Table 5.3 shows a few of the possible permutations of column temperature and solvent that may be utilized for the separation of the PAH solutes. For the case of one solvent, only one sequence of temperatures is investigated and not the reverse, because solute retention will be independent of the column order. For each pairwise combination of column temperatures, the length of column is systematically varied and the minimum CRS is stored in a file and used to identify the optimum conditions. For the case of optimizing temperature alone, the best combination of temperatures is predicted to occur using columns at 23° C and 40° C. The minimum resolution predicted under this condition is 1.31 with a total

Table 5.3 Evaluation of the permutations of a two-temperature/one-solvent and two-temperature/two-solvent chromatographic system for the separation of polynuclear aromtic hydrocarbons. The column is polymeric octadecylsilica; the solvents are 100% methanol and acetonitrile as given in Tables 5.1 and 5.2. The analysis time (t_f), minimum resolution ($(R_{i,i+1})_{min}$) and minimum hromatogrphic Resolution Statistic (CRS_{min}) function correponding to the optimum conditions are given.

COLUMN 1 TEMP(°C)	COLUMN 2 TEMP(°C)	SOLVENT 1	SOLVENT 2	$(t_r)_{max}$	$(R_{i,i+1})_{min}$	CRS_{min}
23	35	100% CH_3OH		120.5	1.29	2.6
23	40	100% CH_3OH		120.0	1.31	2.4
23	45	100% CH_3OH		119.5	1.28	2.6
23	35	100% CH_3CN		67.0	1.29	3.1
23	40	100% CH_3CN		67.0	1.29	3.1
23	45	100% CH_3CN		64.0	1.32	2.6
23	40	100% CH_3OH	100% CH_3CN	102.0	1.33	2.3
40	23	100% CH_3OH	100% CH_3CN	80.0	1.34	2.3
23	40	100% CH_3CN	100% CH_3OH	87.0	1.35	2.2
40	23	100% CH_3CN	100% CH_3OH	83.0	1.34	2.2

analysis time of 120 min. For the case of optimizing both the sequence nd length of the column at two temperatures are varied. The optimum corresponds to column temperature of 23° C and 40° C and using acetonitrile and methanol. The minimum resolution predicted under this condition is 1.35 with a total analysis time of 87 min. Since the optimum obtained using both mobile phase and temperature is not significantly better than that using temperature alone, a two-temperature modulation sequence with one mobile phase was pursued for the optimization, because of the ease with which it can be implemented.

The topographic and contour maps are shown in Figures 5.6A and 5.6B, as a function of the column length at each temperature. It is observed that the overall quality of the separation improves continuously with the length of column at 23° C, and remains fairly constant for length of column at 40° C for all lengths greater than 5 cm. Thus, for the total column length of 90 cm, the predicted optimum length of column at 23° C and 40° C are 85 cm and 5 cm, respectively, using pure methanol as mobile phase. The predicted chromatogram shown in Figure 5.7 shows excellent separation of the PAHs. Because the CRS response surface shown in Figure 5.6A is relatively flat in the vicinity of the optimum, small discrepancies in column length at the two temperatures should have little effect upon the quality of the separation. Thus, the analytical method should be rugged.

Experimental verification of the predicted optimum was obtained by the separation of the PAHs in Figure 5.8 using the predicted optimum conditions. The experimental chromatogram shows an excellent separation of all solutes. Table 5.4 shows a comparison of the experimental and predicted retention times and peak widths. There is an excellent agreement of the predicted retention times and peak width with average errors of ± 0.9% and ± 6.9% respectively. Thus temperature and mobile phase can be used simultaneously to affect solute

Figure 5.6A Topographic map of the CRS response surface as a function of the column length (cm) at temperatures 23° C (Temp. 1) and 40° C (Temp. 2)

Figure 5.6A

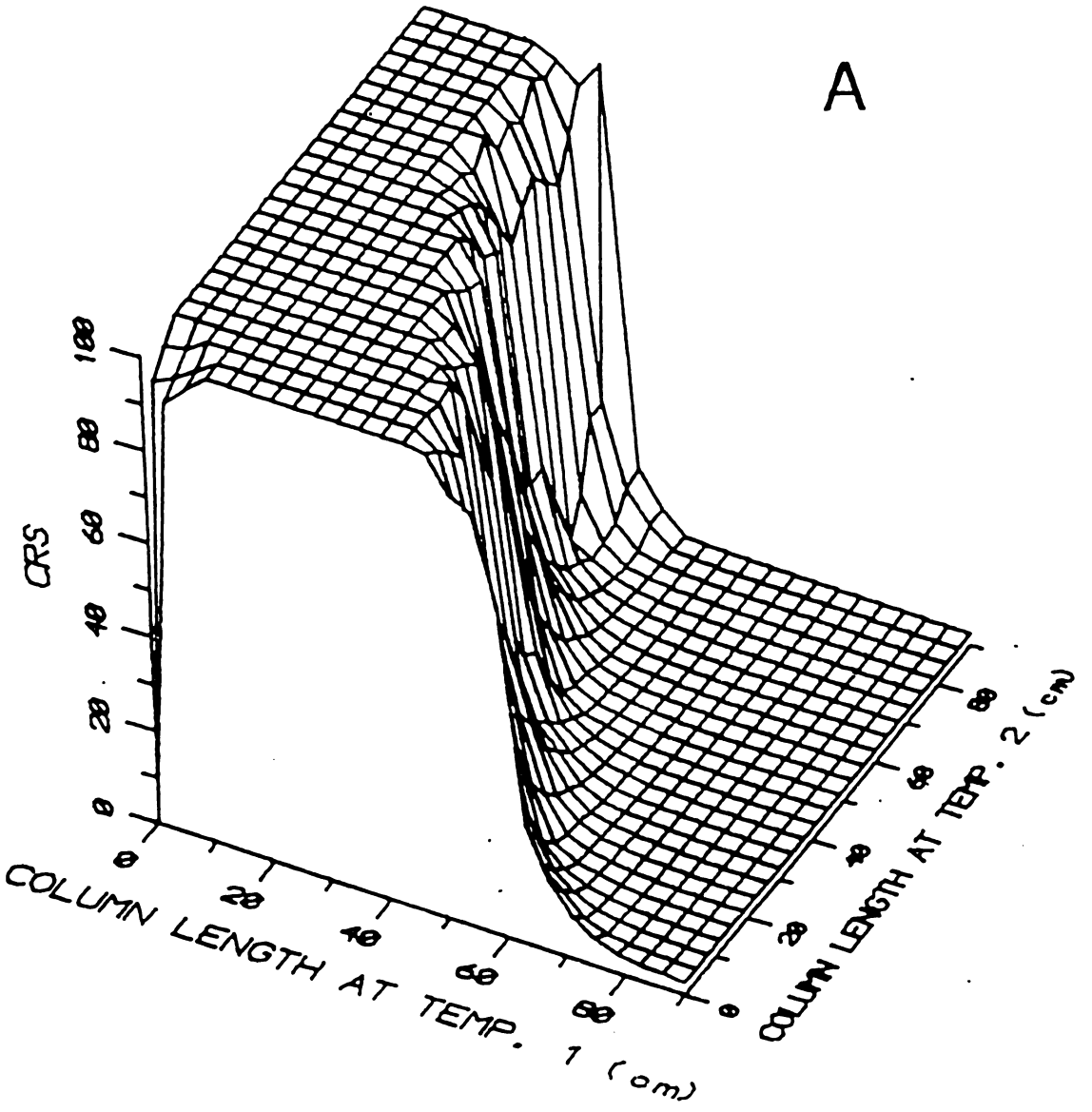
A
CRS
0
20
40
60
80
100
COLUMN LENGTH AT TEMP. 1 (cm)
COLUMN LENGTH AT TEMP. 2 (cm)

Figure 5.6A Contour map of the CRS response surface as a function of the column length (cm) at temperatures 23° C (Temp. 1) and 40° C (Temp. 2)

Figure 5.6B

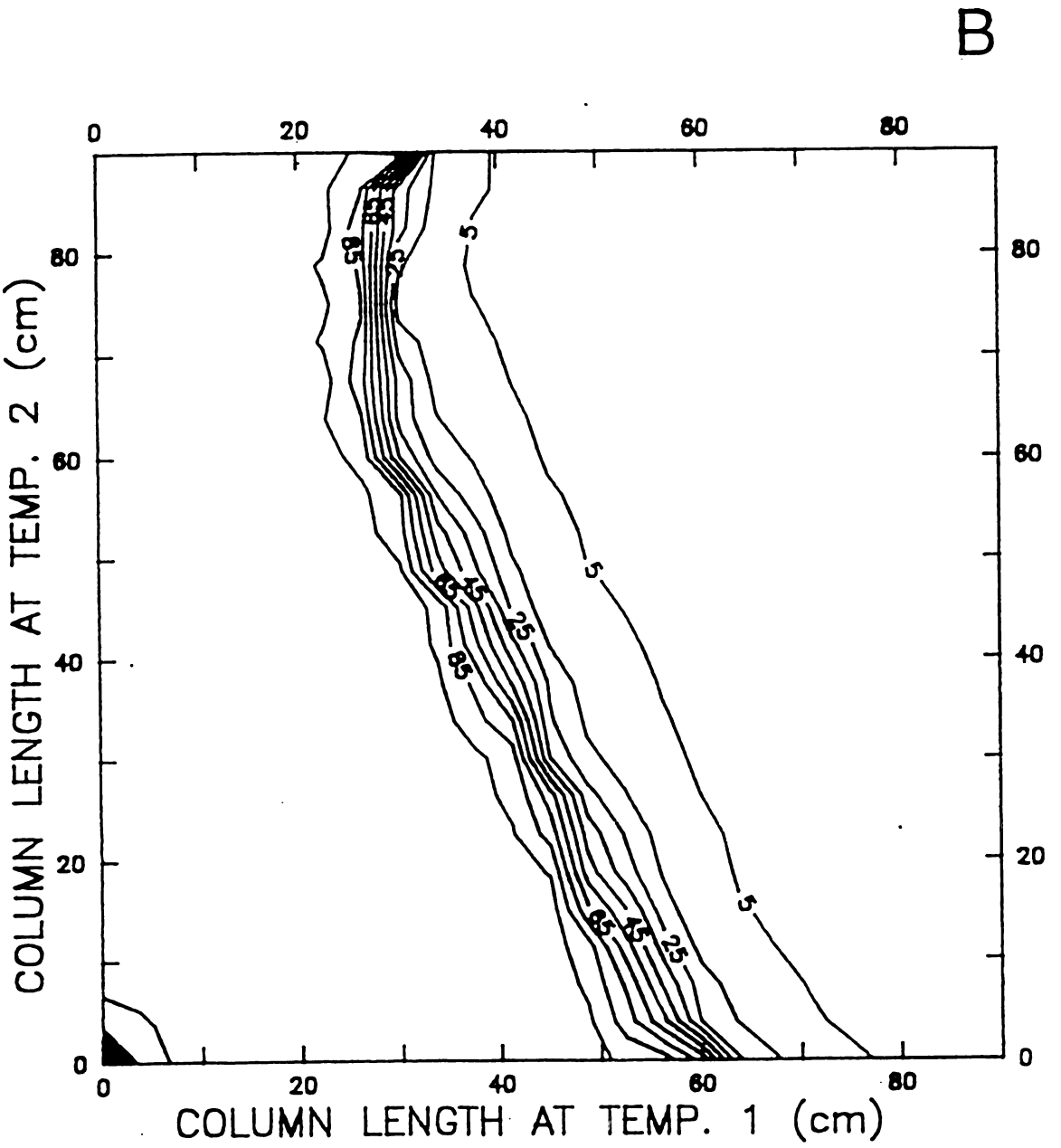
B
COLUMN LENGTH AT TEMP. 2 (cm)
COLUMN LENGTH AT TEMP. 1 (cm)
0
20
40
60
80
5
25
45
65
85

Figure 5.7 Predicted chromatogram for the polynuclear aromatic hydrocarbons on polymeric octadecylsilica column using the optimal conditions of 5 cm of column maintained at 23° C and 85 cm maintained at 40° C; using 100% methanol as the mobile phase. Solutes: (1) Benzo[c]phenanthrene (2) pyrene (3) phenanthrophenanthrene (4) benz[a]anthracene (5) tetrabenzonaphthacene (6) chrysene (7) benzo[e]pyrene (8) perylene (9) benzo[a]pyrene.

Figure 5.7

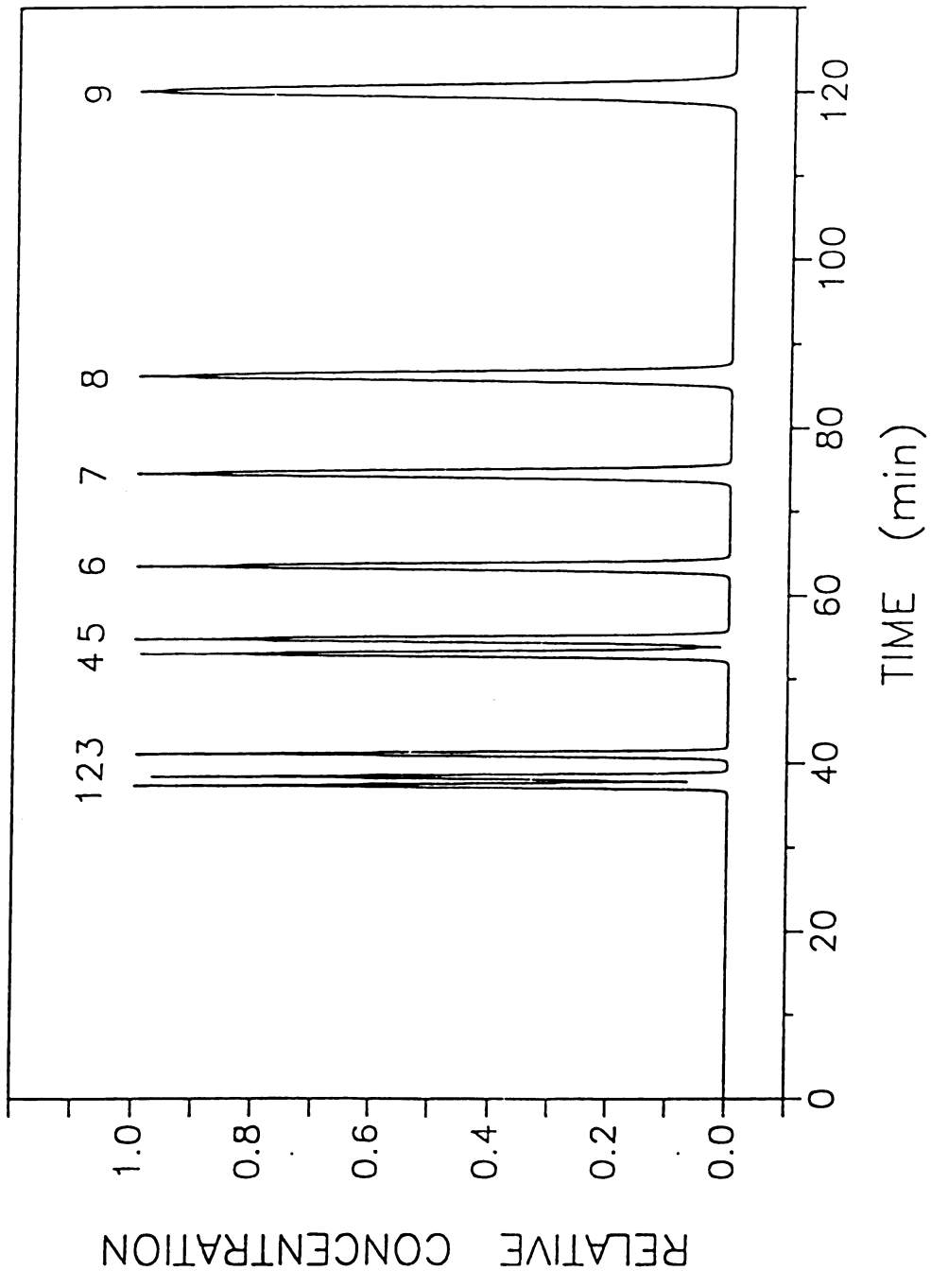
123
45
6
7
8
9
1.0
0.8
0.6
0.4
0.2
0.0
RELATIVE CONCENTRATION
0
20
40
60
80
100
120
TIME (min)

Figure 5.8 Experimental chromatogram obtained under the predicted optimum conditions. Column: 200 mm I.D. x 75 cm fused silica capillary, packed with 5.5 mm polymeric octadecylsilica. Mobile phase: 100% methanol at 1.2 µL/min. Detector: Laser-induced fluorescence with excitation at 325 nm and emission at 420 nm. Solutes : (1) Benzo[c]phenanthrene (2) pyrene (3) phenanthrophenanthrene (4) benz[a]anthracene (5) tetrabenzonaphthacene (6) chrysene (7) benzo[e]pyrene (8) perylene (9) benzo[a]pyrene.

Figure 5.8

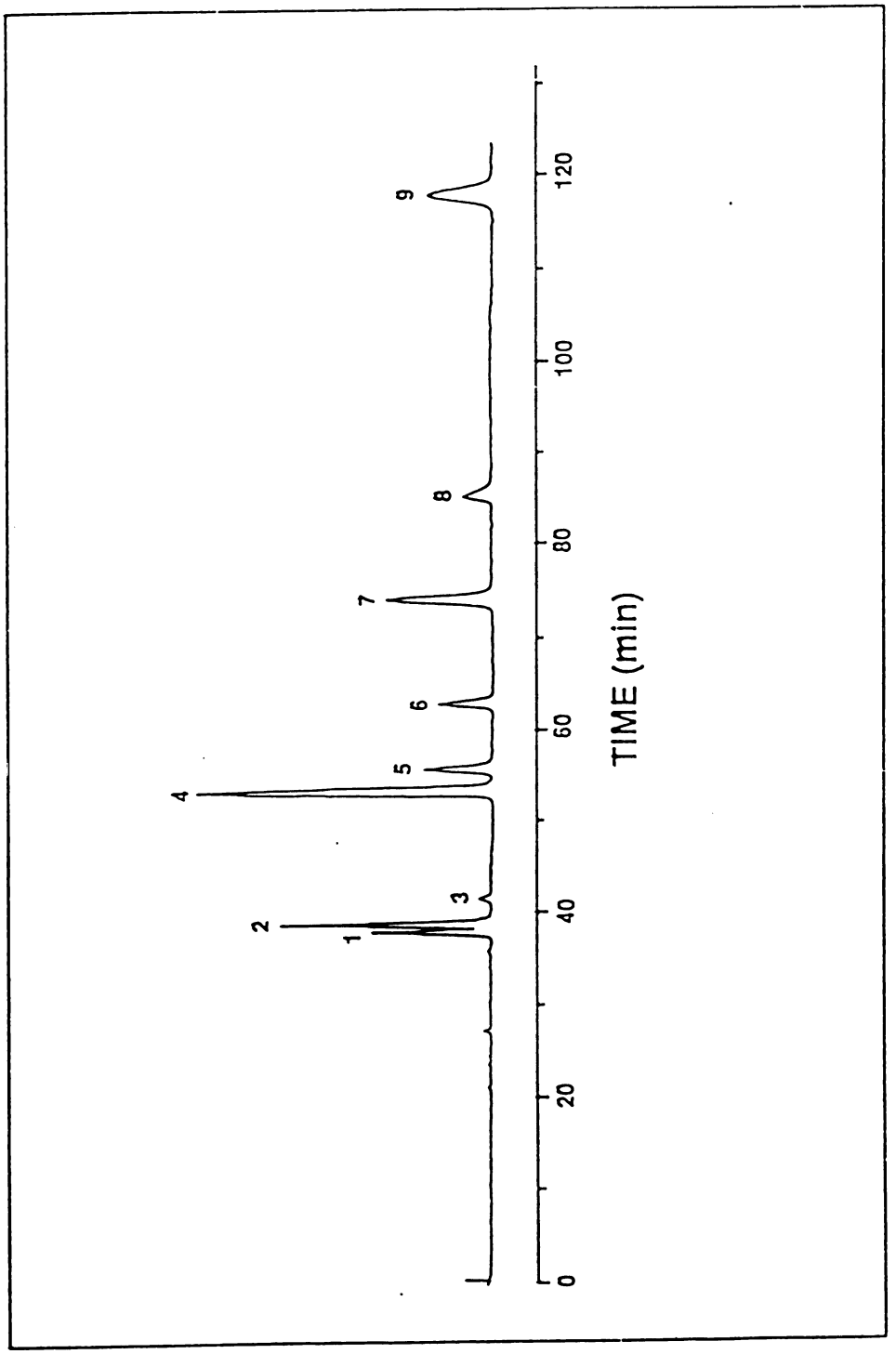

Table 5.4 Comparison of experimental (EXPT) and theoretical (Theory) retention time and peak width under the predicted optimum conditions illustrted in Figures 5.7 and 5.8

POLYNUCLEAR AROMATIC HYDROCARBONS	RETENTION TIME (min)			WIDTH (min)		
	EXPT	THEORY[a]	% ERROR[b]	EXPT	THEORY[c]	% ERROR[b]
BENZO[c]PHENANTHRENE	37.7	37.3	1.1	0.7	0.8	-13.2
PYRENE	38.6	38.3	0.8	0.8	0.8	2.0
PHENANTHROPHENANTHRENE	41.9	41.0	2.2	1.0	0.9	10.7
BENZ[a]ANTHRACENE	53.3	53.0	0.6	1.0	1.1	-8.3
TETRABENZONAPTHACENE	55.9	54.7	2.2	1.22	1.1	6.7
CHRYSENE	63.2	63.4	-0.3	1.4	1.3	2.1
BENZO[e]PYRENE	74.4	74.5	-0.1	1.5	1.6	-4.4
PERYLENE	85.7	86.1	-0.5	2.0	1.8	12.4
BENZO[a]PYRENE	119.2	120.0	-0.7	2.6	2.5	2.1
AVERAGE			±0.9			±6.9

[a] Calculated from Equation [5.1].
[b] % ERROR = 100 (EXPT – THEORY)/THEORY
[c] Calculated from Equation [5.2], assuming a peak width of 4 $(\sigma_i)_t$.

selectivity and the optimization strategy developed in this work enables an accurate prediction of the experimental conditions for the optimization.

5.5 Conclusions

The complete optimization of mobile phase and temperature is achieved for the separation of isomeric polynuclear aromatic hydrocarbons. By subjecting portions of polymeric octadecylsilica column to different temperatures, an optimum combination of temperature along the length of the column is found to provide adequate separation of the PAH molecules. Because the individual temperature regions are spatially separated from one another, solute retention is a simple, time-weighted average of each environment to which the solute is exposed. From these measurements, retention may be accurately predicted for any sequence and length of column at each temperature. The strategy developed in this work appears to be a promising approach for systematically searching all possible combinations of temperature and mobile phase parameters required to achieve the optimum separation.

5.6 References

1. T. D. Schlabach and J. L. Excoffier, J. Chromatogr., **439**, 173 (1988)
2. J.C. Gluckman, A. Hirose, V.L. McGuffin, and M. Novotny, *Chromatographia* **17**, 303 (1983).
3. M. A. Heindorf and V. L. McGuffin, *J. Chromatogr.*, **464**, 186 (1989)
4. L. K. Moore and E. Synovec, *Anal. Chem.*, **65**, 2663 (1993)
5. J. Chmielowiec, and H. *J.* Sawatzky, *Chromatogr. Sci.*, **17**, 245 (1979)
6. L. C. Sander and S. A. Wise, *Anal. Chem.*, **61**, 1749 (1989)
7. K. Jinno, T. Nagoshi, W. Tanaka, M. Okamoto, J. Fetzer, J. R. Biggs, P. R. Griffiths, J. M. Olinger, *J. Chromatogr.* **461**, 209 (1989)
8. R. K. Gilpin, *Anal. Chem.*, **57**, 1465A (1985)
9. D. W. Sindorf, G. E. Marciel, *J. Am Chem. Soc.*, **105**, 1848 (1983)
10. D. W. Sindorf, G. E. Marciel, *J. Am Chem. Soc.*, **105**, 3767 (1983)
11. L. C. Sander, J. B. Callis, L. R. Field, *Anal Chem.*, **55**, 1068 (1983)
12. D. E. Leyden, D. S. Kendal, L. W. Burgraf, F. J. Pern, M. Debello, *Anal. Chem.*, **54**, 101 (1982)
13. D. Morel, K. Tabar, J. Serpinet, P. Claudy, J. M. Letoffe, *J. Chromatogr.*, **395**, 73 (1987)
14. S. H. Chen and V. L. McGufffin, *Anal. Chem.*, Manuscript in preparation.
15. P. H. Lukulay and V. L. McGuffin, *J. Chromatogr.*, **691**, 171 (1995)

CHAPTER 6

EXPERIMENTAL AND COMPUTER SIMULATION STUDIES OF SOLUTE-SOLUTE INTERACTIONS IN LIQUID CHROMATOGRAPHY

In the most complete and rigorous theoretical models of chromatography, discussed in Chapter 1, the interaction of all species is predicted to contribute to solute retention and dispersion. However, in the practical application of chromatographic theories, solute-mobile phase and solute-stationary phase interactions are considered predominant, whereas solute-solute interactions are invariably neglected. In this chapter, an experimental and computer simulation study of solute-solute interactions is presented, and its effect on solute retention and dispersion discussed.

6.1 Introduction

Solute-solute interactions may be broadly defined as an intimate contact or short-range association between molecules that persists as the concentration of solute is decreased. Solute-solute interactions have been studied extensively in bulk solution by measurement of colligative properties such as vapor pressure, melting point, freezing point, conductance, etc. (1-3). In addition, infrared, NMR, and other spectroscopic methods have been used to examine solute-solute interactions at the molecular level in order to identify the bonding sites and to determine the aggregation number (4-6). By combining the information obtained

from these two types of experimental measurements, the equilibrium constant(s) for solute aggregation as well as the activity coefficients and excess thermodynamic functions for the solution may be calculated for comparison with theoretical models.

From a theoretical perspective, solute-solute interactions represent a deviation from ideal solution behavior by violation of the assumption of random molecular distribution. A variety of theoretical models have been developed to account for these deviations. In the classical paper by McMillan and Mayer (7), the grand canonical ensemble method was applied to the generalized case for multicomponent gas or liquid systems. This statistical thermodynamic approach enabled the prediction of the radial distribution function and, henceforth, the thermodynamic properties of the solution. Stigter (8) combined the McMillan–Mayer theory together with simple models of van der Waals and hydrogen bonding forces to interpret the thermodynamics of aqueous solutions of sucrose and glucose. Kozak, Knight, and Kauzmann (1) similarly combined the McMillan-Mayer theory with several lattice models for aqueous solutions of hydrophobic solutes. Nemethy and Scheraga (9,10) as well as Pratt and Chandler (11,12) subsequently developed models of solute-solute interactions based on the hydrophobic theory (13-15). Although the thermodynamic consequences of solute–solute interactions are reasonably well understood in bulk solution, this understanding has not been widely applied to multiple phase systems such as extraction and chromatography.

At the present time, very few studies have documented the effect of solute-solute interactions in chromatography. Amaya and Sasaki (16) investigated the gas chromatographic retention behavior of a binary mixture of chloroform and methyl ethyl ketone on a nonpolar stationary phase (Apiezon J). In addition, they examined binary mixtures of chloroform with carbon tetrachloride

and with toluene on a polar stationary phase (polyethylene glycol). In every case, they observed an increase in the retention time of both solutes in the binary mixture, which was attributed to solute-solute interactions in the stationary phase. These effects were qualitatively explained by using a theoretical model in which the mobile phase was treated as an ideal gas and the stationary phase as a regular solution (16). More recently, solute-solute interactions have been implicated in supercritical fluid and liquid chromatography (17-19). However, because of the innate complexity of condensed phases, a rigorous and comprehensive theoretical model has yet to be developed. Classical thermodynamic models based on regular solution theory (20-24) and the hydrophobic theory (25,26), as well as statistical thermodynamic models (27-29) have been developed for the prediction of solute retention. In practical application of such models, solute-mobile phase and solute-stationary phase interactions are considered predominant, whereas solute-solute interactions are invariably neglected. This neglect is often justified by an argument of statistical probability, since the concentration of solute molecules is small with respect to that of the phases. However, if the energy of interactions is sufficiently large, solute-solute interactions may become important despite the low concentration.

In this study, the self-association and mixed association of corticosteroids are demonstrated to arise under routine operating conditions in reversed-phase liquid chromatography. In order to facilitate understanding of the origin and nature of these strong solute-solute interactions, molecular mechanics and dynamics calculations are employed. Finally, these results are used to explain the observed deviations in chromatographic retention and dispersion behavior.

6.2 Experimental Section

Materials and Methods. The following corticosteroids are utilized in this investigation: cortisone (17α,21-dihydroxy-pregn-4-ene-3,11,20-trione), tetrahydrocortisol (3α,11β,17α,21-tetrahydroxy-5β-pregnane-20-one), tetrahydrocortisone (3α,17α,21-trihydroxy-5β-pregnane-11,20-dione), and methylprednisolone (11β,17α,21-trihydroxy-6α-methyl-pregna-1,4-diene-3,20-dione). These corticosteroids, shown in Figure 6.1, are obtained from the Sigma Chemical Company (St. Louis, MO, USA). Standard solutions are prepared in methanol at 10^{-6} M concentration for cortisone and methylprednisolone and at 10^{-3} M concentration for tetrahydrocortisol and tetrahydrocortisone. Organic solvents are high-purity, distilled-in-glass grade (Baxter Healthcare, Burdick & Jackson Division, Muskegon, MI, USA); water is deionized and double distilled in glass (Model MP-3A, Corning Glass Works, Corning, NY, USA).

Experimental System. A chromatographic pump equipped with two 40-mL syringes (Model 140, Applied Biosystems, Foster City, CA, USA) is used to deliver the mobile phase, 35% aqueous acetonitrile, at 0.5 mL/min. The solutes are introduced by means of a 10-μL injection valve (Model EQ 60, Valco Instrument Co., Houston, TX, USA) to the reversed-phase liquid chromatography column (47 cm × 0.46 cm i.d., 5-μm octadecylsilica, Spheri-5 RP-18, Applied Biosystems). Solute detection is accomplished by using a variable-wavelength UV-VIS absorbance detector (240 nm, 0.005 AUFS, Model 166, Beckman Instruments, San Ramon, CA, USA).

The chromatographic figures of merit, such as area, capacity factor, plate number, skew, etc., are assessed by manual calculation according to the method of Foley and Dorsey (30) for exponentially modified Gaussian peak profiles.

Figure 6.1 Structures of corticosteroids.

Figure 6.1

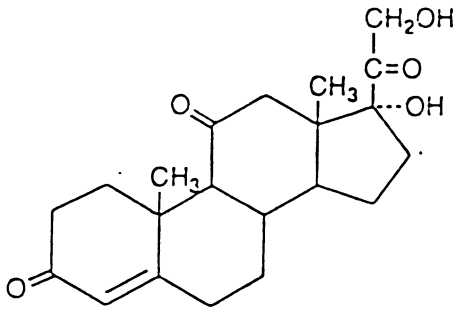

CORTISONE

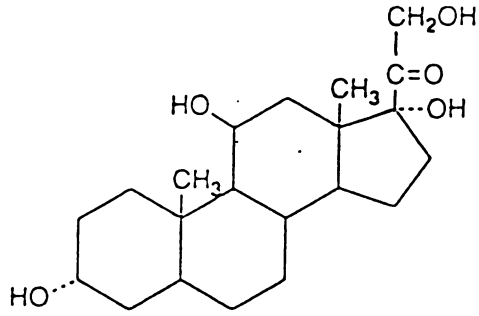

TETRAHYDROCORTISOL

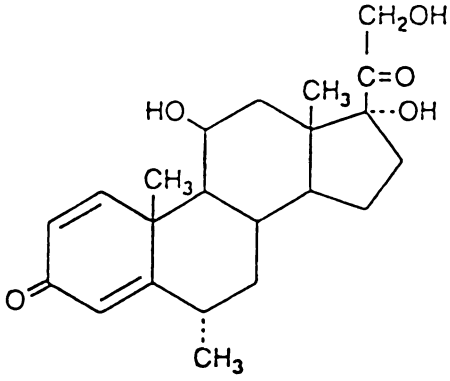

METHYLPREDNISOLONE

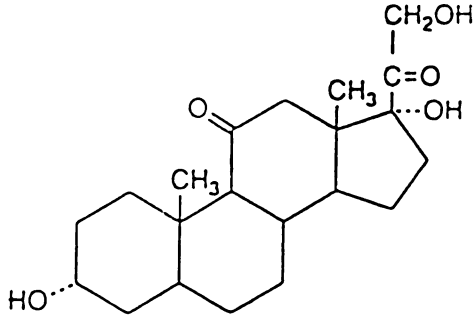

TETRAHYDROCORTISONE

Molecular Mechanics and Dynamics Simulations. Simulations of the interaction between corticosteroid molecules are performed using classical molecular mechanics and dynamics methods (BioGraf version 3.0, Biodesign Inc., Pasadena, CA, USA) on a Silicon Graphics Indigo computer (Model CMNB003, Mountain View, CA, USA). A generic force field, Dreiding (31), is employed to calculate the total energy of the molecule as the sum of the bonding and non-bonding interactions. The bonding interactions include contributions from stretching (E_s), bending (E_b), and torsional (E_ω) energy between atoms that are covalently bonded. The non-bonding interactions consist of contributions from van der Waals (E_{vdw}), electrostatic (E_Q), and hydrogen bond (E_{hb}) energy between atoms that are not covalently bonded. The van der Waals energy is expressed by a standard Lennard-Jones equation

$$E_{vdw} = AR_{ij}^{-12} - BR_{ij}^{-6} \qquad [6.1]$$

where R_{ij} is the distance between atoms i and j, and A and B are empirically derived constants. The electrostatic energy (E_Q) is calculated by using Coulomb's law

$$E_Q = 332.0637\ Q_i\, Q_j / \varepsilon\ R_{ij} \qquad [6.2]$$

where Q_i and Q_j are the net charge on atoms i and j, respectively. The dielectric constant is assumed to be that of a vacuum environment ($\varepsilon = 1$). The hydrogen bonding energy is expressed as:

$$E_{hb} = D_{hb}\ [5\,(R_{hb} / R_{DA})^{12} - 6\,(R_{hb} / R_{DA})^{10}]\ \cos^4(\theta_{DHA}) \qquad [6.3]$$

where θ_{DHA} is the bond angle between the hydrogen donor (D), the hydrogen atom (H), and the hydrogen acceptor (A), while R_{DA} is the distance between the donor and acceptor. D_{hb} and R_{hb} are the energy and the maximum distance used

to define the hydrogen bond, the magnitude of which depend on the convention used for assigning charges in the force field model (31).

To simulate the solute–solute interactions between the corticosteroids, a systematic three-step approach is used. First, the bonding energies are minimized in order to determine the optimum three-dimensional structure and charge distribution for each corticosteroid. These individually optimized structures are then arranged in pairwise combinations. Next, a Monte-Carlo search is performed to examine all possible spatial orientations and to identify those with lowest energy (32). For this study, the steroid pairs are randomly varied in 200 different relative spatial positions and the non-bonding energy is minimized in 30 incremental steps at each of these positions. The final stage of the optimization involves a more refined energy minimization of the most promising orientations (typically 50) identified from the Monte-Carlo search. The annealed dynamics method simulates the exchange of thermal energy between the environment and the steroid pair, thereby allowing translational, vibrational, and rotational motion to minimize the total energy. For this study, the steroid pairs are simulated to be annealed in the temperature range from 300 to 600 K in 20 incremental steps. From among all of these conformations, the one with the lowest total energy is identified as the optimum structure for the steroid pair.

The total interaction energy (ΔE) is calculated by subtracting the energy at the optimum separation distance from that at infinite distance.

$$\Delta E = E_{opt} - E_{\infty} \qquad [6.4]$$

In the same manner, the van der Waals (ΔE_{vdw}), electrostatic (ΔE_{Q}), and hydrogen bonding (ΔE_{hb}) components of the total energy can be calculated:

$$\Delta E_{vdw} = E_{opt,vdw} - E_{\infty,vdw} \qquad [6.5]$$

$$\Delta E_Q = E_{opt,Q} - E_{\infty,Q} \quad [6.6]$$

$$\Delta E_{hb} = E_{opt,hb} - E_{\infty,hb} \quad [6.7]$$

When defined in this manner, the most stable solute–solute pair will have the greatest negative interaction energy.

6.3 Results

Experimental Studies. In a previous study discussed in Chapter 3, the routine analytical separation of eight corticosteroids was performed by reversed-phase liquid chromatography using an octadecylsilica stationary phase and aqueous methanol and acetonitrile mobile phases. During the course of this study, it was observed that specific pairs of steroids exhibited different retention and dispersion behavior when they were analyzed individually and in mixtures (33). Because of the theoretical and practical significance, it was desirable to evaluate this anomalous behavior in greater depth and detail.

The chromatograms of the steroids cortisone and tetrahydrocortisol are shown individually in Figures 6.2A and 6.2B, respectively, and their mixture is shown in Figure 6.2C. The chromatographic figures of merit derived from these chromatograms are summarized in Table 6.1. Within the error of the manual measurements, the sum of the areas for the individual steroid peaks is approximately equal to the area for the composite peak, which confirms that the steroids are co-eluting. However, the capacity factor for the composite peak (1.47) is less than that for the individual peaks (1.56 and 1.48). The standard deviation of replicate measurements is ±0.02 (n = 6), thus the difference in capacity factor is statistically significant at the 99% confidence level (34).

Figures 6.2A,B Chromatograms of individual corticosteroids Column: 47 x 0.46 cm i.d., packed with 5-µm octadecylsilica material. Mobile phase: 35% aqueous acetonitrile; 0.5 mL/min. Detector: UV–visible absorbance detector (240 nm, 0.005 AUFS). Solutes: (A) cortisone (10^{-6} M), (B) tetrahydrocortisol (10^{-3} M).

Figures 6.2A,B

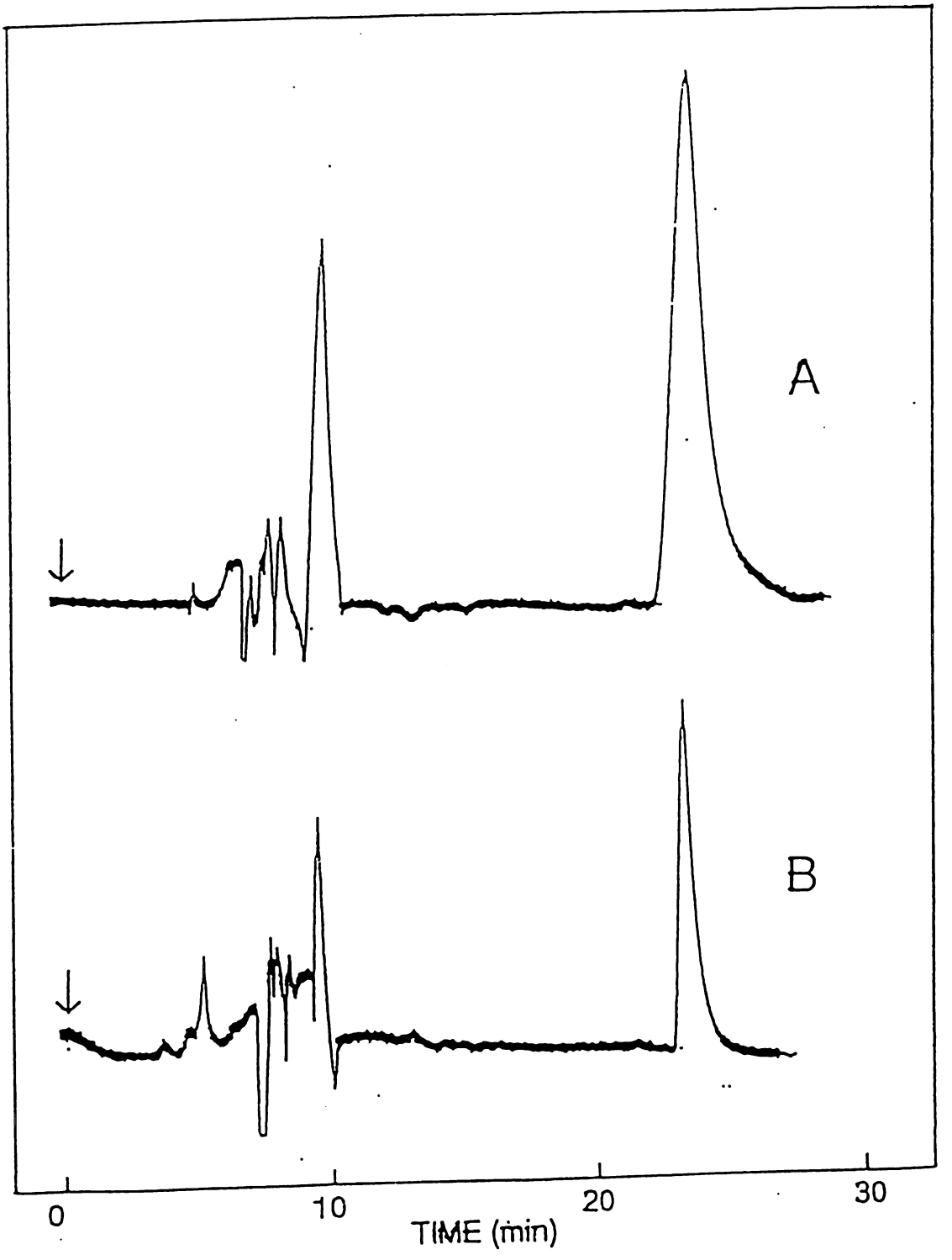

Figure 6.2C Chromatograms of a mixture of cortisone and tetrahydrocortisol. Column: 47 x 0.46 cm i.d., packed with 5-µm octadecylsilica material. Mobile phase: 35% aqueous acetonitrile; 0.5 mL/min. Detector: UV–visible absorbance detector (240 nm, 0.005 AUFS).

Figure 6.2C

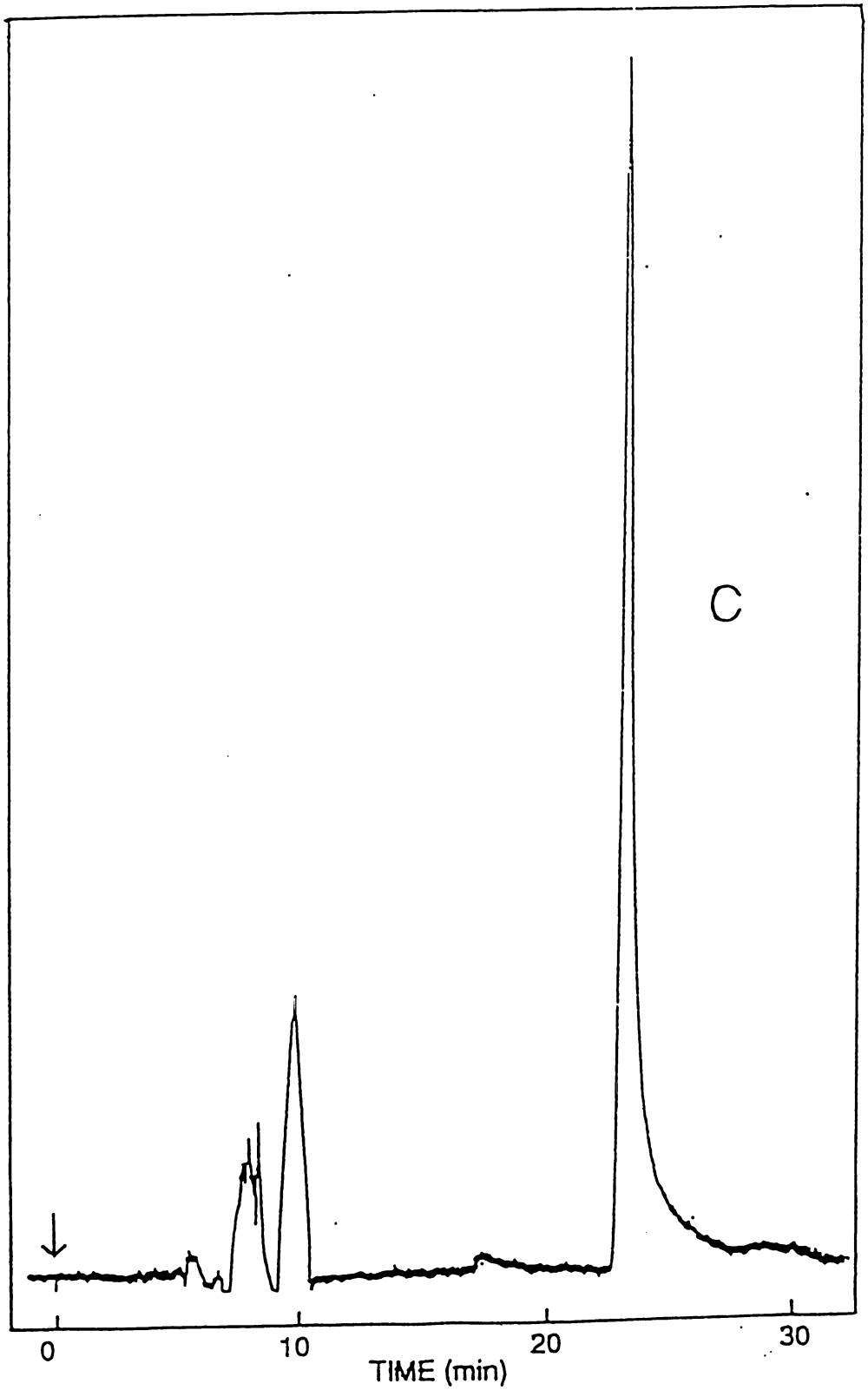

Table 6.1 Comparison of the chromatographic figures of merit for corticosteroids analyzed individually and in mixtures. Experimental conditions as given in Figure 6.2.

CORTICOSTEROID	AREA		CAPACITY FACTOR		PLATE NUMBER		SKEW	
	individual	mixture	individual	mixture	individual	mixture	individual	mixture
Cortisone	0.580	0.727	1.56	1.47	900	4700	1.49	1.33
Tetrahydrocortisol	0.164		1.48		4000		1.56	
Methylprednisolone	0.517	0.677	2.36	2.02	1200	8900	1.65	0.87
Tetrahydrocortisone	0.209		2.26		3200		1.62	

Furthermore, the number of theoretical plates is significantly higher and the skew is significantly lower for the composite peak than for the individual steroid peaks.

The chromatograms of the steroids methylprednisolone and tetrahydrocortisone are shown individually in Figures 6.3 and 6.3B, respectively, and their mixture is shown in Figure 6.3C. The chromatographic figures of merit derived from these chromatograms are summarized in Table 6.1. As in the previous case, the capacity factor for the composite peak is significantly lower than that for the individual steroids. The plate number is significantly higher and the skew is significantly lower for the composite peak than for the individual steroid peaks.

These results clearly demonstrate that the retention and dispersion of these specific pairs of corticosteroids differ when they are analyzed individually and in mixtures. Thus, contrary to traditional theoretical models, the chromatographic behavior of one solute is influenced by the presence of another solute. Strong solute-solute interactions have been reported previously by Bennet *et al.* (35) for bile acids, which have similar skeletal structure to the steroids examined herein. These authors observed little association at the 10^{-3} M concentration level for monohydroxy bile acids, but increasingly stronger interaction for two or more hydroxyl substituents. Hydroxyl groups on the flexible side chain at C-17 showed less interaction than those on the more rigid skeleton, particularly the α face. In addition, carbonyl groups on the side chain played a relatively minor role. These associations were attributed to hydrogen bonding between dimers, however tetramers and higher oligomers were implicated at higher concentrations. Although other workers have suggested that hydrophobic interactions play an important role (36), the predominance of hydrogen bonding effects has been confirmed for the bile salts (37-39) as well as for cholesterol (35,40,41).

Figure 6.3A,B Chromatograms of individual corticosteroids Solute: (A) methylprednisolone (10^{-6} M), (B) tetrahydrocortisone (10^{-3} M). Experimental conditions as given in Figure 6.2.

Figure 6.3A,B

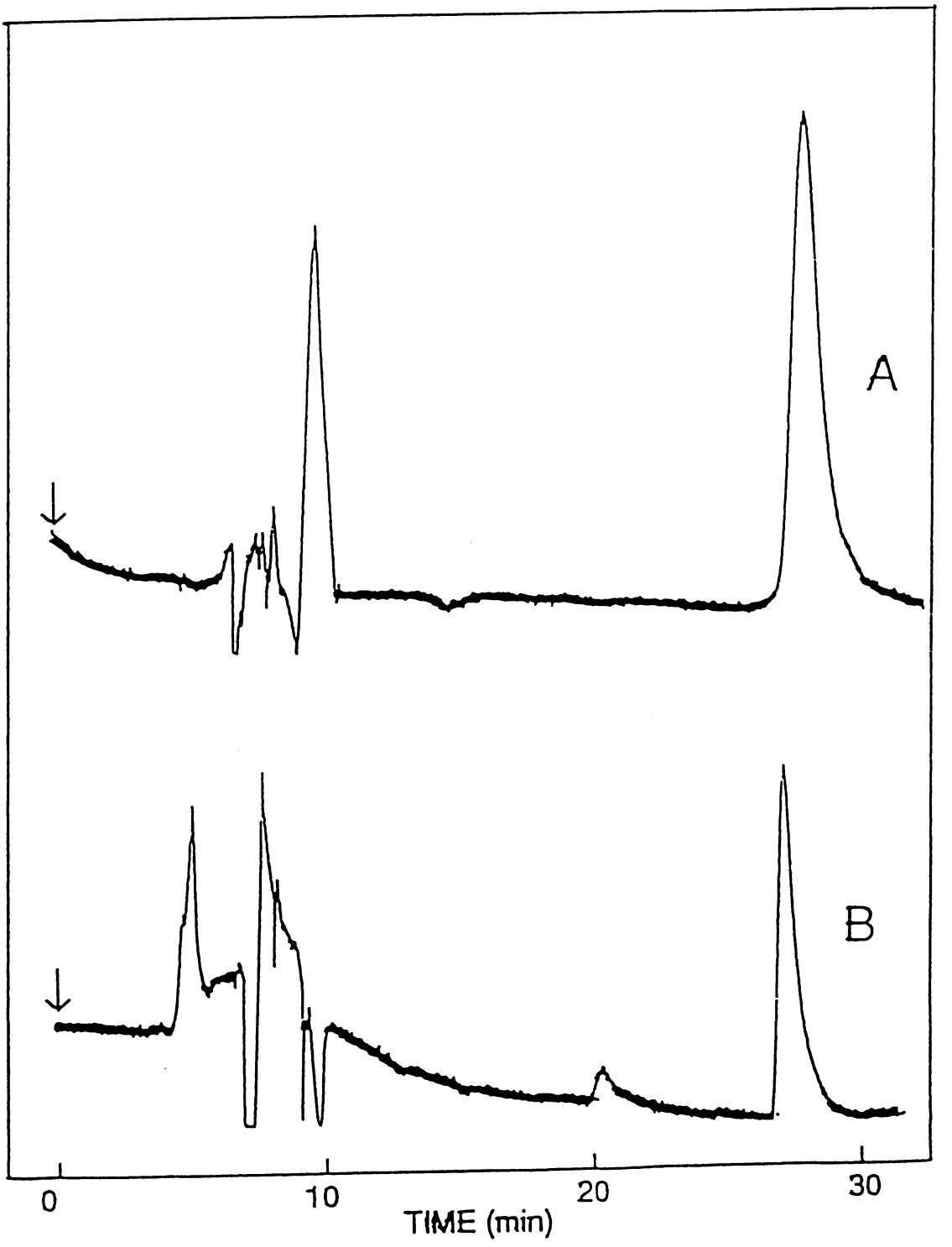

Figure 6.3C Chromatograms of mixture of methylprednisolone (10^{-6} M) and tetrahydrocortisone (10^{-3} M). Experimental conditions as given in Figure 6.2.

Figure 6.3C

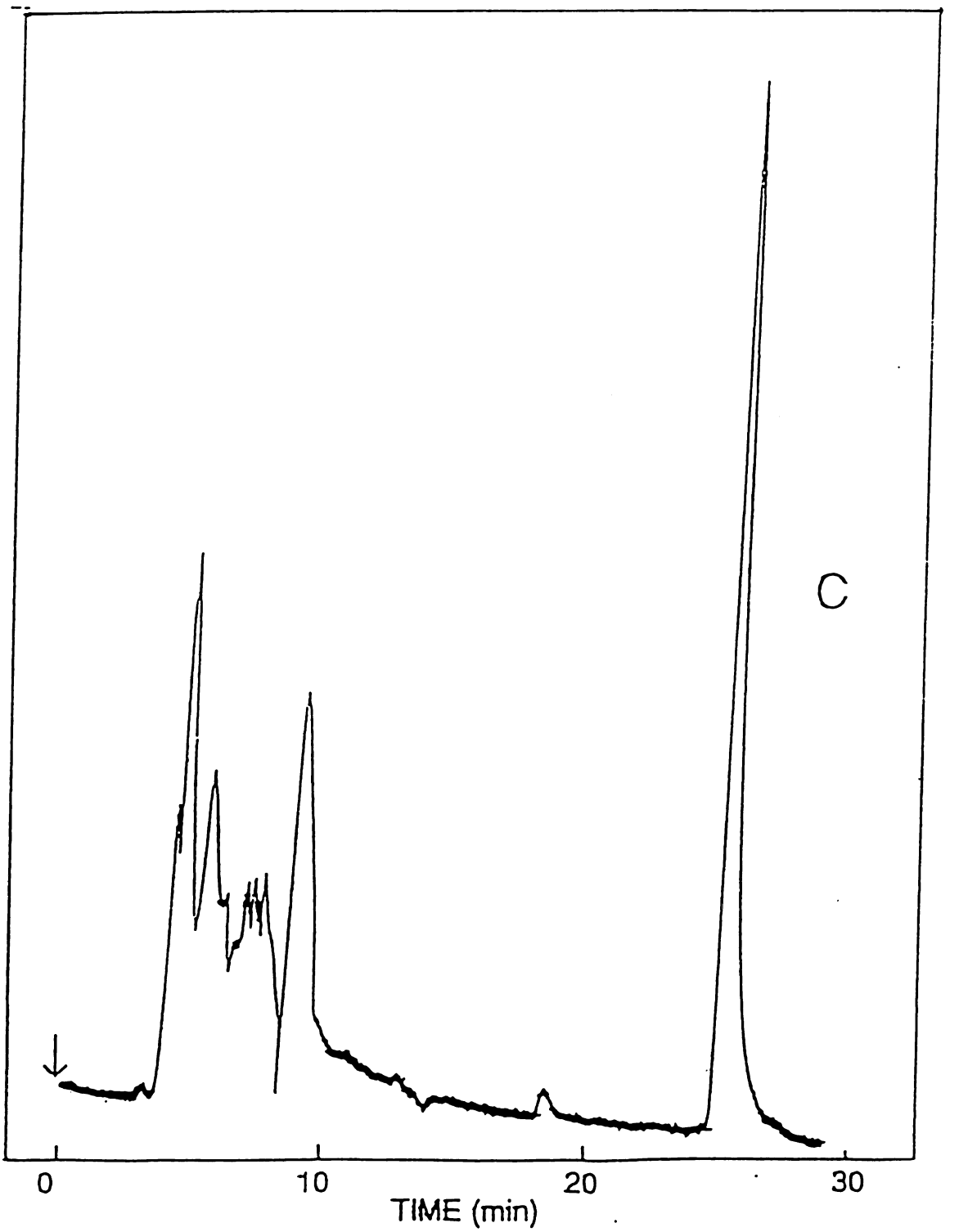

In order to investigate the nature and strength of solute–solute interactions between the corticosteroids, computer simulations are performed by molecular mechanics and dynamics methods. This approach has been used successfully by Hanai *et al.* (42-44) to examine solute–stationary phase interactions in chromatography.

Computer Simulation Studies. The two cases of solute–solute interactions to be examined are cortisone with tetrahydrocortisol and methylprednisolone with tetrahydrocortisone. For each case, there are three possible pairwise combinations, two of which are homogeneous and the other heterogeneous. By examining each of these pairwise combinations, we gain an appreciation for the nature and strength of interactions that exist for self-association as well as for mixed association. Molecular mechanics and dynamics calculations have been performed in order to determine the optimum conformation and to estimate the interaction energy for each of these pairwise combinations.

Figure 6.4 shows the optimized structures for each of the pairwise combinations of cortisone with tetrahydrocortisol. Each pair of steroids is held together by van der Waals, electrostatic, and hydrogen bonding forces. The magnitude of these forces varies with the structure and orientation of the functional groups. The carbonyl and hydroxyl groups interact predominantly by electrostatic and hydrogen bonding forces whereas the hydrocarbon skeleton interacts via van der Waals forces. The optimum conformation for the cortisone-cortisone pair (Figure 6.4A) is a head-to-head orientation that permits intermolecular hydrogen bonding between the carbonyl and hydroxyl groups on the side chain at C-17. In contrast, the tetrahydrocortisol–tetrahydrocortisol pair (Figure 4B) prefers a head-to-tail orientation that allows interaction between the hydroxyl group at C-11 of one molecule with the carbonyl and hydroxyl groups on

Figure 6.4A The optimum configuration for interaction between two cortisone molecules. (O) carbon, (o) hydrogen, (●) oxygen, (- - -) nonbonding atoms that meet the defined energy and distance constraints for hydrogen bonds according to Equation [6.3].

Figure 6.4A

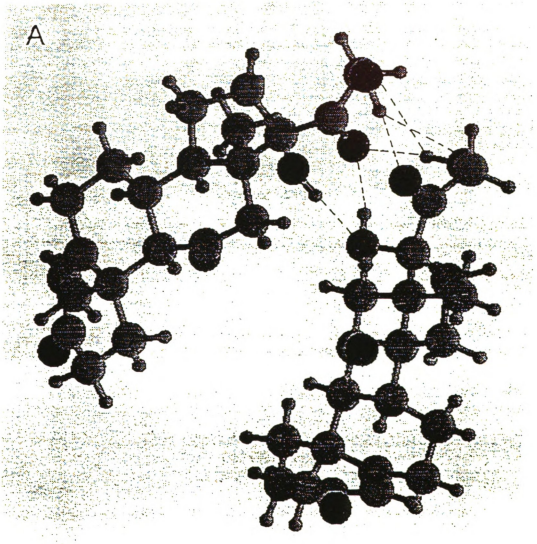

Figure 6.4B The optimum configuration for interaction between two tetrahydrocortisol molecules. (O) carbon, (o) hydrogen, (●) oxygen, (- - -) nonbonding atoms that meet the defined energy and distance constraints for hydrogen bonds according to Equation [6.3].

Figure 6.4B

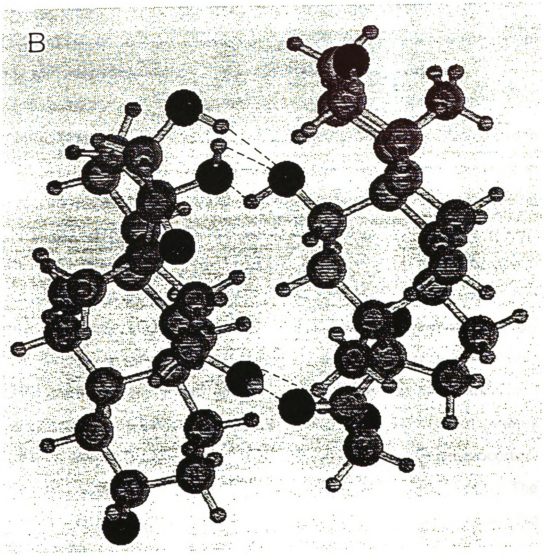

the side chain of the other molecule. Finally, the cortisone-tetrahydrocortisol pair (Figure 6.4C) prefers a head-to-head orientation that allows interaction between the carbonyl group at C-11 of cortisone with the hydroxyl group at C-11 of tetrahydrocortisol, as well as between the carbonyl group on the side chain of cortisone with the hydroxyl group on the side chain of tetrahydrocortisol.

The total energy for each pairwise combination of cortisone with tetrahydrocortisol at infinite and at optimum separation distance is summarized in Table 6.2. The total energy is comprised of the bonding interactions, such as stretching, bending, and torsional energy, as well as the non-bonding interactions, such as van der Waals, electrostatic, and hydrogen bonding energy. Because the bonding energy at infinite separation distance is nearly identical to that at the optimum distance, the interaction energy is dependent primarily upon the non-bonding interactions. From Table 6.2, it is apparent that the van der Waals component is large but remains relatively constant as the molecules approach from infinite to optimum distance. In contrast, the electrostatic and hydrogen bonding components vary considerably. The electrostatic energy decreases for the cortisone-cortisone pair and the cortisone-tetrahydrocortisol pair, but increases for the tetrahydrocortisol-tetrahydrocortisol pair. The hydrogen bonding energy decreases notably for all pairwise combinations, but especially so for the tetrahydrocortisol-tetrahydrocortisol pair. These results suggest that the molecular interactions are controlled predominantly by electrostatic and hydrogen bonding forces. The total interaction energy of the cortisone-cortisone and tetrahydrocortisol-tetrahydrocortisol pairs is less negative than that of the cortisone-tetrahydrocortisol pair, which indicates that formation of the latter pair is more energetically favorable.

In a similar manner, Figure 6.5 shows the optimized structures for each of the pairwise combinations of methylprednisolone with tetrahydrocortisone. The

Figure 6.4C The optimum configuration for interaction between cortisone and tetrahydrocortisol molecules. (O) carbon, (o) hydrogen, (●) oxygen, (- - -) nonbonding atoms that meet the defined energy and distance constraints for hydrogen bonds according to Equation [6.3].

Figure 6.4C

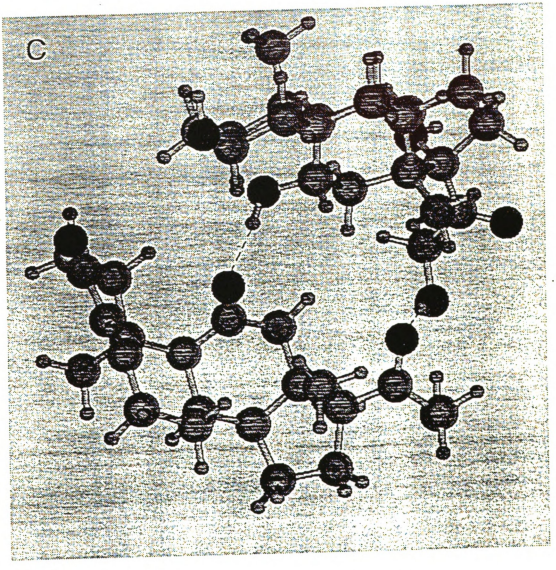

Table 6.2 Total energy (E) and the components of van der Waals energy (E_{vdw}), electrostatic energy (E_Q), and hydrogen bonding energy (E_{hb}) at infinite separation distance (∞) and at the optimum separation distance (opt) for the pairwise configurations of corticosteroids shown in Figures 6.4A to 6.4C.

CORTICOSTEROID PAIR	ENERGY (kcal/mol)											
	E_∞	E_{opt}	ΔE	$E_{\infty,vdw}$	$E_{opt,vdw}$	ΔE_{vdw}	$E_{\infty,Q}$	$E_{opt,Q}$	ΔE_Q	$E_{\infty,hb}$	$E_{opt,hb}$	ΔE_{hb}
Cortisone – Cortisone	196.1	168.2	−27.9	101.0	101.0	0.0	8.3	4.5	−3.8	−11.2	−31.0	−19.8
Tetrahydrocortisol – Tetrahydrocortisol	192.0	160.1	−31.9	100.2	101.1	0.9	1.3	5.4	4.1	−11.1	−39.0	−27.9
Cortisone – Tetrahydrocortisol	198.0	165.4	−32.6	98.1	101.1	3.0	10.2	5.3	−4.9	−11.0	−31.0	−20.0

optimum conformation for the methylprednisolone-methylprednisolone pair (Figure 6.5A) is a head-to-tail orientation that permits hydrogen bonding between the carbonyl group at C-3 and the hydroxyl group at C-11 of one molecule with the hydroxyl and carbonyl groups on the side chain of the other molecule. The tetrahydrocortisone-tetrahydrocortisone pair (Figure 6.5B) prefers a head-to-head orientation that allows interaction between the carbonyl and hydroxyl groups on the side chains. Finally, the methylprednisolone-tetrahydrocortisone pair (Figure 6.5C) prefers a head-to-tail orientation that allows interaction between the hydroxyl group at C-11 of methylprednisolone with the carbonyl group at C-11 of tetrahydrocortisone, between the carbonyl group at C-3 of methylprednisolone with the side chain of tetrahydrocortisone, as well as between the side chain of methylprednisolone with the hydroxyl group at C-3 of tetrahydrocortisone.

The total energy for each pairwise combination of methylprednisolone with tetrahydrocortisone at infinite and at optimum separation distance is summarized in Table 6.3. As in the previous case, the van der Waals component remains relatively constant whereas the electrostatic and hydrogen bonding components decrease significantly as the molecules approach from infinite to optimum distance. The methylprednisolone-methylprednisolone and methylprednisolone-tetrahydrocortisone pairs have the most negative interaction energy and, hence, are the most energetically favorable combinations.

From these molecular mechanics and dynamics simulations, we may conclude that significant non-bonding interactions exist between cortisone and tetrahydrocortisol and between methylprednisolone and tetrahydrocortisone. For both cases, the total interaction energy is of comparable magnitude (approximately –33 kcal/mole) and arises predominantly from electrostatic and hydrogen bonding interactions.

Figure 6.5A The optimum configuration for interaction between two methylprednisolone molecules. (O) carbon, (o) hydrogen, (●) oxygen, (- - -) nonbonding atoms that meet the defined energy and distance constraints for hydrogen bonds according to Equation [6.3].

Figure 6.5A

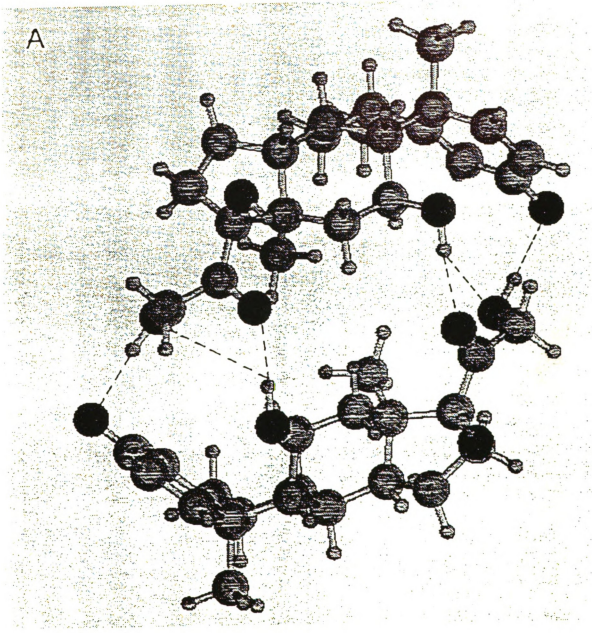

Figure 6.5B The optimum configuration for interaction between two tetrahydrocortisone molecules. (O) carbon, (o) hydrogen, (●) oxygen, (- - -) nonbonding atoms that meet the defined energy and distance constraints for hydrogen bonds according to Equation [6.3].

Figure 6.5B

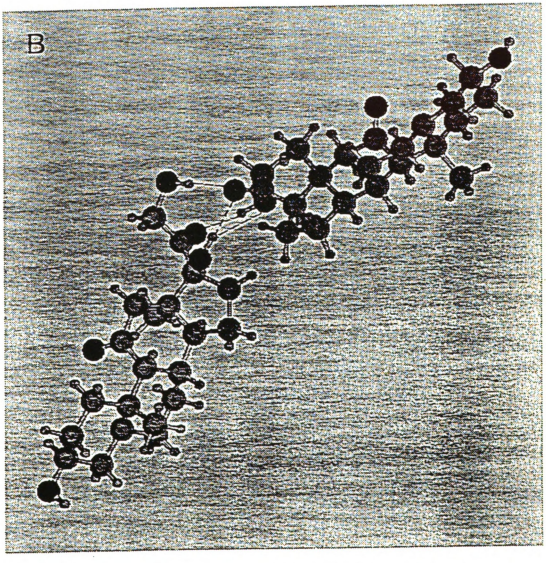

Figure 6.5C The optimum configuration for interaction between methylprednisolone and tetrahydrocortisone molecules. (O) carbon, (o) hydrogen, (●) oxygen, (- - -) nonbonding atoms that meet the defined energy and distance constraints for hydrogen bonds according to Equation [6.3].

Figure 6.5C

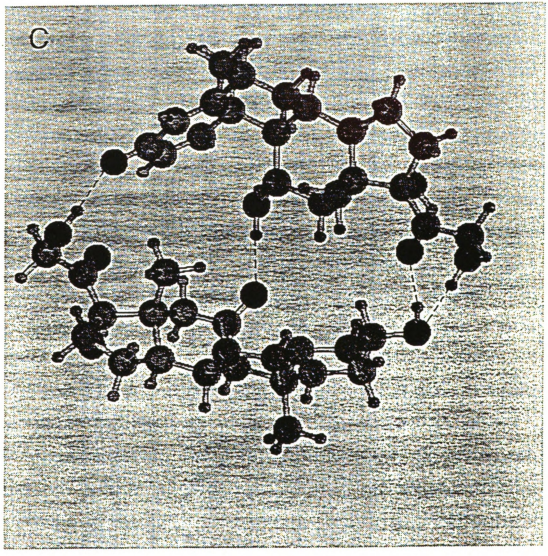

Table 6.3 Table 6.3 Total energy (E) and the components of van der Waals energy (E_{vdw}), electrostatic energy (E_Q), and hydrogen bonding energy (E_{hb}) at infinite separation distance (∞) and at the optimum separation distance (opt) for the pairwise configurations of corticosteroids shown in Figures 6.5A to 6.5C.

CORTICOSTEROID PAIR	ENERGY (kcal/mol)											
	E_∞	E_{opt}	ΔE	$E_{\infty,vdw}$	$E_{opt,vdw}$	ΔE_{vdw}	$E_{\infty,Q}$	$E_{opt,Q}$	ΔE_Q	$E_{\infty,hb}$	$E_{opt,hb}$	ΔE_{hb}
Methylprednisolone – Methylprednisolone	197.4	159.3	−38.1	99.1	99.3	0.2	11.2	1.8	−9.4	−11.1	−31.0	−19.9
Tetrahydrocortisone – Tetrahydrocortisone	194.2	168.2	−26.0	100.4	102.1	1.7	10.3	4.1	−6.2	−11.1	−30.1	−19.0
Methylprednisolone – Tetrahydrocortisone	194.1	161.4	−32.7	101.2	101.3	0.1	10.1	2.4	−7.7	−11.4	−36.3	−24.9

6.4 Discussion

In order to understand the effect of these solute-solute interactions, it is helpful to discuss briefly the structure of octadecylsilica and the associated mechanism(s) of solute retention (45-49). Octadecylsilica is comprised of alkyl chains covalently bonded to the silica surface, with residual silanol and siloxane groups. Nonpolar solute molecules may interact predominantly with the alkyl chains, whereas polar functional groups may interact with the weakly acidic silanol groups or weakly basic siloxane groups. The former interactions arise from relatively weak van der Waals forces and, thus, tend to be rapidly reversible. In contrast, the latter interactions arise from stronger electrostatic and hydrogen bonding forces, which are characterized by slow mass transfer kinetics (50). These interactions often result in lower plate number and higher asymmetry or skew.

For solutes such as the corticosteroids, which possess a hydrocarbon skeleton together with varying numbers of carbonyl and hydroxyl groups, a dual retention mechanism is likely to occur (51). In the aqueous acetonitrile mobile phases utilized for the present study, steroids with readily accessible carbonyl groups exhibit the lowest plate number and highest asymmetry. For example, the plate number for cortisone, which has carbonyl groups at C-3 and C-11, is significantly less than that for tetrahydrocortisol, which has hydroxyl groups at these positions (Table 6.1). However, in aqueous methanol mobile phases, which can form hydrogen bonds with the carbonyl groups, the plate number is significantly increased and the asymmetry is reduced. These observations suggest that interaction of the carbonyl group, which is weakly basic, with silanol groups or other Lewis-acid impurities in the silica is largely responsible for the observed peak profiles.

The retention and dispersion of the individual steroids and their mixtures can, therefore, be rationalized in terms of the number of carbonyl groups that are available to adsorb at the silica surface. For the case of cortisone with tetrahydrocortisol, the cortisone-tetrahydrocortisol pair is more energetically favorable than either of the homogeneous pairwise combinations. Because of the extensive intermolecular and intramolecular hydrogen bonding in the cortisone-tetrahydrocortisol pair, there are fewer free carbonyl groups than in the individual steroids. Similarly for the case of methylprednisolone and tetrahydrocortisone, the methylprednisolone-tetrahydrocortisone pair is energetically favorable and provides extensive hydrogen bonding to mask the carbonyl groups. In each case, the solute-solute interactions serve to reduce adsorption at the silanol groups, hence the composite peak is less retained and has higher plate number and lower skew than the individual steroids.

Based on the interaction energy in Table 6.3, one would expect the homogeneous methylprednisolone-methylprednisolone pair to be at least as prevalent as the heterogeneous pairs discussed above. To test this hypothesis, the chromatographic peak profile was analyzed as the concentration of methylprednisolone was increased from 10^{-6} M to 10^{-3} M, comparable to tetrahydrocortisone. The plate number correspondingly increased from 1200 to 2100, and the skew decreased from 1.65 to 1.60. Thus, methylprednisolone appears to undergo self association in addition to mixed association with tetrahydrocortisone. The molecular mechanics and dynamics simulations may prove to be useful in predicting other cases of solute-solute interactions.

6.5 Conclusion

By a combination of experimental and computer simulation techniques, corticosteroids are shown to undergo both self-association and mixed association at the 10^{-3} M concentration level. Like the structurally similar bile acids, the steroids interact primarily by electrostatic and hydrogen bonding forces. These interactions have a significant influence upon solute retention and dispersion under routine operating conditions for reversed-phase liquid chromatography. Because solute-solute interactions are invariably neglected in theoretical and semi-empirical models, they may have a detrimental effect on the prediction and optimization of chromatographic separations.

6.6 References

1. J. J. Kozak, W. S. Knight and W. Kauzmann, *J. Chem. Phys.* **48**, 675 (1968).

2. T. H. Lilley and R. P. Scott, *J. Chem. Soc. Faraday Trans. 1*, **72**, 184 (1976).

3. E. Matteoli and L. Lepori, *J. Phys. Chem.* **86**, 2994 (1982) .

4. K. Nakanishi, *Infrared Absorption Spectroscopy: Practical*, Holden-Day, San Francisco, California, 1964.

5. N. S. Bhacca and D. H. Williams, *Applications of NMR Spectroscopy in Organic Chemistry*, Holden-Day, San Francisco, California, 1964.

6. K. L. Mittal, *Solution Chemistry of Surfactants*, Vol. 1 and 2, Plenum Press, New York, 1979.

7. W. G. McMillan and J. E. Mayer, *J. Chem. Phys.* **13**, 276 (1945).

8. D. Stigter, *J. Phys. Chem.* **64**, 118 (1960).

9. G. Nemethy and H. A. Scheraga, *J. Chem. Phys.* 36, 3382 (1962).

10. G. Nemethy and H. A. Scheraga, *J. Phys. Chem.* 66, 1773 (1962).

11. L. R. Pratt and D. Chandler, *J. Chem. Phys.* **67**, 3683 (1977).

12. L. R. Pratt and D. Chandler, *J. Solution Chem.* **9**, 1 (1979).

13. C. Tanford, *The Hydrophobic Effect*, Wiley Interscience, New York, 1973.

14. A. Ben-Naim, *Water and Aqueous Solutions*, Plenum Press, New York, 1974.

15. A. Ben-Naim, *Hydrophobic Interactions*, Plenum Pres, New York, 1980.

16. K. Amaya and K. Sasaki, *Bull. Chem. Soc. Japan* **35**, 1507 (1962).

17. D. K. Johnson, H. L. Chum and J. A. Hyatt, *ACS Symp. Ser.* **397**, 109 (1989).

18. T. Malfait and F. Van Cauwelaert, *J. Chromatogr.* **504**, 369 (1990).

19. S. Gupta, D. Ghonasgi, K. M. Dooley and F. C. Knopf, *J. Supercrit. Fluids* **4**, 181 (1991).

20. J. H. Hildebrand and R. L. Scott, *The Solubility of Non-electrolytes*, Reinhold, New York, 1950, Chap. 23.

21. A. F. M. Barton, *Chem. Rev.* **75**, 731 (1975).

22. D. E. Martire and D. C. Locke, *Anal. Chem.* **43**, 68 (1971)

23. P. J. Schoenmakers, H. A. H. Billiet and L. de Galan, *J. Chromatogr.* **185**, 179 (1979).

24. P. J. Schoenmakers, H. A. H. Billiet and L. de Galan, *J. Chromatogr.* **205**, 13 (1981).

25. C. Horvath, W. Melander and I. Molnar, *J. Chromatogr.* **125**, 129 (1976).

26. W. R. Melander and C. Horvath, in *High-Performance Liquid Chromatography: Advances and Perspectives*, Vol. 2, C. Horvath, Ed., Academic Pres, New York, 1980, pp. 113-319.

27. D. E. Martire and R. E. Boehm, *J. Phys. Chem.* **87**, 1045 (1983).

28. D. E. Martire, *J. Liq. Chromatogr.*, **10**, 1569 (1987).

29. K. A. Dill, *J. Phys. Chem.* **91**, 1980 (1987).

30. J. P. Foley and J. G. Dorsey, *Anal. Chem.* **55**, 730 (1983).

31. L. M. Stephen, B. D. Olafson and W. A. Goddard, *J. Phys. Chem.* **94**, 8897 (1990).

32. J. Gasteiger and M. Marsili, *Tetrahedron* **36**, 3219 (1980).

33. P. H. Lukulay and V. L. McGuffin, *J. Liq. Chromatogr.*, in press.

34. S. L. Meyer, *Data Analysis for Scientists and Engineers*, John Wiley and Sons, New York, 1975, pp. 274-282.

35. W. S. Bennet, G. Eglinton and S. Kovac, *Nature* **214**, 776 (1967).

36. D. M. Small, *Adv. Chem. Ser.* **84**, 31 (1968).

37. D. G. Oakenfull and L. R. Fisher, *J. Phys. Chem.* **81**, 1838 (1977).

38. L. R. Fisher and D. G. Oakenfull, *J. Phys. Chem.* **84**, 937 (1980).

39. J. Robeson, B. W. Foster, S. N. Rosenthal, E. T. Adams and E. J. Fendler, *J. Phys. Chem.* **85**, 1254 (1981).

40. J. J. Feher, L. D. Wright and D. B. McCormick, *J. Phys. Chem.* **78**, 250 (1974).

41. B. W. Foster, J. Robeson, N. Tagata, J. M. Beckerdite, R. L. Huggins and E. T. Adams, *J. Phys. Chem.* **85** 3715 (1981).

42. T. Hanai, H. Hatano, N. Nimura and T. Kinoshita, *Supramolecular Chemistry* **3**, 243 (1992).

43. T. Hanai, H. Hatano, N. Nimura and T. Kinoshita, *Analyst* **118**, 1371 (1993).

44. T. Hanai, H. Hatano, N. Nimura and T. Kinoshita, *J. Liq. Chromatogr.* **17**, 241 (1994).

45. L. C. Sander and S. A. Wise, *CRC Crit. Rev. Anal. Chem.* **18**, 299 (1987).

46. J. G. Dorsey and K. A. Dill, *Chem. Rev.* **89**, 331 (1989).

47. J. F. Wheeler, T. L. Beck, S. J. Klatte, L. A. Cole and J. G. Dorsey, *J. Chromatogr.* **656**, 317 (1993).

48. J. Nawrocki, *Chromatographia*, **31**, 177 (1991).

49. J. Nawrocki, *Chromatographia*, **31**, 193 (1991).

50. L. R. Snyder, *Principles of Adsorption Chromatography*, Marcel Dekker, New York, 1968.

51. A. Nahum and C. Horvath, *J. Chromatogr.* **203**, 53 (1981).

CHAPTER 7

SUMMARY AND FUTURE WORK

7.1 Summary

In this work, a novel method for optimizing chromatographic separation is developed and validated. This methodology is in sharp contrast to the more commonly used method, the regression technique, for optimizing chromatographic parameters. In regression techniques, a mathematical function is assumed for the functional relationship between retention and the variables. Optimization of the parameters is accomplished by measuring retention at a few levels of the parameters and using these experimental data to fully characterize the retention surface. From the retention surface, solute retention can be predicted as a function of any level of the parameters in the model equation. The accuracy of the predictions depends on the accuracy of the model used. Due to interactions between chromatographic parameters, the mathematical models used often do not adequately represent the dependence of the parameters on the overall retention. This inadequacy is even more problematic in multivariate optimization.

In order to overcome this limitation, parametric modulation has been developed as an alternative approach for the optimization of univariate and multivariate optimization. The fundamental strategy of this approach is that chromatographic retention may be accurately predicted if the solute is constrained to undergo interaction independently within a segment of each parameter, such as mobile phase, stationary phase, and temperature environment. By maintaining each of these variables in discrete and separate

zones along the chromatographic column, the overall retention time (t_i) of the solute may be calculated by summation of its retention within each individual environment. Thus the prediction of retention is more accurate because it is calculated by summation of known and measured behavior, rather than by numerical regression of poorly characterized interacting parameters. Additionally, this method is advantageous because only a few initial experiments may be necessary to fully characterize the response surface. From these preliminary experiments, the retention time for any combination, sequence and length of the parameter zones may be calculated. Thus, a complete multivariate response surface may be systematically generated and the optimum conditions may be identified by visual inspection or by computer-assisted search methods.

Experimental verification of this method was performed for the univariate optimization of mobile phase, for the separation of corticosteroids on octadecylsilica stationary phase in Chapter 3. The performance of this method was compared to DryLab, a commercially available program which uses the regression technique for the univariate optimization of mobile phase composition. The error of prediction of retention times was comparable, but a slightly better separation was obtained for the least resolved solute molecules using parametric modulation. Next, the efficacy of the method was demonstrated for multivariate optimization. Two experimental studies were performed for the separation of isomeric four- and five-ring polynuclear aromatic hydrocarbons (PAH). In the first study in Chapter 4, mobile and stationary phases were optimized using aqueous methanol and acetonitrile mixtures as mobile phases and octadecylsilica and β-cyclodextrinsilica as stationary phases. The experimental and predicted retention times and peak widths were in very good agreement, with an error of ±3.5% and ±21%, respectively. The optimum length of octadecylsilica and cyclodextrinsilica columns were 75 cm and 0 cm, respectively. The optimum solvent modulation

sequence was 70% aqueous acetonitrile and 80% aqueous methanol in zones of 203 and 634 cm length, respectively. In the second study, temperature and mobile phase were optimized for the separation of polynuclear aromatic hydrocarbons. Two temperatures were found to be optimum with column lengths of 85 cm maintained at 23° C and 5 cm maintained at 40° C. The optimum mobile phase was 100% methanol. The experimental chromatogram agreed well with theoretical predictions having relative error in retention time and peak widths of 0.9% and 16%, respectively. The results of this study are given in Chapter 5. Based on these results, the parametric modulation approach appears to be a powerful and versatile strategy for the univariate and multivariate optimization of chromatographic separations.

Finally, a theoretical and experimental study was undertaken to investigate solute-solute interaction in liquid chromatography, and its effect on chromatographic figures of merit, such as solute capacity factor and plate number. In the practical application of chromatographic theory, solute-solute interaction is considered negligible. Thus, the solute capacity factor of one solute should be independent of others in a mixture. An experimental and computer simulation study of solute-solute interaction was undertaken for the interaction between corticosteroids, and the results presented in Chapter 6. Two pairs of steroids were observed to interact significantly: cortisone with tetrahydrocortisol and methylprednisolone with tetrahydrocortisol. The interaction between these corticosteroids was investigated using a commercially available program, BioGraf, which uses molecular mechanics calculations to estimate the energy of interaction. The steroids in each pair were found to interact significantly with each other via hydrogen bonding when the concentration of one of the steroids was as high as 10^{-3} M. This preferential interaction caused a change in the capacity factor and variance of the solutes when they were injected singly and as

a mixture. Thus, based on these results, solute-solute interactions can lead to significant variation in chromatographic figures of merit.

7.2 Future Work

The concept of parametric modulation presents an opportunity for the optimization of chromatographic variables without knowledge about the interaction between these variables. The current expressions developed for predicting retention as a function of length of mobile and stationary phases as well as temperature zones include other variables such as flow rate, porosity, column radius and particle size. The inclusion of these variables in the expression developed herein allows a theoretical prediction of retention as a function of these variables, as well as their optimization. Thus, future studies could be directed at the optimization of these variables using the expressions developed in this work.

In addition to chromatographic optimization, there is potential for this method to be applied to the optimization of capillary zone (1) and isoelectric focussing (2) electrophoretic separations. One of the parameters which can be optimized is the length of buffer zone at different pH (3). Retention surfaces can be obtained for the quality criterion as a function of this variable.

Finally, this method can be incorporated into an expert system for the optimization of various chromatographic parameters (4). After selection of the appropriate parameters for a given separation by the expert system, optimization of the parameters can be achieved by combining regression techniques and parametric modulation. The regression techniques can be used to make a

coarse identification of the optimum parameter level and parametric modulation can be used to more accurately determine the optimum separation conditions.

7.3 References

1. S. Hjerten, *Chromatogr. Rev.* **9**, 11 (1967)
2. P. G. Righetti, *J. Chromatogr.* **300**, 165 (1984)
3. M. Bier, Ed.; *Electrophoresis - Theory, Methods and Applications*; Academic Press Inc.; New York, 1959
4. S. V. Medlin, *Ph.D. Dissertation*, Michigan State University, 1993

APPENDIX 1

COMPUTER PROGRAM

In this appendix, a description of the computer program used to implement the parametric modulation method is given, and the program is listed in Appendix A1.2

A1.1 Program Description

The program to calculate solute retention and optimize chromatographic separation under the conditions of parametric modulation is written in the FORTRAN 77 language and executed on a VAXstation II computer (Digital Equipment Corporation). A flow chart for the program is given in Figure A1.1. The current version of the program can optimize any two parameters simultaneously by the parametric modulation approach. In order to accomplish this, it requires an input of solute capacity factor for each parameter investigated. For example, if two mobile phases and two columns are to be optimized, then the program requires capacity factors of each solute in each mobile phase on each column. Hence, for a system composed of n mobile phases and q columns, only $n \cdot q$ retention measurements are necessary for the calculation of solute capacity factor for the parameters chosen. In order to calculate the overall retention time, the program requires an input of flow rate (F), radius (r_p) and porosity (ε_p) of the column. In addition to solute retention, the variance of each solute is also calculated in order to estimate the resolution between the solutes. The variance calculation requires an input of the reduced plate height (h_p) and particle

Figure A1.1 A flow chart of the computer program used to optimize chromatographic parameters by the parametric modulation method.

Figure A1.1

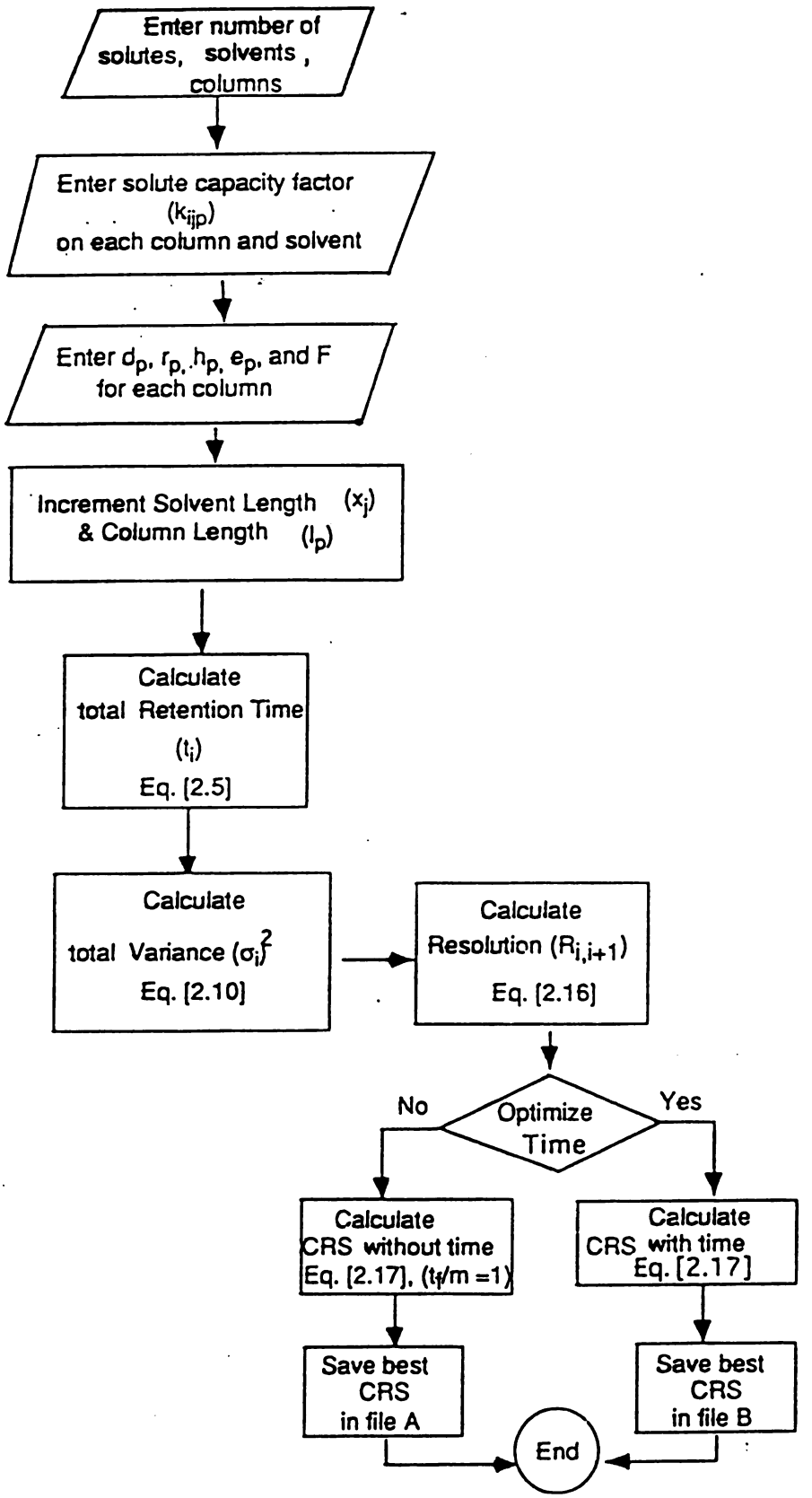
Enter number of solutes, solvents, columns
Enter solute capacity factor (k_{ijp}) on each column and solvent
Enter d_p, r_p, h_p, e_p, and F for each column
Increment Solvent Length (x_j) & Column Length (l_p)
Calculate total Retention Time (t_i) Eq. [2.5]
Calculate total Variance $(\sigma_i)^2$ Eq. [2.10]
Calculate Resolution ($R_{i,i+1}$) Eq. [2.16]
Optimize Time
No
Yes
Calculate CRS without time Eq. [2.17], ($t_i/m = 1$)
Calculate CRS with time Eq. [2.17]
Save best CRS in file A
Save best CRS in file B
End

diameter (d_p). During execution, the program increments the length of each parameter, e.g. the length of solvent or column, and calculates the overall retention time for each solute. Next, the variance is calculated. These retention times are then sorted in increasing order using a bubble sort routine (1) in order to calculate the resolution between adjacent solutes. For each possible combination and sequence of parameters, the minimum CRS is stored in a file. Two types of CRS are calculated and stored (2). The CRS with and without time optimization are evaluated and stored in the first and second file, respectively. The former criteria is used if time optimization is important and the latter if time optimization is not important. The values of the parameters corresponding the minimum CRS are identified as the optimum conditions for the separation.

A1.2 Optimization Program

Program Name: Paramod1.for

Written by: Patrick H. Lukulay

```
* This is a program to optimize liquid chromatographic *separations by
the PARAMETRIC MODULATION method. It is code-named Paramod1.for

      DOUBLE PRECISION RFRAC, COL1, COL2, SOLVA, SOLVB,
     & LTEMP2, TCOL1, TCOL2, S1MAX, S2MAX, LTEMP1, QTEMP,
     & S1MIN, S2MIN, SOLCAP, CAP, S1, S2, TEST, PNUM, NTEMP,
     & CAPAC, PLTNUM, PULSE, RR, NT, CRS1, CRS2, SIGMA,MINRES,
     & N1, N2, K1,K2,CAPTOT, CRS, PLTHT1, FRAC, RMIN, ROPT,
     & PLTHT2, dp1,dp2, HIGH1A, HIGH2A, HIGH1B, HIGH2B, ID2,
     & CL1MIN, CL1MAX, CL2MIN, CL2MAX, RETENT, RETEN, WIDTH,
     & L1MIN, L1MAX, L2MIN, L2MAX, SAMIN, SAMAX, SBMIN,
     & SBMAX, FPULSE, COLEN1, COLEN2, WIDTHS, ID1, SEPTIME,
     & BCOL1, BCOL2, BSOLVA BSOLVB, CRST, BCRS, FLOW, C1, C2,
     & CRSTT, BCRSTT, BCOL1T, BCOL2T, BSOLVAT, BSOLVBT, CRITRT,
     & SEPTIMT
      PARAMETER ( MYFILE = 2,
     & PORUS1 = 0.90, PORUS2 = 0.90, PI = 3.14159)
      INTEGER*4 OUTPUT, I, P, J, M, N, MAXSOL, MAXCOL,
     & MAXSOV, COUNTA, COUNTB, COUNTC, COUNTD, RRSOLA,
     & RRSOLB, REPTA, REPTB, COUNT, TPULSE
      CHARACTER FILE1*20, FILE2*20, RESP1, RESP2
      LOGICAL DONE
      DIMENSION SOLCAP( 20, 2, 2), RETENT(100), PULSES(100),
     & WIDTHS(100), COUNT(5)

*        ------------Input statements--------------------

1007   WRITE (6, 1) 'ENTER OUTPUT FILENAME FOR FILE1 '
1     FORMAT (A)
      READ (5, 2) FILE1
2     FORMAT (A)
      OPEN (UNIT = 20 , FILE = FILE1, STATUS = 'NEW')
       WRITE (6, 1008) 'ENTER OUTPUT FILENAME FOR FILE2 '
1008     FORMAT (A)
      READ (5, 1009) FILE2
1009     FORMAT (A)
      OPEN (UNIT = 10 , FILE = FILE2, STATUS = 'NEW')

      WRITE (6,*) 'PLEASE ENTER THE NUMBER OF SOLUTES,'
      READ (5,*) MAXSOL
      WRITE (6, 666)
666   FORMAT(1X, 'PLEASE ENTER THE NUMBER OF COLUMN TYPES,'
     & ' 1 OR 2' )
      READ (5, *) MAXCOL
```

```
      WRITE (6, 667)
667   FORMAT (1X, 'PLEASE ENTER THE NUMBER OF MOBILE,'
     & ' PHASES, 1 0R 2')
      READ (5, *) MAXSOV

      DO 10 I = 1, MAXSOL
      DO 11 P = 1, MAXCOL
      DO 12 J = 1, MAXSOV

      WRITE (6, 71) I, P, J
71    FORMAT (1X, 'PLEASE ENTER THE CAPACITY FACTOR OF'
     &' SOLUTE', I3, ' IN COLUMN', I3, ' AND IN MOBILE'
     & ' PHASE', I3)

      READ (5, 81 ) SOLCAP (I,P,J)
81     FORMAT ( F8.3 )

12    CONTINUE
11     CONTINUE
10      CONTINUE
      WRITE (6,778)

778   FORMAT(1X, ' PLEASE ENTER THE FLOW RATE ON COLUMN(S)'
     & 'IN cm3 / MIN')
      READ (5,*) FLOW

        IF (MAXCOL .GT. 1) THEN
      WRITE (6,7)
7      FORMAT (1X,  'ENTER THE PARTICLE DIAMETER IN cm FOR '
     & ' COLUMN 1 ')

      READ (5, *) dp1
      WRITE (6, 2007)

2007     FORMAT (1X, 'ENTER THE COLUMN DIAMETER IN (cm) FOR'
     & ' COLUMN 1 ')

      READ (5, *) ID1


      WRITE(6,696)
696   FORMAT(1X, 'ENTER THE REDUCED PLATE HEIGHT IN cm OF COLUMN 1')
      READ (5, *) hp1

      WRITE (6, 91)

91     FORMAT (1X, 'ENTER THE PARTICLE DIAMETER IN (cm) FOR'
     & ' COLUMN 2 ')

      READ (5, *) dp2
      WRITE (6, 2006)

2006     FORMAT (1X, 'ENTER THE COLUMN DIAMETER IN (cm) FOR'
     & ' COLUMN 2 ')
```

```
      READ (5, *) ID2

      WRITE(6,796)
796   FORMAT(1X, 'ENTER THE REDUCED PLATE HEIGHT IN cm OF COLUMN 2')
      READ (5, *) hp2

        ELSE
      WRITE (6,8)
8      FORMAT (1X,  'ENTER THE PARTICLE DIAMETER IN cm FOR '
     & ' THE COLUMN ')
       dp2 = 0.0
      READ (5,*) dp1

      WRITE (6, 2008)
2008     FORMAT (1X, 'ENTER THE COLUMN DIAMETER IN (cm) FOR'
     & ' THE COLUMN ')

      READ (5, *) ID1

      WRITE(6,896)
896   FORMAT(1X, 'ENTER THE REDUCED PLATE HEIGHT IN cm OF COLUMN')
      READ (5, *) hp1

        ENDIF

      WRITE (6,901)
901   FORMAT (1X, 'WOULD YOU LIKE TO INPUT ROPT AND RMIN '
     & ' Y OR TYPE N IF YOU WANT TO USE DEFAULT VALUES ? ')
      READ (5,902) RESP1
902   FORMAT(A)
             IF ( RESP1 .EQ. 'Y' ) THEN

      WRITE (6,801)
801   FORMAT (1X, ' INPUT A VALUE FOR THE OPTIMUM '
     & ' RESOLUTION, ROPT ')
      READ (5, 802) ROPT
802   FORMAT (F8.3)
      WRITE (6,803)
803   FORMAT (1X, ' INPUT A VALUE FOR THE MINIMUM '
     & ' ACCEPTABLE RESOLUTION, RMIN ')
      READ (5,804) RMIN
804   FORMAT (F8.3)

           ELSE
      ROPT = 1.5
      RMIN = 0.5
           ENDIF

         IF (MAXCOL .GT. 1) THEN

      WRITE (6, 13)
      READ (5, *)  CL1MIN, CL1MAX
      WRITE (6, 14)
```

```
      READ (5, *) CL2MIN, CL2MAX
13    FORMAT (1X, ' ENTER THE MINIMUM AND MAXIMUM '
     & ' LENGTH OF COLUMN1 THAT YOU WISH TO TRY.')
      WRITE (6, 5001)
5001  FORMAT(1X, 'ENTER COLUMN 1 INCREMENTS ')
      READ (5, *) C1

14    FORMAT (1X, ' ENTER THE MINIMUM AND MAXIMUM '
     & ' LENGTHS OF COLUMN2 THAT YOU WISH TO TRY.')
      WRITE (6, 5002)
5002  FORMAT(1X, 'ENTER COLUMN 2 INCREMENTS ')
      READ (5, *) C2


         ELSE

      WRITE (6, 670)
      READ (5, *)  CL1MIN, CL1MAX
670   FORMAT (1X, ' ENTER THE MINIMUM AND MAXIMUM '
     & ' LENGTH OF THE COLUMN THAT YOU WISH TO TRY.')
      WRITE (6, 5003)
5003  FORMAT(1X, 'ENTER THE COLUMN INCREMENTS ')
      READ (5, *) C1
         ENDIF

       HIGH1A = 0.00
       HIGH1B = 0.00
       HIGH2A = 0.00
       HIGH2B = 0.00
       REPTA = 0.0
       REPTB = 0.0
       TEST = 0.0D0
             BCRS = 1.0E20
             BCRSTT = 1.0E20
       DO 100 I = 1, MAXSOL
         IF (SOLCAP(I,1,1) .GT. HIGH1A) THEN
          HIGH1A = SOLCAP(I,1,1)
         END IF
         IF (SOLCAP(I,2,1) .GT. HIGH2A) THEN
          HIGH2A = SOLCAP(I,2,1)
         END IF
         IF (SOLCAP(I,1,2) .GT. HIGH1B) THEN
          HIGH1B = SOLCAP(I,1,2)
         END IF
         IF (SOLCAP(I,2,2) .GT. HIGH2B) THEN
         HIGH2B = SOLCAP(I,2,2)
         END IF

100    CONTINUE

          HIGH1A = HIGH1A + 1
          HIGH2A = HIGH2A + 1
          HIGH1B = HIGH1B + 1
          HIGH2B = HIGH2B + 1
```

```
          IF (MAXCOL .LT.2) THEN
          HIGH2A = 0.0
          HIGH2B = 0.0
          END IF

          IF (MAXSOV .LT.2) THEN
          HIGH1B = 0.0
          HIGH2B = 0.0
          END IF

       IF (MAXSOV .GT. 1) THEN
        WRITE (6,101)
101     FORMAT(1X, ' DO YOU WANT TO ENTER YOUR OWN VALUES '
     & ' FOR THE SOLVENT LENGTHS ?, Y OR N ')
        READ (5, 102) RESP2
102     FORMAT(A)
          IF (RESP2 .EQ. 'Y') THEN
        WRITE (6,104)
104     FORMAT(1X, 'ENTER THE MINIMUM AND MAXIMUN LENGTH OF '
     & ' SOLVENT 1 THAT YOU WISH TO TRY ')
        READ (5, *) S1MIN, S1MAX
       WRITE (6, 5004)
5004   FORMAT(1X, 'ENTER SOLVENT 1 INCREMENTS ')
       READ (5, *) S1
        WRITE (6,106)
106     FORMAT(1X, 'ENTER THE MINIMUM AND MAXIMUN LENGTH OF '
     & ' SOLVENT 2 THAT YOU WISH TO TRY ')
        READ (5, *) S2MIN, S2MAX
       WRITE (6, 5005)
5005   FORMAT(1X, 'ENTER SOLVENT 2 INCREMENTS ')
       READ (5, *) S2
           L1MIN = S1MIN
           L1MAX = S1MAX
           L2MIN = S2MIN
           L2MAX = S2MAX
           TEST = 1.0D0
           ENDIF
       ENDIF
       IF ((MAXSOV .LT. 2) .OR. (RESP2 .EQ. 'N')) THEN
       WRITE(6,*) 'ENTER SOLVENT1 INCREMENT'
       READ(5,*) S1
       WRITE(6,*) ' ENTER SOLVENT2 INCREMENT'
       READ(5,*) S2
       ENDIF

112    FORMAT (1X, '-----------------------------------------------')

*     -----------------Calculation of overall capacity ----*---factor as
a function of solvent length and column length

        DO 17 COL1 = CL1MIN, CL1MAX, C1
          IF (MAXCOL .LT. 2) THEN
          CL2MIN = 0.0
```

```
        CL2MAX = 0.0
        C2 = 0.0
        GOTO 616
        END IF
       DO 18 COL2 = CL2MIN, CL2MAX, C2
616         SAMIN = 15 * SQRT((hp1* dp1 * COL1)
     & + (hp2* dp2 * COL2))
        SAMAX = (COL1 * HIGH1A) + (COL2 * HIGH2A)

        SBMIN = 15 * SQRT((hp1* dp1 * COL1)
     & + (hp2 * dp2 * COL2))
        SBMAX = (COL1 * HIGH1B) + (COL2 * HIGH2B)
        IF (TEST .EQ. 1.0D0) THEN
        GOTO 333
        END IF
            IF (MAXSOV .GT. 1) THEN
         L1MIN = SAMIN
         L1MAX = SAMAX
         L2MIN = SBMIN
         L2MAX = SBMAX
            ELSE
         L1MIN = SAMAX
         L1MAX = SAMAX
            ENDIF
*333       WRITE (6,*)
333        CONTINUE

         DO 19 SOLVA = L1MIN, L1MAX, S1
        IF (MAXSOV .LT. 2) THEN
        L2MIN =0.0
        L2MAX = 0.0
        S2 = 0.0
        GOTO 108
        END IF
          DO 20 SOLVB = L2MIN, L2MAX, S2
      REP1 = 0
108      REP2 = 0

         DO 21 I = 1, MAXSOL

      LTEMP1 = 0
      LTEMP2 = 0
      TCOL1 = 0
      TCOL2 = 0
      K1 = 0.0
      K2 = 0.0
      CAPTOT = 0.0
       PULSE = 0.0
      DO 22 N = 1, 1000, 1
           IF (((N/2.) - INT(N/2.)) .GT. 0.2) THEN
           X = SOLVA
           CAP = SOLCAP(I,1,1)
           ELSE
           X = SOLVB
```

```
          CAP = SOLCAP(I,1,2)
          COUNTB = COUNTB + 1
          END IF

         IF (X .EQ. 0.0) THEN
         GOTO 2002
         END IF
            LTEMP1 = LTEMP1 + (X/CAP)
            IF (LTEMP1 .LE. COL1) THEN
            PULSE = PULSE + 1
      TCOL1 = TCOL1 + ((PI * (ID1/2)**2 * PORUS1)/FLOW)
    & * X * ((1 + CAP)/ CAP)
            ELSE
            GOTO 222
            END IF
22    CONTINUE
222      FRAC = (X - ((LTEMP1 - COL1) * CAP)) / X
           IF  (FRAC .LT. (1.0 D -10)) THEN
         FRAC = 0.0D0
           END IF
        PULSE = PULSE + FRAC
      TCOL1 = TCOL1 + ((PI * (ID1/2)**2 * PORUS1)/FLOW)
    & * X * ((1 + CAP)/ CAP) * FRAC

            IF (MAXCOL .LT. 2) THEN
            GOTO 888
            ENDIF

      IF (((N/2.) - INT(N/2.)) .GT. 0.2) THEN
                X = SOLVA
                CAP = SOLCAP(I,2,1)

                LTEMP2 = X * (1 - FRAC) / CAP
              IF (LTEMP2 .LE. COL2) THEN
                  PULSE = PULSE + (1 - FRAC)
      TCOL2 = TCOL2 + ((PI * (ID2/2)**2 * PORUS2)/FLOW)
    & * X * ((1 + CAP)/ CAP) * (1 - FRAC)
              ELSE
            X = (1 - FRAC) * X
            FRAC = (X - ((LTEMP2 - COL2) * CAP)) / X
            IF  (FRAC .LT. (1.0 D -10)) THEN
         FRAC = 0.0D0
            END IF
            PULSE = PULSE + FRAC
              GOTO 247
              END IF
                DO 24 M = 1, 1000, 1
                   IF (((M/2.) - INT(M/2.)) .GT. 0.2) THEN
                   X = SOLVB
                   CAP = SOLCAP(I,2,2)
                   ELSE
                   X = SOLVA
                   CAP = SOLCAP(I,2,1)
                   END IF
```

```
                    LTEMP2 = LTEMP2 + (X/CAP)
                       IF (LTEMP2 .LE. COL2) THEN
                       PULSE = PULSE + 1
      TCOL2 = TCOL2 + ((PI * (ID2/2)**2 * PORUS2)/FLOW)
     & * X * ((1 + CAP)/ CAP)
                       ELSE
                       GOTO 246
                       END IF
24                CONTINUE
       ELSE
                  X = SOLVB
                  CAP = SOLCAP(I,2,2)
                  LTEMP2 = X * (1 - FRAC) / CAP
                IF (LTEMP2 .LE. COL2) THEN
                PULSE = PULSE + (1 - FRAC)
      TCOL2 = TCOL2 + ((PI * (ID2/2)**2 * PORUS2)/FLOW)
     & * X * ((1 + CAP)/ CAP) * (1 - FRAC)
                ELSE
              X = (1 - FRAC) * X
              FRAC = (X - ((LTEMP2 - COL2) * CAP)) / X
              IF  (FRAC .LT. (1.0 D -10)) THEN
            FRAC = 0.0D0
              END IF
              PULSE = PULSE + FRAC
                GOTO 247
                END IF

                    DO 25 M = 1, 1000, 1
                    IF (((M/2.) - INT(M/2.)) .GT. 0.2 ) THEN
                    X = SOLVA
                    CAP = SOLCAP(I,2,1)
                    COUNTC = COUNTC + 1
                    ELSE
                    X = SOLVB
                    CAP = SOLCAP(I,2,2)
                    COUNTD = COUNTD + 1
                    END IF
                    LTEMP2 = LTEMP2 + (X/CAP)
                      IF (LTEMP2 .LE. COL2) THEN
                      PULSE = PULSE + 1
      TCOL2 = TCOL2 + ((PI * (ID2/2)**2 * PORUS2)/FLOW)
     & * X * ((1 + CAP)/ CAP)
                      ELSE
                      GOTO 246
                      END IF
25                  CONTINUE
246             FRAC = (X-((LTEMP2 - COL2) * CAP))/X
            IF (FRAC .LT. (1.0 D -10)) THEN
            FRAC = 0.0D0
            END IF
            PULSE = PULSE + FRAC

247          TCOL2 = TCOL2 + ((PI * (ID2/2)**2 * PORUS2)/FLOW)
     & * X * ((1 + CAP)/ CAP) * FRAC
```

```
      END IF

888      RETEN = (TCOL1 + TCOL2)
       RETENT (I) = RETEN
       PULSES(I) = PULSE
          IF (PULSE .GT. INT(PULSE)) THEN
          FPULSE = (PULSE - INT(PULSE)) * 100
          TPULSE = INT(PULSE) + 1
          ELSE
           FPULSE = 100
           TPULSE = PULSE
          END IF
*       WRITE (20,*) PULSE, FPULSE, TPULSE
          IF ((COL1 .EQ. 0.0) .AND. (COL2 .EQ. 0.0)) THEN
          GOTO 2002
          END IF
          IF (COL1 .EQ. 0.0) THEN

*    ---------Calculation of variance of solute-----------

       SIGMA = SQRT((hp2* dp2 * COL2) * (TCOL2/COL2)**2)
          GOTO 2001
          ELSE
             IF (COL2 .EQ. 0.0) THEN
       SIGMA = SQRT((hp1* dp1 * COL1) * (TCOL1/COL1)**2)
          GOTO 2001
             END IF
          END IF
        IF (MAXCOL .GT. 1) THEN
       SIGMA = SQRT((hp1* dp1 * COL1) * (TCOL1/COL1)**2
     & + (hp2* dp2 * COL2) * (TCOL2/COL2)**2)
        ELSE
       SIGMA = SQRT((hp1* dp1 * COL1) * (TCOL1/COL1)**2)
        END IF

2001        PNUM = (RETEN**2)/(SIGMA**2)
       WIDTH = 4 * SIGMA

       WIDTHS (I) = WIDTH



21      CONTINUE

      CALL SORT (MAXSOL, RETENT, WIDTHS, ROPT, RMIN, CRST, MINRES)

      CRSTT = CRST * (RETENT(MAXSOL)) / MAXSOL

          IF (CRST .LT. BCRS) THEN
          BCRS = CRST
          BCOL1 = COL1
          BCOL2 = COL2
          BSOLVA = SOLVA
          BSOLVB = SOLVB
```

```
          SEPTIME = RETENT(MAXSOL)
          CRITRS = MINRES
          END IF

          IF (CRSTT .LT. BCRSTT) THEN
          BCRSTT = CRSTT
          BCOL1T = COL1
          BCOL2T = COL2
          BSOLVAT = SOLVA
          BSOLVBT = SOLVB
          SEPTIMT = RETENT(MAXSOL)
          CRITRT = MINRES
          END IF

         IF (MAXSOV .LT. 2) THEN
         GOTO 19
         END IF
20       CONTINUE
19     CONTINUE
2002          IF ((COL1 .EQ. 0.0)  .AND. (COL2 .EQ. 0.0)) THEN
         BCRS = 0.0
         BCOL1 = 0.0
         BCOL2 = 0.0
         BSOLVA = 0.0
         BSOLVB = 0.0
         SEPTIME = 0.0
         CRITRS = 0.0

         BCRSTT = 0.0
         BCOL1T = 0.0
         BCOL2T = 0.0
         BSOLVAT = 0.0
         BSOLVBT = 0.0
         SEPTIMT = 0.0
         CRITRT = 0.0
              END IF

*    ----------Output optimum conditions----------------

      WRITE(20, 74) BCOL1,BCOL2, BCRS, BSOLVA, BSOLVB, SEPTIME, CRITRS
74     FORMAT(1X, 2(1X, F10.3), E10.2, 2(1X,F10.3), 2(1X, F10.2))
      WRITE(10, 704) BCOL1T,BCOL2T,BCRSTT,BSOLVAT,BSOLVBT,SEPTIMT,CRITRT
704     FORMAT(1X, 5(1X, F10.3), 2(1X, F10.2))

            BCRS = 1.0E20
            BCRSTT = 1.0E20
         IF (MAXCOL .LT. 2) THEN
         GOTO 17
         END IF

18     CONTINUE
17    CONTINUE
      END
**-------------------------------------------------------------*
```

```
*------------Bubble Sort Routine------------------

*This program is meant to sort a list of numbers in an *array in *an
ascending order.and determine resolutions *between adjacent *peaks and
their CRS values

      SUBROUTINE SORT (LIMIT, INDEX, ENDEX, ROPT, RMIN, CRS, MINRES)
      REAL*8 INDEX, RES, RSUM, RAVG,CS1,CS2,CRS1,CRS2,
     & CRS, RMIN, ROPT, RESOL, ENDEX, MINRES
      INTEGER*4 PAIRS, I, J, COUNT1, LIMIT
      LOGICAL DONE
      DIMENSION INDEX (100), ENDEX (100), RESOL(100)
      PAIRS = LIMIT - 1

      DONE = .FALSE.

20    IF (.NOT. DONE) THEN
      DONE = .TRUE.

      DO 30 I = 1, PAIRS
       IF (INDEX(I) .GT. INDEX(I + 1)) THEN
        TEMP = INDEX(I)
        INDEX(I) = INDEX(I + 1)
        INDEX(I + 1) = TEMP
        TEMP = ENDEX (I)
        ENDEX (I) = ENDEX (I + 1)
        ENDEX (I + 1) = TEMP
      DONE = .FALSE.
      END IF
30    CONTINUE
      PAIRS = PAIRS - 1
      GO TO 20
      END IF
      RSUM = 0
      COUNT1 = 0
       MINRES = 1.0E20
      DO 201 I = 1, LIMIT - 1
      RES = (ABS(INDEX (I) - INDEX (I + 1))) * 2
     & / (ENDEX (I) + ENDEX (I + 1))
      RESOL (I) = RES
       IF (RES .LT. MINRES) THEN
       MINRES = RES
       END IF
      RSUM = RSUM + RES
      COUNT1 = COUNT1 + 1

201   CONTINUE

      RAVG = RSUM/ COUNT1
      CRS1 = 0
      CRS2 = 0
      DO 300 I = 1, LIMIT - 1
         IF (RESOL (I) .LT. (RMIN + 0.01)) THEN
```

```
          CS1 = ((( ROPT - RMIN) * 100) ** 2) * (1 / RMIN)
          ELSE
       CS1 = (((RESOL(I) - ROPT) / (RESOL(I) - RMIN)) ** 2)
      & / RESOL(I)
          END IF
          CS2 = (RESOL(I) ** 2) / (COUNT1 * (RAVG ** 2))
          CRS1 = CRS1 + CS1
          CRS2 = CRS2 + CS2
300       CONTINUE
          CRS = CRS1 + CRS2
          END

*-------------------------------------------------------------*
*-------------------------------------------------------------*
```

A1.3 References

1. L. Nyhoff and S Leestma, *Fortran 77 for Engineers and Scientist*, 2nd Ed., Macmillan Publishing Co., New York, Chapter 7.

2. T. D. Schlabach and J. L. Excoffier, *J. Chromatogr.* **439**, 173 (1988)

MICHIGAN STATE UNIV. LIBRA
3129301417211